

RADIOPHARMACEUTICAL APPLICATIONS OF TECHNETIUM  
3-OXY-4-PYRONES AND 3-OXY-4-PYRIDINONES  
AND GALLIUM 3-OXY-4-PYRIDINONES

by

Gordon A. Webb

B. Sc., Mount Allison University, 1986

A THESIS SUBMITTED IN PARTIAL FULFILLMENT OF  
THE REQUIREMENTS FOR THE DEGREE OF  
MASTER OF SCIENCE

in

THE FACULTY OF GRADUATE STUDIES

(Department of Chemistry)

We accept this thesis as conforming  
to the required standard

The University of British Columbia

December 1989

© Gordon A. Webb, 1989



In presenting this thesis in partial fulfilment of the requirements for an advanced degree at the University of British Columbia, I agree that the Library shall make it freely available for reference and study. I further agree that permission for extensive copying of this thesis for scholarly purposes may be granted by the head of my department or by his or her representatives. It is understood that copying or publication of this thesis for financial gain shall not be allowed without my written permission.

Department of CHEMISTRY

The University of British Columbia  
Vancouver, Canada

Date Dec 20 / 1989

## ABSTRACT

Ammonium pertechnetate  $[\text{NH}_4][\text{TcO}_4]$  was reacted with the following ligands *via* the reduction route: 3-hydroxy-2-methyl-4-pyrone (maltol), 5-hydroxy-2-hydroxymethyl-4-pyrone (kojic acid), 3-hydroxy-2-methyl-4-pyridinone (Hmpp), 3-hydroxy-1,2-dimethyl-4-pyridinone (Hdpp), 3-hydroxy-2-methyl-1-hexyl-4-pyridinone (Hmhpp), 3-hydroxy-2-methyl-1-undecanato-4-pyridinone (Hmupp), and  $\beta$ -[N-(3-hydroxy-4-pyridinone)]- $\alpha$ -aminopropionic acid (*l*-mimosine). The products from the reduction route were characterized by mass spectrometry, infrared spectrometry, ultraviolet spectroscopy, and conductivity measurements. Initial results indicate the formation of mono-cationic tris-ligand complexes of tin and technetium ( $[\text{TcL}_3]^+$  and  $[\text{SnL}_3]^+$ ). The formation of Tc (V) complexes *via* a substitution route was also investigated.  $[\text{Bu}_4\text{N}][\text{TcOCl}_4]$  was reacted with: 3-hydroxy-2-methyl-4-pyrone (maltol), 5-hydroxy-2-hydroxymethyl-4-pyrone (kojic acid), and  $\beta$ -[N-(3-hydroxy-4-pyridinone)]- $\alpha$ -aminopropionic acid (*l*-mimosine). The 3-hydroxy-4-pyridinone used in this study (except mimosine) were prepared by the conversion of an oxygen heterocycle, 3-hydroxy-2-methyl-4-pyrone, to the corresponding nitrogen heterocycle by reaction with a primary amine. These potentially bidentate ligands contain an  $\alpha$ -hydroxyketone moiety and their conjugate bases form mono-cationic tris-ligand technetium complexes. Hmupp, a new compound, was fully characterized by mass spectrometry, infrared spectrometry, proton NMR, ultraviolet spectroscopy, and elemental analysis.

Initial clearance studies were done in a rabbit with the products of the reactions of  $[\text{}^{99\text{m}}\text{TcO}_4]^-$  with Hdpp and Mimosine. Analogous to the synthetic procedure above using  $[\text{}^{99}\text{TcO}_4]^-$ , two products are formed ( $[\text{}^{99\text{m}}\text{TcL}_3]^+$  and  $[\text{SnL}_3]^+$ ). The  $[\text{SnL}_3]^+$  complex is not radioactive and is therefore not visualized by the imaging procedure. The observed

distribution is therefore that of the  $[^{99m}\text{TcL}_3]^+$  complex. The results of the clearance study with  $[^{99m}\text{Tc}(\text{dpp})_3]^+$  show a small amount of liver, heart, and gall bladder uptake; however, the majority of the activity is rapidly excreted *via* the kidneys and bladder. There is also some gut uptake observed, and this is cleared much more slowly. The clearance study conducted with  $[^{99m}\text{Tc}(\text{mimo})_3]^+$  shows results similar to those conducted with  $[^{99m}\text{Tc}(\text{dpp})_3]^+$ ; however, less gut uptake and faster bladder clearance are observed with the mimosine complex.

In addition to the technetium radiopharmaceutical work, some gallium-67 work was also done. This was done in collaboration with William Nelson and Don Lyster to complete an ongoing study of the *in vitro* and *in vivo* coordination chemistry of gallium 3-oxy-4-pyridinones as a model for the biodistribution of aluminum.  $^{67}\text{Ga}$ -biodistribution studies were conducted with the following 3-hydroxy-4-pyridinone ligands: 3-hydroxy-2-methyl-4-pyridinone (Hmpp), 3-hydroxy-1,2-dimethyl-4-pyridinone (Hdpp), 3-hydroxy-2-methyl-1-hexyl-4-pyridinone (Hmhpp), and  $\beta$ -[N-(3-hydroxy-4-pyridinone)]- $\alpha$ -aminopropionic acid (*l*-mimosine). The results of the biodistribution show that under conditions of excess ligand  $^{67}\text{Ga}$  is redirected from transferrin; however, the  $^{67}\text{Ga}$ -ligand complexes do not localize in any organs.

## TABLE OF CONTENTS

	page
ABSTRACT .....	ii
TABLE OF CONTENTS .....	iv
LIST OF TABLES .....	vii
LIST OF SCHEMES .....	vii
LIST OF FIGURES .....	viii
LIST OF ABBREVIATIONS .....	x
ACKNOWLEDGEMENTS .....	xii
CHAPTER I. GENERAL INTRODUCTION .....	1
CHAPTER II. SYNTHESIS AND CHARACTERIZATION OF 3-HYDROXY-4-PYRIDINONE LIGANDS	
2.1 Introduction .....	18
2.2 Materials and Methods .....	19
2.2.1 Preparation of Hmpp .....	20
2.2.2 Preparation of Hdpp .....	20
2.2.3 Preparation of Hmhpp .....	21
2.2.4 Preparation of Hmupp .....	21
2.3 Characterization .....	22
2.3.1 Elemental Analysis .....	22
2.3.2 Infrared Spectroscopy .....	23
2.3.3 Proton NMR Spectroscopy .....	25
2.3.4 Electron Impact Mass Spectrometry .....	26
2.3.5 Ultraviolet Spectroscopy .....	28

CHAPTER III. SYNTHESIS OF TECHNETIUM COMPLEXES BY THE  
REDUCTION ROUTE

3.1 Introduction .....	30
3.2 Materials and Methods .....	33
3.2.1 Reaction of $[\text{TcO}_4]^-$ with maltol .....	33
3.2.2 Reaction of $[\text{TcO}_4]^-$ with kojic acid .....	33
3.2.3 Reaction of $[\text{TcO}_4]^-$ with Hmpp .....	33
3.2.4 Reaction of $[\text{TcO}_4]^-$ with Hdpp .....	34
3.2.5 Reaction of $[\text{TcO}_4]^-$ with Hmhpp .....	34
3.2.6 Reaction of $[\text{TcO}_4]^-$ with Hmupp.....	34
3.2.7 Reaction of $[\text{TcO}_4]^-$ with mimosine .....	35
3.3 Discussion of Synthetic Procedure .....	35
3.4 Characterization .....	36
3.4.1 Infrared Spectroscopy .....	38
3.4.2 Mass Spectrometry .....	41
3.4.3 Ultraviolet Spectroscopy .....	43
3.4.4 Conductivity Measurements .....	44

CHAPTER IV. SYNTHESIS OF TECHNETIUM COMPLEXES BY THE  
SUBSTITUTION ROUTE

4.1 Introduction .....	46
4.2 Materials and Methods .....	47
4.2.1 Reaction of $[\text{Bu}_4\text{N}][\text{TcOCl}_4]$ with maltol .....	47
4.2.2 Reaction of $[\text{Bu}_4\text{N}][\text{TcOCl}_4]$ with kojic acid.....	47
4.2.3 Reaction of $[\text{Bu}_4\text{N}][\text{TcOCl}_4]$ with Hmpp .....	48
4.3 Discussion of Synthetic Procedure .....	48

4.4 Characterization .....	49
4.4.1 Infrared Spectroscopy .....	49
4.4.2 Mass Spectrometry .....	51
4.5 Results and Discussion .....	53
CHAPTER V. RADIOPHARMACEUTICAL APPLICATIONS OF TECHNETIUM AND GALLIUM	
5.1 Gallium Biodistribution Studies	
5.1.1 Introduction .....	55
5.1.2 Materials and Methods .....	55
5.1.3 Results and Discussion .....	56
5.2 Technetium Biodistribution Studies	
5.2.1 Introduction .....	62
5.2.2 Chromatography .....	64
5.2.3 Materials and Methods.....	66
5.2.4 Results and Discussion .....	67
CHAPTER VI. CONCLUSIONS AND SUGGESTIONS FOR FUTURE WORK .....	
REFERENCES .....	81
APPENDIX .....	87

## LIST OF TABLES

Table 1.1	Isotopes of technetium .....	2
Table 2.1	Hmupp elemental analysis .....	23
Table 2.2	Selected infrared absorption bands ( $\text{cm}^{-1}$ ) for Hmupp .....	23
Table 2.3	Proton NMR chemical shift ( $\delta$ ) data for Hmupp at 400 MHz (ppm) .....	25
Table 2.4	Mass spectral data (m/z) for Hmupp .....	26
Table 3.1	Selected infrared absorption bands ( $\text{cm}^{-1}$ ) for the tris-ligand metal chloride complexes .....	40
Table 3.2	Data from FAB-MS spectra of the tris-ligand metal chloride complexes (m/z) .....	41
Table 3.3	Ultraviolet spectral data for the tris-ligand metal chloride complexes .....	43
Table 3.4	Resistance values ( $\text{k}\Omega$ ) for the tris-ligand metal chloride complexes .....	45
Table 4.1	Negative DCI mass spectrum for the organic soluble product from the reaction of $[\text{Bu}_4\text{N}][\text{TcOCl}_4]$ and maltol .....	51
Table 4.2	FAB mass spectrum for the organic soluble product from the reaction $[\text{Bu}_4\text{N}][\text{TcOCl}_4]$ and maltol .....	52
Table 5.1	Biodistribution of $^{67}\text{Ga}$ after 24 hours as a function of ligand in mice .....	59

## LIST OF SCHEMES

Scheme 1	Reduction route .....	7
Scheme 2	Substitution route.....	8

## LIST OF FIGURES

Figure 1.1	Nuclear reaction for the formation of $^{95m}\text{Tc}$ and $^{97m}\text{Tc}$ .....	1
Figure 1.2	Scintigraphic Scanner .....	4
Figure 1.3	$^{99m}\text{TcO}_4^-$ Generator .....	4
Figure 1.4	Decay scheme of $^{99}\text{Mo}$ .....	5
Figure 1.5	Substituted 3-hydroxy-4-pyrones and 3-hydroxy-4-pyridinones .....	14
Figure 1.6	Gallium complexes of 3-oxy-4-pyridinonato.....	16
Figure 2.1	Mechanism for the conversion of 4-pyrones to 4-pyridinones .....	18
Figure 2.2	3-hydroxy-2-methyl-4-pyridinone ligands .....	19
Figure 2.3	Infrared spectrum of Hmupp.....	24
Figure 2.4	EI-MS spectrum of Hmupp .....	27
Figure 2.5	UV Spectrum of Hmupp .....	28
Figure 3.1	Five-membered chelate ring .....	30
Figure 3.2	Synthesis of $[\text{M}(\text{dpp})_3]^+$ ( $\text{M} = \text{Tc}, \text{Sn}$ ) <i>via</i> the reduction route .....	32
Figure 3.3	Infrared spectra of Hdpp (top) and $[\text{M}(\text{dpp})_3]^+$ ( $\text{M} = \text{Tc}, \text{Sn}$ ) (bottom) .....	39
Figure 3.4	FAB-MS spectrum of $[\text{M}(\text{dpp})_3]^+$ ( $\text{M} = \text{Tc}, \text{Sn}$ ).....	42
Figure 4.1	Infrared spectra of the two solids from the reaction of $[\text{Bu}_4\text{N}][\text{TcOCl}_4]$ and maltol .....	50
Figure 5.1	Percent uptake per gram of organ for blood and liver 24 hours post-injection of various $^{67}\text{Ga}$ -ligand solutions in mice .....	60
Figure 5.2	Clearance study of $^{67}\text{Ga}(\text{dpp})_3$ (bold trace) and $^{67}\text{Ga}(\text{citrate})$ (thin trace) in a rabbit .....	61
Figure 5.3	Distribution for $[\text{}^{99m}\text{Tc}(\text{dpp})_3]^+$ twenty minutes post-injection (upper chest region) .....	69

Figure 5.4	Distribution for $[^{99m}\text{Tc}(\text{dpp})_3]^+$ twenty minutes post-injection (lower chest region) .....	70
Figure 5.5	Distribution for $[^{99m}\text{Tc}(\text{dpp})_3]^+$ one hour post-injection and post-urination (posterior view) .....	71
Figure 5.6	Clearance curves for $[^{99m}\text{Tc}(\text{dpp})_3]^+$ (right kidney upper trace left kidney lower trace) .....	72
Figure 5.7	Clearance curves for $[^{99m}\text{Tc}(\text{dpp})_3]^+$ (kidneys upper traces bladder lower trace) .....	73
Figure 5.8	Distribution for $[^{99m}\text{Tc}(\text{mimo})_3]^+$ twenty minutes post-injection (upper chest region) .....	74
Figure 5.9	Distribution for $[^{99m}\text{Tc}(\text{mimo})_3]^+$ twenty minutes post-injection (lower chest region) .....	75
Figure 5.10	Clearance curves for $[^{99m}\text{Tc}(\text{mimo})_3]^+$ (right kidney upper trace left kidney lower trace) .....	76
Figure 5.11	Clearance curves for $[^{99m}\text{Tc}(\text{mimo})_3]^+$ (kidneys upper traces bladder lower trace) .....	77

## LIST OF ABBREVIATIONS

Abbreviation	Meaning
$\alpha$	alpha decay
$\beta^+$	beta decay; positron emission
$\beta^-$	beta decay; electron emission
Bq	Becquerel; equals 1 disintegration per second
Ci	Curie; equals $3.7 \times 10^{10}$ disintegrations per second
(d, n)	induced nuclear process; involves the bombardment of an isotope by a deuteron and subsequent emission of a neutron
DCI	desorption chemical ionization
DMG	dimethylglyoxime
DTPA	diethylenetriamine pentaacetic acid
$\epsilon_{\max}$	molar absorptivity at wavelength of maximum absorbance
EI	electron impact
FAB	fast atom bombardment
$\gamma$	gamma decay; electromagnetic radiation ( $\gamma$ -ray)
Hdpp	3-hydroxy-1,2-dimethyl-4-pyridinone
HIDA	N-(2,6-dimethylphenylcarbamoylmethyl)-iminodiacetate
Hmepp	3-hydroxy-2-methyl-1-ethyl-4-pyridinone
Hmhpp	3-hydroxy-2-methyl-1-hexyl-4-pyridinone
Hmpp	3-hydroxy-2-methyl-4-pyridinone
Hmupp	3-hydroxy-2-methyl-1-undecanato-4-pyridinone
HPLC	high performance liquid chromatography
IR	infrared

IT	isomeric transition
$J_{ab}$	NMR coupling constant between a and b
keV	kilo electron volt
$\lambda_{\max}$	wavelength of maximum absorbance
ma (maltol)	3-hydroxy-2-methyl-4-pyrone
mimo (mimosine)	$\beta$ -[N-(3-hydroxy-4-pyridinone)]- $\alpha$ -aminopropionic acid
$\Omega$	ohms
$p$	n-octanol/water partition coefficient
$t_{1/2}$	half life
TLC	thin layer chromatography
UV	ultraviolet
X	halide (F, Cl, Br, I)

## ACKNOWLEDGEMENTS

I would like to give my special thanks to Dr. Guenter Eigendorf and the technical staff of the Mass Spectrometry Department for running my radioactive samples. I would also like to thank Zaihui for his help in running my NMR samples.

Financial support in the form of the Sir Walter C. Sumner Memorial Fellowship, a UBC Teaching Assistantship, and a research grant from DuPont are gratefully acknowledged.

I would especially like to thank Chris Orvig (and his former English teacher) for all his support and help.

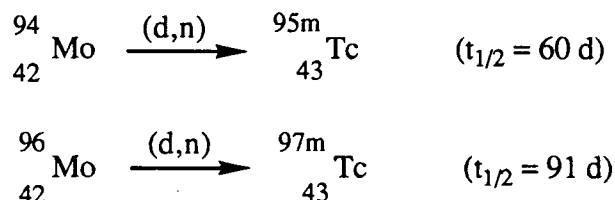
I would also like to thank Don Lyster and Terri Rihela for their help in the biodistribution and clearance studies.

Finally, to Inalga and Arnold "thanks, for bringing a bit of joy to a joyless time", (I love those feeding frenzies) and to Sir Isaac Newt, who has been found, "may he rest in peace."

## CHAPTER I GENERAL INTRODUCTION

Technetium was discovered by Perrier and Segrè in 1937 in Italy.<sup>1,2</sup> They showed that radioactivity, obtained by irradiation of a plate of molybdenum with deuterons in the Berkeley cyclotron, resulted in isotopes of technetium. They had produced mainly  $^{95m}\text{Tc}$  and  $^{97m}\text{Tc}$  by the nuclear reactions shown in Figure 1.1.

Figure 1.1 Nuclear reactions for the formation of  $^{95m}\text{Tc}$  and  $^{97m}\text{Tc}$ .



This artificial element was not named until 1938 when it was named "technetium" from *tecnetos*, the Greek word meaning artificial.<sup>3</sup> At present 21 isotopes and numerous isomers of mass numbers 90 to 110 are known; these are listed in Table 1.1.

Technetium, although called an artificial element, is present in the earth's crust.  $^{99}\text{Tc}$  is formed by the spontaneous fission of  $^{238}\text{U}$ .  $^{99}\text{Tc}$  is the only isotope which can be obtained in weighable amounts and it exists as a bright silver grey metal. Like rhenium, it crystallizes in the hexagonal close packed arrangement.

Technetium is a second row transition, or d-block, element whose chemistry is expected to resemble that of its neighbors molybdenum and ruthenium. Further, because of

Table 1.1 Isotopes of Technetium

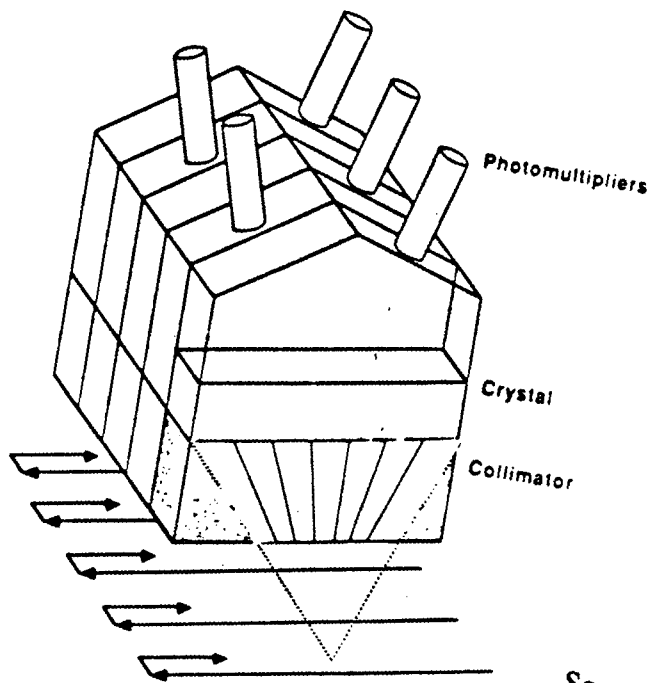
Isotope	Mode of decay	Half-life	$\gamma$ Energies (keV)	Mode of production
$^{90}\text{Tc}$	$\beta^+$	50 sec	948; 1054; 511	$^{92}\text{Mo}(p, 3n)^{90}\text{Tc}$
$^{91}\text{Tc}$	$\beta^+$ , EC	3.3 min	218-2888; 511	$^{92}\text{Mo}(p, 2n)^{91}\text{Tc}$
$^{92}\text{Tc}$	$\beta^+$ , EC	4.4 min	329; 773; 511	$^{92}\text{Mo}(d, 2n)^{92}\text{Tc}$
$^{93\text{m}}\text{Tc}$	IT, EC	43 min	392; 2645	$^{92}\text{Mo}(d, n)^{93\text{m}}\text{Tc}$ ; $^{92}\text{Mo}(p, \gamma)^{93\text{m}}\text{Tc}$
$^{93}\text{Tc}$	$\beta^+$ , EC	2.7 hr	1363; 1477; 511	$^{92}\text{Mo}(d, n)^{93}\text{Tc}$ ; $^{92}\text{Mo}(p, \gamma)^{93}\text{Tc}$
$^{94\text{m}}\text{Tc}$	IT, $\beta^+$ , EC	52 min	871; 1869; 511	$^{93}\text{Nb}(\alpha, 3n)^{94\text{m}}\text{Tc}$ ; $^{94}\text{Mo}(d, 2n)^{94\text{m}}\text{Tc}$
$^{94}\text{Tc}$	$\beta^+$ , EC	4.88 hr	704; 650; 511	$^{94}\text{Mo}(d, 2n)^{94}\text{Tc}$
$^{95\text{m}}\text{Tc}$	IT, $\beta^+$ , EC	61 days	204; 786; 511	$^{95}\text{Mo}(p, n)^{95\text{m}}\text{Tc}$ ; $^{94}\text{Mo}(d, n)^{95\text{m}}\text{Tc}$
$^{95}\text{Tc}$	EC	20 hr	766; 1074	$^{95}\text{Mo}(p, n)^{95}\text{Tc}$ ; $^{94}\text{Mo}(d, n)^{95}\text{Tc}$
$^{96\text{m}}\text{Tc}$	IT, $\beta^+$ , EC	52 min	34; 481; 778	$^{93}\text{Nb}(\alpha, n)^{96\text{m}}\text{Tc}$ ; $^{96}\text{Mo}(d, 2n)^{96\text{m}}\text{Tc}$
$^{96}\text{Tc}$	EC	4.3 days	778; 850; 1127	$^{96}\text{Mo}(p, n)^{96}\text{Tc}$ ; $^{95}\text{Mo}(d, n)^{96}\text{Tc}$
$^{97\text{m}}\text{Tc}$	IT	90 days	97	$^{96}\text{Ru}(n, \gamma)^{97}\text{Ru}(\text{EC})^{97\text{m}}\text{Tc}$
$^{97}\text{Tc}$	EC	$2.6 \times 10^6$ years		$^{96}\text{Ru}(n, \gamma)^{97}\text{Ru}(\text{EC})^{97}\text{Tc}$
$^{98}\text{Tc}$	$\beta^-$	$4.2 \times 10^6$ years	652; 745	$^{98}\text{Mo}(p, n)^{98}\text{Tc}$
$^{99\text{m}}\text{Tc}$	IT	6.02 hr	141	$^{98}\text{Mo}(n, \gamma)^{99}\text{Mo}(\beta^-)^{99\text{m}}\text{Tc}$
$^{99}\text{Tc}$	$\beta^-$	$2.1 \times 10^5$ years		fission
$^{100}\text{Tc}$	$\beta^-$	15.8 sec	540; 591	$^{99}\text{Tc}(n, \gamma)^{100}\text{Tc}$
$^{101}\text{Tc}$	$\beta^-$	14.3 min	307; 532	$^{100}\text{Mo}(n, \gamma)^{101}\text{Mo}(\beta^-)^{101}\text{Tc}$
$^{102\text{m}}\text{Tc}$	IT, $\beta^-$	4.4 min	475; 628; 1103	$^{102}\text{Ru}(n, p)^{102\text{m}}\text{Tc}$ ; fission
$^{102}\text{Tc}$	$\beta^-$	5.3 sec	475; 628	$^{102}\text{Ru}(n, p)^{102}\text{Tc}$ ; fission
$^{103}\text{Tc}$	$\beta^-$	50 sec	136; 531; 884	Fission
$^{104}\text{Tc}$	$\beta^-$	18.1 min	360; 531; 884	Fission
$^{105}\text{Tc}$	$\beta^-$	7.6 min	108; 143; 322	Fission
$^{106}\text{Tc}$	$\beta^-$	36 sec	270; 2239	Fission
$^{107}\text{Tc}$	$\beta^-$	21.2 sec	103	Fission
$^{108}\text{Tc}$	$\beta^-$	5.17 sec		Fission
$^{109}\text{Tc}$	$\beta^-$	1.4 sec		Fission
$^{110}\text{Tc}$	$\beta^-$	0.82 sec		Fission

the lanthanide contraction the chemistry of technetium will more closely resemble that of its third row congener rhenium than that of manganese. The electronic configuration of technetium in the ground state is  $[\text{Kr}] 4d^5 5s^2$  and Tc is expected to exhibit a wide variety of oxidation states with an extensive redox chemistry. As expected, compounds of technetium in the formal oxidation states (+7) to (-1) have been synthesized. Generally, those of the (+7) and (+5) oxidation states are more stable; however, those of the lower oxidation states can be stabilized by the appropriate ligands. When coordinated, Tc (III), Tc (IV) and Tc (V) predominate in the lower oxidation states.

Technetium-99m is the most widely utilized radioisotope for the preparation of radiopharmaceuticals. Its physical properties compatible with nuclear medicine, as is its availability. The wide-spread use of technetium-99m may be attributed to two major technological developments: the development of the Anger scintillation camera, and the development of the pertechnetate generator.

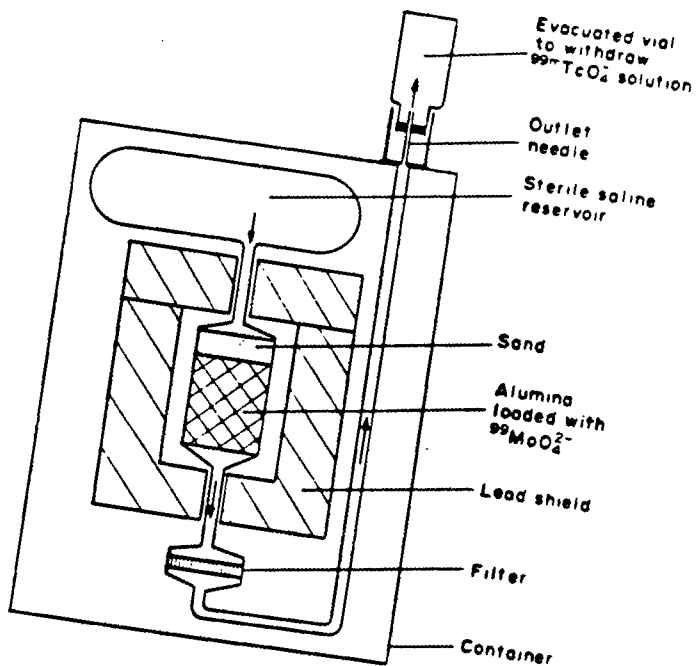
The development of the Anger scintillation camera (Figure 1.2) made it possible to visualize, and to take photographs of,  $\gamma$  radiation in the body. Radiopharmaceuticals are introduced into the body in a number of ways; the most common is by injection into the blood stream. They may be used to image the blood pool or some other area in which they localize. Scintigraphic scanners or cameras have three main parts: the collimator, a thick thallium-activated sodium iodide crystal, and a photomultiplier or photodiode. The collimator collects and focuses  $\gamma$  radiation from the radiopharmaceutical onto the crystal, which upon absorption of the radiation ejects a core electron which imparts its kinetic energy to the crystal matrix. The resulting emission of visible light photons is directly proportional to the number and energies of the incident  $\gamma$  rays. This is then converted by a photomultiplier tube or photodiode array into an electrical pulse proportional in magnitude to the amount of light produced. This can then be displayed graphically.

Figure 1.2 Scintigraphic Scanner



Source Ref. 90

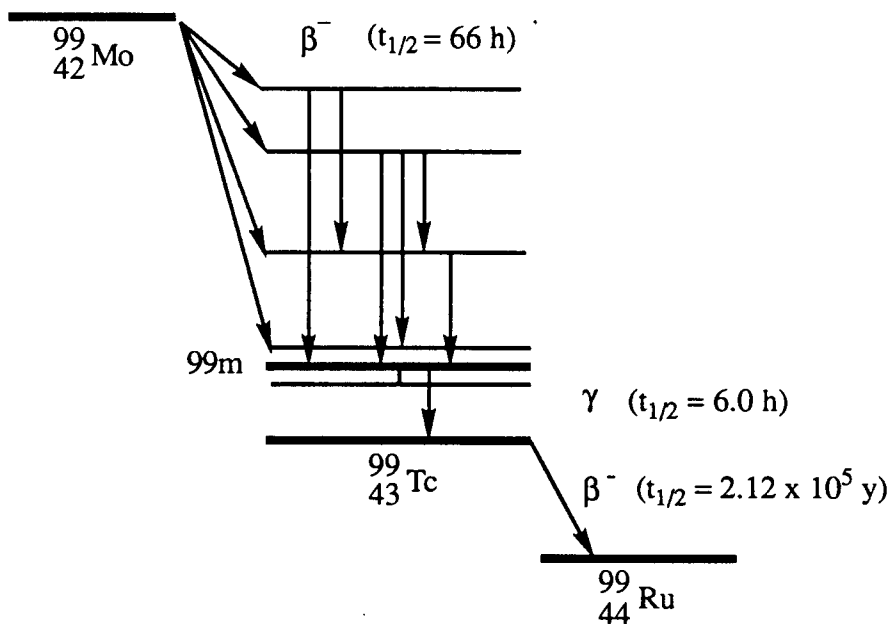
Figure 1.3  $^{99m}\text{TcO}_4^-$  Generator



Source Ref. 91

The development of the pertechnetate generator is the second, and most important reason for the increased use of  $^{99m}\text{Tc}$  in nuclear medicine. The pertechnetate generator (Figure 1.3) works on the basis of a chromatographic separation by charge of  $[\text{}^{99}\text{MoO}_4]^{2-}$  and  $[\text{}^{99m}\text{TcO}_4]^-$ . The parent  $[\text{}^{99}\text{MoO}_4]^{2-}$  (or mother as it is often called) decays *via* a  $\beta^-$  cascade to give the metastable  $[\text{}^{99m}\text{TcO}_4]^-$  (the daughter). The eluent from the column is then drawn off in a process known as milking. This eluent may be injected directly into radiopharmaceutical kits; these consist of a ligand, a reducing agent (commonly a salt of Sn (II)) and sometimes a buffer and/or a stabilizing agent. Due to the short half life of  $^{99m}\text{Tc}$  ( $t_{1/2} = 6 \text{ h}$ ) which undergoes a  $\gamma$  decay (IT 99+%) to  $^{99}\text{Tc}$  (a long lived isotope ( $t_{1/2} = 2.12 \times 10^5 \text{ y}$ )) there is a build-up of  $^{99}\text{Tc}$  over time. To obtain carrier-free  $[\text{}^{99m}\text{TcO}_4]^-$  the first milking is discarded. The complete decay scheme for  $^{99}\text{Mo}$  is shown in Figure 1.4.

Figure 1.4 Decay Scheme of  $^{99}\text{Mo}$



$^{99m}\text{Tc}$  also has other chemical and physical properties which make it the radionuclide of choice for imaging. The  $\gamma$  energy (140 keV) is in the ideal range for detection and resolution by scintillation cameras, and the half life (6.0 h), although long enough for chemical manipulation, is short enough that mCi amounts can be administered to the patient while minimizing the radiation exposure. The average radiation dose from a scanning procedure is about equivalent to that of a chest X-ray. The radiation exposure to the patient is also kept down by the absence of  $\alpha$  or  $\beta^-$  radiation which would needlessly increase the radiation dose. Another advantage of using  $^{99m}\text{Tc}$  is that it has an isomer:  $^{99}\text{Tc}$ . The long half life ( $t_{1/2} = 2.12 \times 10^5 \text{ y}$ ) and weak  $\beta^-$  emission (292 keV) of  $^{99}\text{Tc}$  mean that it may be handled at the mCi ( $3.70 \times 10^{10} \text{ Bq}$ ) level without special precautions, other than those normally required for contamination control and compliance with legislation relating to radioactive material; whereas  $^{99m}\text{Tc}$  is a short lived  $\gamma$  emitter and a large number of precautions must be taken in the handling of it.

Being isomers, the chemistries of  $^{99}\text{Tc}$  and  $^{99m}\text{Tc}$  are identical and no example has yet been presented where  $^{99}\text{Tc}$  and  $^{99m}\text{Tc}$  differ significantly, ignoring obvious cases such as large differences in concentration, and insufficient tin (II) available for complete reduction of  $^{99}\text{Tc}$  pertechnetate. In theory the chemistry may be worked out with  $^{99}\text{Tc}$  and may then be transferred to  $^{99m}\text{Tc}$ . In practice however, differences arise due to the variation in concentrations at which the reactions are done. Reactions with  $^{99m}\text{Tc}$  are done on the nanomolar scale ( $10^{-8}$  to  $10^{-12} \text{ M}$ ) while reactions with  $^{99}\text{Tc}$  are performed on the millimolar scale ( $10^{-1}$  to  $10^{-4} \text{ M}$ ). Reactions which are second-order in technetium will be very sensitive to total concentration of technetium and as such, differences may arise between the chemistry of the two isomers.

For the reasons already mentioned  $[\text{}^{99m}\text{TcO}_4]^-$  is the preferred starting material for the preparation of radiopharmaceuticals and was chosen as a starting point for the research described herein. The  $[\text{}^{99m}\text{TcO}_4]^-$  obtained from the generator has itself been used for

diagnostic purposes, but its applications are limited. The principal sites of accumulation are the thyroid and salivary glands, as well as the stomach. In addition to thyroid scanning,  $[^{99m}\text{TcO}_4]^-$  has been used for brain scanning since, although  $[^{99m}\text{TcO}_4]^-$  does not penetrate the blood-brain barrier, it does accumulate to some extent in regions where the barrier is disturbed, for example by a tumor.

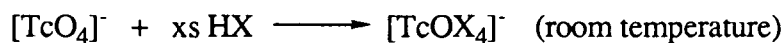
In most medical applications the  $[^{99m}\text{TcO}_4]^-$  will be reduced to a lower oxidation state and bound to a carrier prior to administration. This method for synthesis of technetium complexes may be arbitrarily categorized as the "reduction" route and is displayed as Scheme 1. The reaction generally produces a mixture of reduced technetium complexes and in most cases the chemical form and oxidation state of the components of this mixture are unknown. A variety of reducing agents have been used in this reaction, and these include: concentrated HX, Sn (II), Ti (III), Cu (I), Fe (II),  $\text{Sn}^0$  or  $\text{Zr}^0$  electrodes,  $\text{SCN}^-$ ,  $\text{BH}_4^-$ ,  $\text{S}_2\text{O}_3^{2-}$ ,  $\text{H}_3\text{PO}_2$ ,  $\text{H}_2\text{NNH}_2$ ,  $\text{H}_2\text{NOH}$ , formamidine sulfinic acid and dithiothriitol. Commercial "kits" generally use Sn (II) as the reductant, and this leads to several problems associated with the chemistry of tin and with the fact that Sn (IV) and Tc (IV) are physically very similar.

#### Scheme 1 Reduction Route

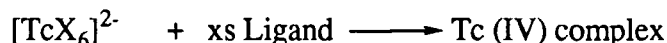


The alternate route to synthesis of technetium complexes is the "substitution" route which is displayed as Scheme 2. This route is a mainstay in the synthesis of macroscopic amounts of Tc (V) and Tc (IV) complexes because of the availability of the starting materials  $[\text{TcOX}_4]^-$  ( $\text{X} = \text{F}, \text{Cl}$ ) and  $[\text{TcX}_6]^{2-}$  ( $\text{X} = \text{Cl}, \text{Br}, \text{I}$ ). However, this route has

## Scheme 2 Substitution Route

Initial preparation of  $[\text{TcOX}_4]^-$  or  $[\text{TcX}_6]^{2-}$ 

Followed by the addition of ligand



not yet been generally applied to the synthesis of  $^{99\text{m}}\text{Tc}$  radiopharmaceuticals because of the difficulty in producing pure  $[\text{99mTcOX}_4]^-$  and  $[\text{99mTcX}_6]^{2-}$  intermediates within a reasonable time. Nevertheless, due to the inherent advantage of this route, (i.e., a known oxidation state for the resulting complex) it would be a desirable route for synthesis of technetium complexes. Now with the widespread use of HPLC (high pressure/performance liquid chromatography) the substitution route may become more widely used for the synthesis of radiopharmaceuticals. When one is using the tetrabutylammonium salt, substitutions onto  $[\text{TcOX}_4]^-$  are usually conducted in organic solvents to prevent hydrolytic disproportionation of the starting material. The  $d^2$  centre is fairly labile and these reactions generally proceed rapidly under mild conditions yielding five-, six-, or seven-coordinate complexes in which the  $\text{TcO}^{3+}$  core remains intact. Substitutions onto  $[\text{TcX}_6]^{2-}$  are also often conducted in organic solvents, the tetrabutylammonium salts being used to provide sufficient solubility. Under anhydrous conditions, this octahedral  $d^3$  centre appears to be substitution inert and forcing reaction conditions must be used to attain a reasonable rate of reaction.

Another possible solution to the problem of obtaining pure  $[^{99m}\text{TcOX}_4]^-$  or  $[^{99m}\text{TcX}_6]^{2-}$ , is the use of different substrates for the substitution reactions, such as  $^{99m}\text{Tc}$ -glucoheptonate,  $^{99m}\text{Tc}$ -gluconate or  $^{99m}\text{Tc}$ -citrate.

As a result of the rapid search for new and better  $^{99m}\text{Tc}$  radiopharmaceuticals the chemistry of technetium has developed rapidly. The most convenient and stable starting materials for the study of technetium compounds are the salts of the pertechnetate ion  $[\text{TcO}_4]^-$ . For this reason Tc (VII) is considered the most important oxidation state of technetium. Pertechnetate, an oxoanion of Tc (VII), is a more powerful oxidizing agent than is its isoelectronic molybdenum (VI) species  $[\text{MoO}_4]^{2-}$ . Its aqueous chemistry is dominated by the driving force for reduction of pertechnetate to the stable oxide  $\text{TcO}_2 \cdot n\text{H}_2\text{O}$ . For example, with aqueous  $\text{Na}_2\text{S}_2\text{O}_4$  the brown-black insoluble technetium (IV) compound  $\text{TcO}_2 \cdot n\text{H}_2\text{O}$  is readily produced. When  $[\text{TcO}_4]^-$  is reduced, the final technetium product depends upon the nature of the reducing agent, the ligands employed and the conditions of the reaction. Other known Tc (VII) compounds are the yellow heptoxide  $\text{Tc}_2\text{O}_7$ , the black heptasulfide  $\text{Tc}_2\text{S}_7$  and the oxohalides  $\text{TcO}_3\text{F}^4$  and  $\text{TcO}_3\text{Cl}^5$ .

Only a few compounds of Tc (VI) are known. The halide  $\text{TcF}_6$  and the oxohalides  $\text{TcOF}_4$  and  $\text{TcOCl}_4$  have been reported.<sup>6, 7, 5</sup> The isolation of  $\text{TcCl}_6$  has been reported but is under dispute.<sup>5</sup> Electrochemical reduction of  $[\text{TcO}_4]^-$  in acetonitrile solution containing tetramethylammonium salts yields violet crystals of  $[(\text{CH}_3)_4\text{N}]_2[\text{TcO}_4]$ .<sup>8</sup> Electrochemical evidence also exists for the transient formation of  $[\text{TcO}_4]^{2-}$  from pertechnetate in aqueous alkaline media.<sup>9</sup>

A relatively large number of Tc (V) complexes have been recently prepared and characterized by X-ray diffraction methods. Technetium (V) complexes can be considered as derived from a two-electron reduction of pertechnetate with the partial elimination of oxygen atoms. Technetium (V) has a  $d^2$  electronic configuration and is diamagnetic or

slightly paramagnetic. The magnetic properties arise from the orbital distortion induced by the polar Tc-X group (X = O, N or S). The presence of at least one oxo group around technetium is characteristic of Tc (V) cores while the geometry of the complexes depends on the nature of the other ligands.  $\text{TcO}^{3+}$ ,  $\text{TcO}_2^+$  and  $\text{Tc}_2\text{O}_3^{4+}$  cores are very common in five-, six-, or seven-coordinate compounds. The oxotechnetium (V) species may be stabilized by a large variety of ligands, mostly bidentate, tridentate, tetradentate, or pentadentate ligands and can have O, N, S, As, or P donor atoms.

Ligands with exclusively sulphur donor atoms tend to lead to five-coordinate complexes with  $\text{TcO}^{3+}$  cores. OS (eg. mercaptoethanol) or OO (eg. ethyleneglycol) donor ligands also tend to form analogous five-coordinate complexes with  $\text{TcO}^{3+}$  cores. Occasionally a sixth ligand binds *trans* to the oxo group and it is usually a phenolic, alcoholic, or hydroxy oxygen, or sometimes a halogen or  $\mu$ -oxo bridging two technetium centres. The sixth group is weakly bonded (the *trans* influence) if it is a monodentate ligand, whereas it is relatively stable when it is part of a polydentate ligand. In technetium (V) oxo complexes the stretching vibration of the Tc=O bond in the IR spectrum falls between 890-1020  $\text{cm}^{-1}$ , and is determined by the ligands in the equatorial plane and by the nature of the sixth ligand *trans* to Tc=O.

In complexes containing N-donor ligands such as pyridine, imidazole, ethylenediamine, 1,2-diaminopropane and cyclam, or even diarsines and diphosphines, two *trans*-oxo groups remain in the complex giving the  $\text{TcO}_2^+$  core.<sup>10</sup> The coordination of the second oxygen is necessary to alleviate the electron deficiency around the technetium centre and occurs with ligands that do not generate enough electron density. As a second oxygen is now coordinated *trans* to Tc=O, the Tc=O stretching vibration is at 790-834  $\text{cm}^{-1}$  for  $\text{TcO}_2^+$  complexes.

Under certain conditions the oxo can be replaced by a nitrogen or sulphur atom. Reduction of pertechnetate with hydrazine or substituted hydrazines in the presence of an

appropriate ligand leads to the formation of technetium nitrido complexes.  $\text{TcN}^{2+}$  is a very stable core and a variety of five- and six-coordinate complexes with various ligands including amines, phosphines, cyclam and aminophosphines are known.<sup>11</sup> The TcN stretching vibration in the IR spectrum is reported at 1050-1070  $\text{cm}^{-1}$ . The structures were determined crystallographically, and generally exhibit a square pyramidal configuration for five-coordinate species and a pseudo-octahedral geometry for six-coordinate complexes. The  $\text{TcS}^{3+}$  core is less common and to date only one example is known:  $[\text{TcS}(\text{HBPz}_3)\text{Cl}_2]$  ( $\text{HBPz}_3$  = hydrotris(1-pyrazolyl)borato) prepared from the known oxo analogue by reaction with  $\text{B}_2\text{S}_3$ .<sup>11</sup>

The first technetium (IV) product discovered was the very insoluble black oxide  $\text{TcO}_2 \cdot n\text{H}_2\text{O}$ . While freshly prepared  $\text{TcO}_2 \cdot n\text{H}_2\text{O}$  is occasionally used as a starting material for the preparation of other Tc(IV) complexes,<sup>12, 13</sup> the hexahalo-dianions  $[\text{TcX}_6]^{2-}$  ( $\text{X} = \text{Cl}, \text{Br}$  or  $\text{I}$ ) are more commonly used.<sup>14</sup> The chloro and bromo complexes are readily synthesized by the reduction of  $[\text{TcO}_4]^-$  in hot solutions of the corresponding hydrohalic acid, whereas the iodo complex is prepared by the treatment of the chloro or bromo species with hot HI.<sup>15</sup>

Technetium (IV) complexes with phosphate or phosphonate ligands are of particular interest since these species represent an important class of bone-imaging radiopharmaceuticals.<sup>16</sup> However, relatively few technetium (IV) complexes have been used as radiopharmaceuticals. Technetium (IV) is an intermediate oxidation state and has been less completely studied because it generally undergoes kinetically fast reactions in which this oxidation state is passed by (or through). Technetium (V) is reduced by a two electron process and goes directly to technetium (III) in many cases.

Technetium (III) is one of the more accessible oxidation states and has been shown to complex with a variety of ligands in several coordination geometries. In general the trivalent state of technetium appears to require the presence of good  $\pi$  acceptor ligands such

as triphenylphosphine, a diarsine, or carbon monoxide for stabilization. The series of complexes  $[\text{TcL}_2\text{X}_2]^+$  ( $\text{L}$  = a diphosphine or diarsine, and  $\text{X}$  = Cl or Br) have been synthesized by allowing the appropriate ligand to react with  $[\text{TcX}_6]^{2-}$  in acidic-ethanol water mixtures. Pertechnetate can also be used as the starting material when phosphine ligands, which serve as both the reductant and the chelating agent, are employed.<sup>17</sup> Technetium (III) species in solution have also been prepared by the reduction of  $[\text{TcO}_4]^-$  with  $\text{SnCl}_2$  in the presence of polydentate organic ligands such as citrate or DTPA.<sup>18, 19</sup>

Seven-coordinate complexes are also becoming more common following the preparation of  $[\text{Tc}(\text{CO})\text{Cl}_3(\text{Me}_2\text{PhP})_3]$  where the carbonyl resides in the center of the three phosphine groups forming a face-capped octahedron.<sup>20</sup> The seven-coordinate species is only attained easily when the ligands are small enough.

Lipophilic Tc(III) complexes with iminodiacetic acid derivatives are readily extracted by the liver and constitute an important class of hepatobiliary imaging agents.<sup>21, 22</sup>

Compounds of the type  $[\text{TcX}_2\text{L}_2]$  ( $\text{L}$  = diphos or diars,  $\text{X}$  = Cl, Br or I), the Tc (II) analogues of the Tc (III) compounds noted above, were the first Tc (II) compounds isolated.<sup>23, 24</sup> Complexes of the type  $[\text{TcX}_2(\text{PPh}(\text{OEt})_2)_4]$  react with carbon monoxide at atmospheric pressure to give *cis*- and *trans*-dicarbonyl isomers by replacement of the halides.<sup>25</sup> The compound  $[\text{n-Bu}_4\text{N}][\text{Tc}(\text{NO})\text{Br}_4]$  can be prepared in high yield by the reaction of nitric oxide with freshly precipitated  $\text{TcO}_2 \cdot \text{nH}_2\text{O}$  in 4M HBr,<sup>12</sup> and has been used to prepare compounds such as  $[\text{n-Bu}_4\text{N}][\text{Tc}(\text{NO})\text{Cl}_4]$  and  $[\text{n-Bu}_4\text{N}]_2[\text{Tc}(\text{NO})(\text{NCS})_5]$ . Subsequently  $[\text{n-Bu}_4\text{N}]_2[\text{Tc}(\text{NO})(\text{NCS})_5]$  can be reduced with hydrazine to yield the analogous Tc (I) species. An organometallic compound, the cyclopentadienyl Tc(II) dimer  $[\text{Tc}(\text{C}_5\text{H}_5)]_2$ , has also been reported.<sup>26</sup>

The low oxidation state Tc (I) can be stabilized by strong  $\pi$ -back bonding ligands such as carbon monoxide, cyanide and aromatic hydrocarbons. Examples are  $[\text{Tc}(\text{CO})_5\text{X}]$

(X = Cl, Br or I)<sup>27</sup>; the large group of compounds of the type  $[\text{Tc}(\text{CO})_3\text{L}_2\text{Cl}]$  (L =  $\text{PPh}_3$ ,  $\text{AsPh}_3$ ,  $\text{SbPh}_3$ , pyridine, isonitrile), and the dithiocarbamates  $[\text{Tc}(\text{CO})_4(\text{S}_2\text{CNR}_2)]$  (R = Me, Et)<sup>28</sup> have been described, as well as many others. Most of these complexes have octahedral geometry, sometimes distorted.

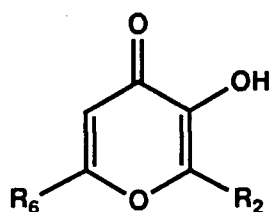
Representatives of Tc (0) are the carbonyls  $[\text{Tc}_2(\text{CO})_{10}]$  and  $[\text{TcRe}(\text{CO})_{10}]$ , which have octahedral geometries.<sup>29, 30</sup>

Species of Tc (-I) are obtained by reduction of  $[\text{NH}_4][\text{TcO}_4]$  with potassium in ethylenediamine.<sup>31</sup> The (-I) oxidation state is stabilized by carbonyl ligands as in  $[\text{Na}][\text{Tc}(\text{CO})_5]$ , prepared by the reduction of  $[\text{Tc}_2(\text{CO})_{10}]$  in tetrahydrofuran with sodium amalgam.<sup>27</sup>

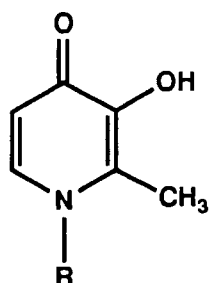
The goal of this work was to synthesize and characterize several complexes of technetium and to investigate their viability as imaging agents. In particular, we were looking for potential brain and heart imaging agents. In searching for a brain imaging agent, constraints on size, lipophilicity, and charge must be considered. The brain is separated from the circulatory system by the blood-brain barrier (BBB) which is the most selective barrier in the body. We therefore focused on ligands that would form low molecular weight complexes which would be neutral or mono-cationic, water soluble, reasonably lipophilic, and easily functionalized. There is also a need for thermodynamic stability to maintain the integrity of the complex *in vivo* in order to direct the radionuclide to a target organ. A heart imaging agent, on the other hand, would require different properties. With a ligand that can be easily functionalized, one can vary the R groups on the ligand to achieve a desired characteristic.

The ligands chosen for this work were the 3-hydroxy-4-pyrones and the 3-hydroxy-4-pyridinones which are shown in Figure 1.5 and which have been studied extensively by our group.

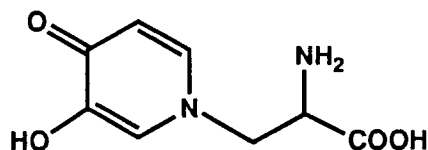
Figure 1.5 Substituted 3-hydroxy-4-pyrones and  
3-hydroxy-2-methyl-4-pyridinones.



$R_2 = \text{CH}_3, R_6 = \text{H}$  Maltol  
 $R_2 = \text{H}, R_6 = \text{CH}_2\text{OH}$  Kojic acid



$R = \text{H}$  Hmpp  
 $R = \text{CH}_3$  Hdpp  
 $R = (\text{CH}_2)_5 \text{CH}_3$  Hmhpp  
 $R = (\text{CH}_2)_{10} \text{COOH}$  Hmupp



Mimosine

More emphasis was placed on the 3-hydroxy-2-methyl-4-pyridinones as a large number of different amines may be used in synthesis of this type of compound allowing the R group on the ring nitrogen to be altered easily, whereas the cyclic ether oxygen in 4-pyrones may not be functionalized with different R groups. The 3-hydroxy-4-pyridinones are also stronger bases as indicated by the second  $\text{pK}_a$  of the hydroxyl group (Hmpp  $\text{pK}_a = 9.80$ ; maltol  $\text{pK}_a = 8.42$ ) and this should result in more stable complexes.

In addition to the development of  $^{99\text{m}}\text{Tc}$  labelled radiopharmaceutical imaging agents the development of  $^{67}\text{Ga}$  labelled radiopharmaceutical imaging agents was also being investigated in our group. Our interest in  $^{67}\text{Ga}$  labelled radiopharmaceutical imaging

agents stemmed from the study of the aqueous coordination chemistry of aluminum *in vitro* and the desire to study the *in vivo* chemistry of aluminum. Aluminum has no suitable isotopes for radiolabelling studies and  $^{67}\text{Ga}$  is the radionuclide that was chosen for these imaging experiments. Despite the differences in electronic configuration and ionic radius, the aqueous coordination chemistry of Al and Ga is very similar. They are only found in the +3 oxidation state in water and their aqueous chemistry is dominated by their shared property of strong Lewis acidity.<sup>37</sup> The similarity of *in vitro* aqueous behavior makes  $^{67}\text{Ga}$  the best model available for Al.

As part of a continuing project to detail the coordination chemistry of gallium as it pertains to the role played by radioactive isotopes in the diagnosis of disease, we have been studying their tris(ligand) complexes containing certain bidentate monobasic ligands.<sup>32-36</sup> These  $^{67}\text{Ga}$  biodistribution experiments can be considered first order approximations of the biological fate of the Al analogues.

The chemistry of gallium is developing rapidly because of the utility of  $^{67}\text{Ga}$  ( $t_{1/2} = 78.1$  hr;  $\gamma = 93.3, 185, 300$  keV) and  $^{68}\text{Ga}$  ( $t_{1/2} = 68.3$  min;  $\gamma = 511$  keV from  $\beta^+$  annihilation) in the field of diagnostic nuclear medicine,<sup>38-47</sup> and because of the antitumor activity of gallium nitrate.<sup>48</sup>

A pertinent example of the application of basic coordination chemistry to Ga imaging is 8-hydroxyquinoline (oxine) which has been chelated to  $^{68}\text{Ga}$  in radiopharmaceutically active tris(ligand) complexes.<sup>40, 49, 50</sup> This bidentate ligand has high formation constants for  $\text{Ga}^{2+}$  and can be used in the labelling of red blood cells, leukocytes, and blood platelets.<sup>39, 40, 49-51</sup> The tris(oxinato) complexes are neutral and lipophilic, and cross cell membranes easily. Labelling must be done *in vitro* to avoid transferrin competition. Subsequently, the labelled blood cells are then returned *in vivo* for the scanning procedure. Tropolone, acetylacetone, and 2-mercaptopyridine-N-oxide have also been investigated as alternatives in the same transport system.<sup>50, 52</sup>



*vitro* by solution potentiometry and *in vivo* by biodistribution studies in mice and a rabbit.

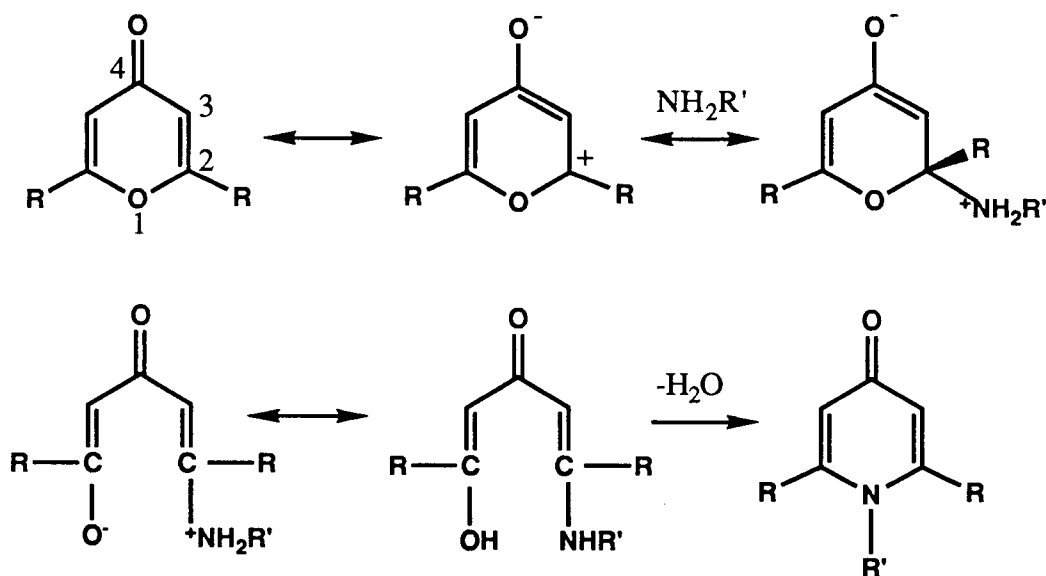
Dr. D. Clevette conducted the potentiometric studies of the gallium 3-oxy-4-pyridinone complexes, while I investigated their biodistributions in mice and a rabbit.

## CHAPTER II SYNTHESIS AND CHARACTERIZATION OF 3-HYDROXY-4-PYRIDINONE LIGANDS

### 2.1 Introduction

The simplest method for the synthesis of 3-hydroxy-4-pyridinone ligands is ring substitution of an analogous pyrone. One of the oldest known ring conversions involves the ammonolysis and aminolysis of the cyclic ether 4-pyrone. The accepted mechanism (Figure 2.1) is nucleophilic attack by a primary amine followed by ring opening, loss of water, and ring closure to give the corresponding 4-pyridinone.<sup>58</sup>

Figure 2.1 Mechanism for the conversion of 4-pyrones to 4-pyridinones



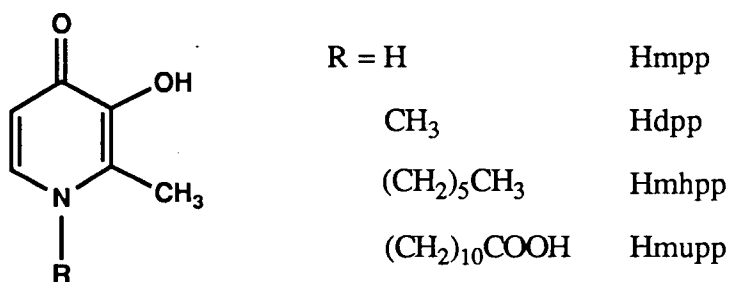
There is no direct proof offered for this mechanism but molecular orbital calculations indicate a higher probability of nucleophilic attack at position 2.<sup>59</sup> Further indirect evidence is the effect of ring substituents on the conversion reaction. Electron-

withdrawing groups enhance reactivity while electron-donating groups decrease reactivity.<sup>60</sup>

Maltol (3-hydroxy-2-methyl-4-pyrone) has been used as a precursor to N-substituted-3-hydroxy-2-methyl-4-pyridinones in our lab and a variety of 3-hydroxy-2-methyl-4-pyridinones have been synthesized by preparations reported in the literature<sup>61, 63</sup> and modifications of these worked out by W. O. Nelson.<sup>63</sup>

The 3-hydroxy-2-methyl-4-pyridinones were synthesized from maltol and the following primary amines: ammonia, methylamine, n-hexylamine and 11-aminoundecanoic acid. The structures of the ligands synthesized are shown in Figure 2.2.

Figure 2.2 3-hydroxy-2-methyl-4-pyridinone ligands



## 2.2 Materials and Methods

All chemicals were reagent grade or better and were used without further purification. The reactions were monitored by thin layer chromatography (TLC) on silica plates with 10% methanol in chloroform as the eluting solvent or on cellulose plates with 50% methanol in water as the eluting solvent. Ninhydrin was used for visualization of the non-ultra-violet (UV) active species. The quoted yields, unless otherwise stated, are for

purified product based on maltol. The melting points were measured on a Mel-Temp apparatus and are uncorrected.

Maltol, n-hexylamine, and 11-aminoundecanoic acid were obtained from Sigma Chemical Company and were used without further purification. Hmpp was prepared by Method B according to W. O. Nelson<sup>63</sup> this is a simplification of the method developed by Harris.<sup>61</sup> Further changes were made in the recrystallization technique, giving a better yield. The synthesis of Hdpp from maltol has been reported by Kontoghiorghes<sup>62</sup> and this method was used in the preparation of Hdpp with minor changes. Hmhpp and Hmupp were prepared in a similar manner to that of Hdpp; however, it was found necessary to control the pH throughout the course of the reactions and also to develop an individual purification method for each ligand.

2.2.1 3-hydroxy-2-methyl-4(1H)-pyridinone, Hmpp. To a chilled solution of maltol (5.06 g, 40.2 mmol) in 60 mL of water was added 8.0 mL of concentrated NH<sub>4</sub>OH (120 mmol) followed by 10.0 mL of 6N HCl; the latter was added dropwise. The pH was adjusted to 9.3 with 1N NaOH and the solution was heated at 60°C for 36 hours under a nitrogen atmosphere. During the reaction the pH was monitored and adjusted to 9.3 when necessary. Concentration in vacuo and cooling to 10°C for 24 hours gave 3.52 g of crystalline product. Recrystallization was achieved by dissolving into a minimum amount of acidic water and then raising the pH to 7.5 which gave 3.03 g of a pink solid (60% yield).

2.2.2 3-hydroxy-1,2-dimethyl-4-pyridinone, Hdpp. To a solution of maltol (10.0 g, 79.4 mmol) in 200 mL of water three equivalents (239.8 mmol) of 40% aqueous methyl amine were added and the resulting solution was refluxed for 8.0 hours. Decolourizing carbon was added and the mixture was stirred for 0.5 hours. The suspension was filtered

and the dark brown filtrate was evaporated in vacuo to give a brown solid. Recrystallization from hot water gave 6.91 g of fine white needles (45% yield).

2.2.3 3-hydroxy-2-methyl-1-hexyl-4-pyridinone, Hmhpp. Maltol (7.1 g, 56.3 mmol) was added to 100 mL of water and three equivalents (168.3 mmol) of n-hexylamine were added. The pH was adjusted to 9.3 with 1 N NaOH and the solution was heated at 60°C under a nitrogen atmosphere for 72 hours. During the course of the reaction the pH was monitored and adjusted to 9.3 when necessary. The product was extracted with methylene chloride (5 x 20 mL), decolorizing charcoal was added to the organic layer and the resulting mixture was stirred for 0.5 hours. The dark brown filtrate was reduced in volume under vacuum to give an oil. The product was then extracted into hot water, the water was removed in vacuo and the white solid was washed with diethyl ether. Recrystallization from hot water gave 2.12 g of a white solid (18% yield).

2.2.4 3-hydroxy-2-methyl-1-undecanato-4-pyridinone, Hmupp. To a solution of maltol (2.02 g, 16.0 mmol) in 80 mL water and 30 mL ethanol four equivalents of 11-aminoundecanoic acid (63.5 mmol) were added. The resulting mixture was adjusted to pH 9.35 with 1 N NaOH and was refluxed under a nitrogen atmosphere for 48 hours. During the course of the reaction the pH was monitored and adjusted to 9.3 when necessary. The solvent was removed in vacuo leaving a brown solid. The solid was dissolved in a minimum amount of methanol; this solution was filtered and chromatographed on a silica column with 10% methanol in methylene chloride as the eluent. The fractions were collected and evaporated leaving an off-white solid. Recrystallization from acidic water by raising the pH to 10 gave 0.90 g of solid (18% yield).

## 2.3 Characterization of the 3-hydroxy-4-pyridinone ligands.

Hmpp, Hdpp, and Hmhpp have all been previously characterized and reported. Characterization of these ligands was performed only to check the purity before further reactions were done. Hmupp, 3-hydroxy-2-methyl-1-undecanato-4-pyridinone, is a new compound and characterization will be reported.

Hmupp was characterized by elemental analysis, infrared (IR), proton NMR, and UV/Visible spectroscopy, and electron impact mass spectrometry (EI-MS). The elemental analyses (C, H, N) were performed by Mr. Peter Borda of the UBC Microanalytical Laboratory. The IR spectra were recorded with a BOMEM MB-100 FTIR in the range 4000-300  $\text{cm}^{-1}$ . All samples were prepared as KBr disks and spectra were referenced to polystyrene film. The proton NMR spectra were recorded with Bruker WP-80 and WP-400 instruments. The 80 MHz spectra and the 400 MHz spectra were graciously run by Zaihui Zhang of our laboratory. The UV/Visible spectra were run on a Shimadzu UV/2100 spectrophotometer. The EI-MS were performed on a Kratos MS 50 spectrometer and all mass spectra were supplied by the UBC Mass Spectrometry Service.

### 2.3.1 Elemental analysis

Upon failure to recrystallize or sublime Hmupp, prior to submission for analysis the sample was purified by column chromatography with 10% methanol in methylene chloride as the eluent. The sample was then dried under vacuum. The results of the elemental analysis are found in Table 2.1. Probable water content would explain the slightly low carbon number.

Table 2.1 Hmupp Elemental Analysis (Found/[calculated])

Ligand	% C	% H	% N
Hmupp	65.54 [66.00]	8.74 [8.80]	4.46 [4.53]

### 2.3.2 Infrared Spectroscopy

Table 2.2 Selected infrared absorption bands ( $\text{cm}^{-1}$ ) for Hmupp.  
All bands are strong except where noted.

Assignment	Wave number
$\nu_{\text{OH}}$	3361 b
$\nu_{\text{CH}}$ aliphatic	2924, 2854
$\nu_{\text{C=O}}$ carboxylic	1692 m
$\nu_{\text{C=O}}$ ketonic	1637
$\nu_{\text{ring}}$	1564, 1515, 1480
	1445 w

(abbreviations: b = broad, w = weak, m = medium)

Of the spectroscopic techniques used in the study of these compounds, IR is the most useful as it gives quick confirmation of the outcome of the conversion reaction. There are typically four ring stretching modes between  $1650$  and  $1400 \text{ cm}^{-1}$ , and the pattern changes predictably when the ring oxygen is replaced by a nitrogen. By examination of the IR spectrum one can readily confirm the transformation of maltol

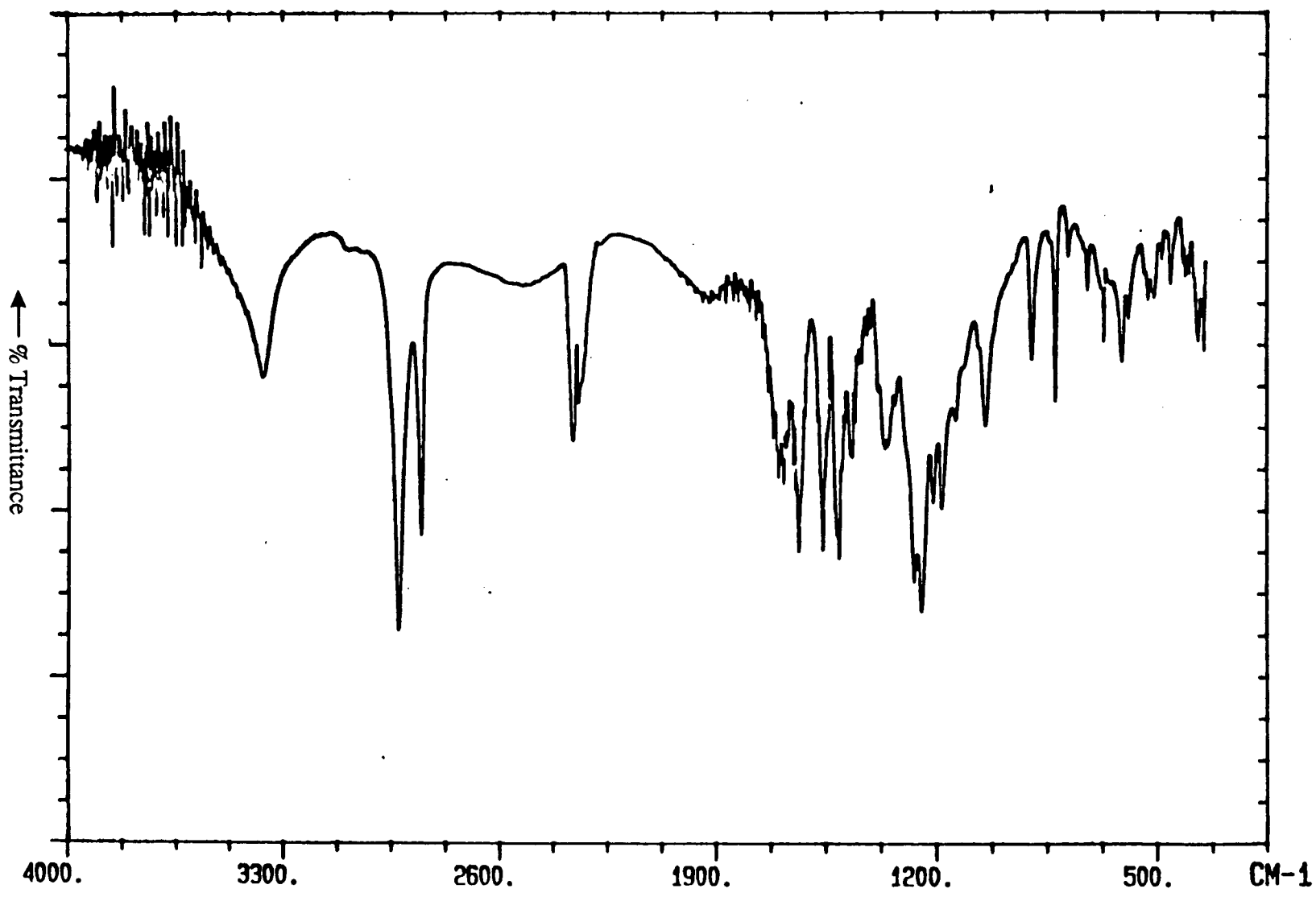
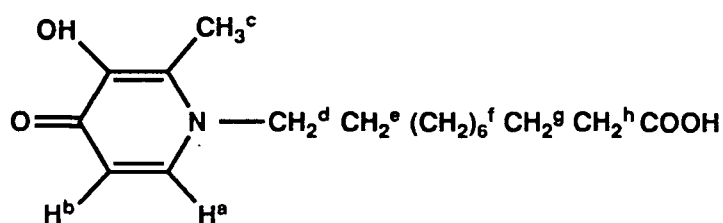


Figure 2.3 Infrared spectrum of Hmupp

to the corresponding 3-hydroxy-4-pyridinone. It is impossible to separate the assignments of  $\nu_{\text{C=O}}$  and the higher  $\nu_{\text{ring}}$  stretches in any of the compounds as the bands are extensively coupled; however, tentative assignments of the IR bands were made by reference to Bellamy.<sup>64</sup> The IR spectrum of Hmupp from 4000 to 350  $\text{cm}^{-1}$  is reproduced as Figure 2.3. The spectral assignments for Hmupp are given in Table 2.2.

### 2.3.3 Proton NMR Spectroscopy

Table 2.3 Proton NMR chemical shift ( $\delta$ ) data for Hmupp at 400 MHz (ppm).



Assignments	Chemical Shift (ppm)
H <sup>a</sup> (d)	7.35
H <sup>b</sup> (d)	6.60
CH <sub>3</sub> <sup>c</sup> (s)	2.47
CH <sub>2</sub> <sup>d</sup> (t)	3.98
CH <sub>2</sub> <sup>e</sup> (m)	1.79
(CH <sub>2</sub> ) <sub>6</sub> <sup>f</sup> (m)	1.33
CH <sub>2</sub> <sup>g</sup> (m)	1.67
CH <sub>2</sub> <sup>h</sup> (t)	2.40

(abbreviations: s = singlet, d = doublet, t = triplet, m = multiplet)

The spectrum of Hmupp was recorded in  $\text{CDCl}_3$  with an internal lock to tetramethylsilane (TMS). The chemical shifts listed in Table 2.3 were recorded at 400 MHz.

The spectrum has AB doublets for the ring protons ( $J_{ab}$  of 7 to 8 Hz), a singlet for the ring methyl group, and a series of signals for the methylene protons on the undecanoic acid group. The signal for the protons on the carbon directly attached to the ring nitrogen is shifted downfield from that of the ring methyl. This is due to deshielding by the electronegative nitrogen. This is also the reason for assigning the lowfield doublet to  $\text{H}^a$ . The methylene group directly attached to the carboxylic acid group is also shifted downfield due to deshielding by the electronegative carboxylic acid group. No attempt was made to resolve the other methylene protons on the undecanoic R group on Hmupp. Assignments are given in Table 2.3.

#### 2.3.4 Electron Impact Mass Spectrometry

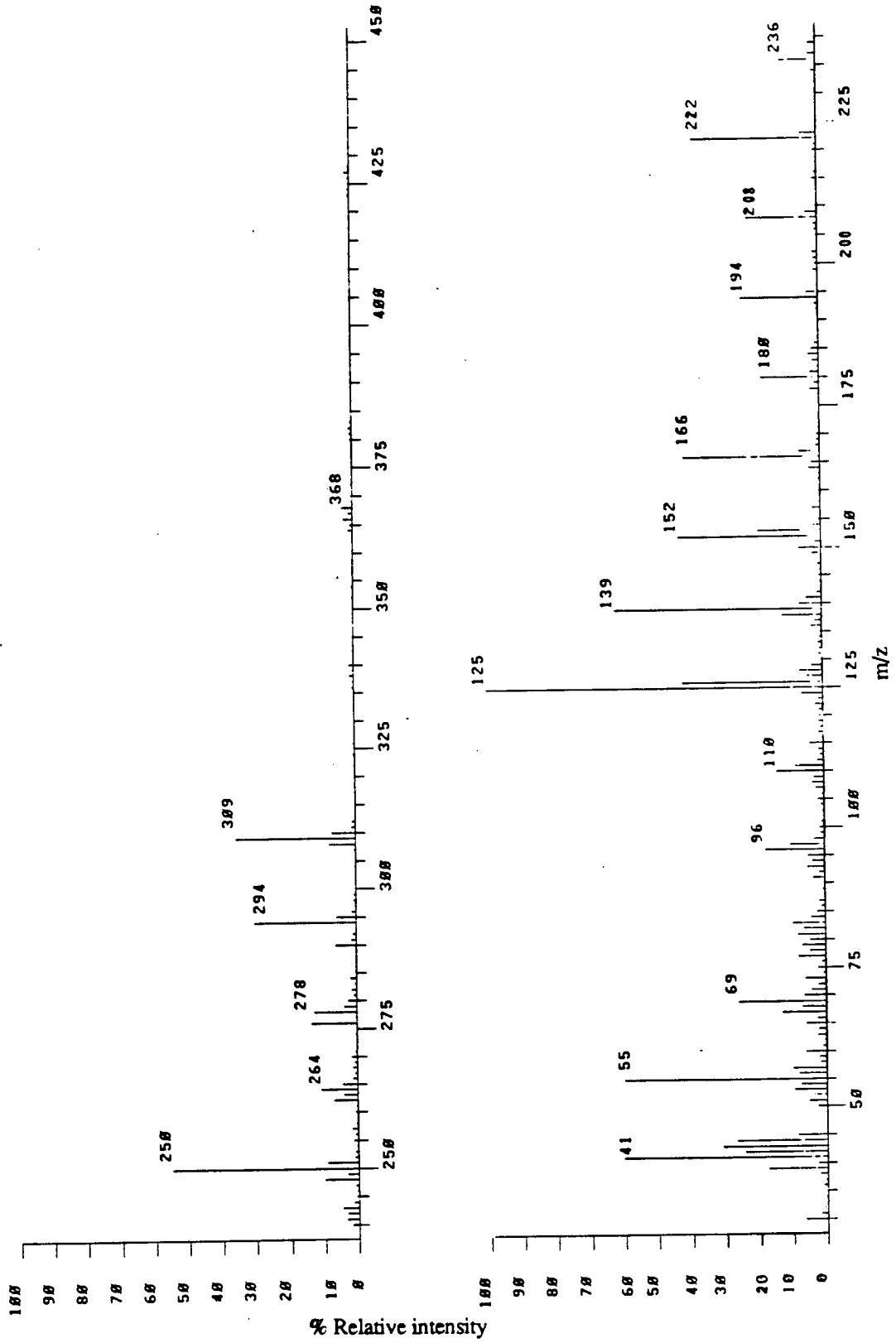
The molecular ions, base peaks, and selected fragment ions for Hmupp are listed in Table 2.4 and the mass spectrum is reproduced as Figure 2.4.

Table 2.4 Mass spectral data ( $m/z$ ) with the percent relative intensity in parentheses.

Ligand	$\text{M}^+$	Fragment Peaks
Hmupp	309 (34.9)	294 (29.5) 250 (54.8) 236 (11.1) 222 (37.3) 208 (21.3) 194 (23.1) 180 (17.6) 166 (40.8) 152 (42.1) 139 (61.7) 125 *

\* Base peak (relative intensity = 100 %).

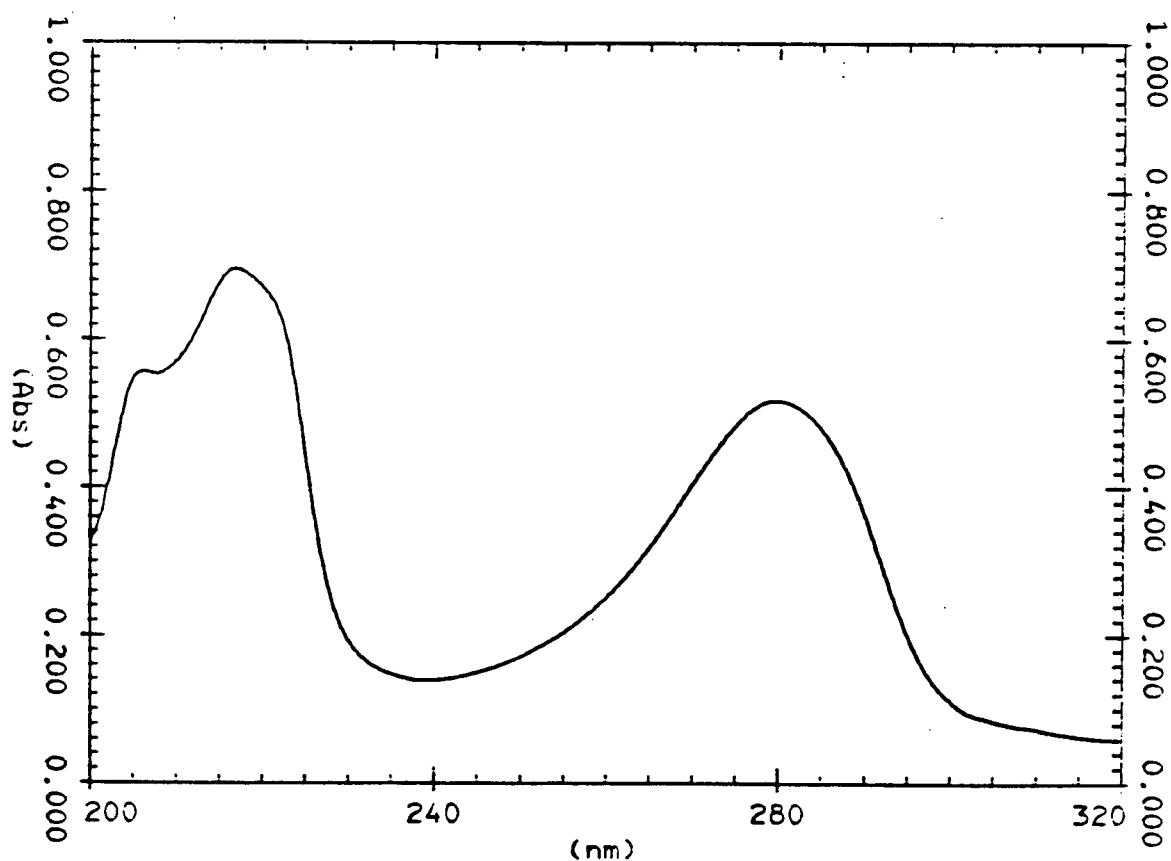
Figure 2.4 EI-MS spectrum of Hmupp



The molecular radical cation ( $M^{\cdot+}$ ) is present in the spectrum and can be attributed to the ability of the ring nitrogen to localize positive charge. The  $m/z$  294 peak is due to loss of a  $CH_3$  group. Loss of  $CH_2COOH$  gives the  $m/z$  250 peak which then fragments by successive loss of the other 9  $CH_2$  groups. Hmupp can also fragment by cleavage of the exocyclic N-C bond with hydrogen migration to give the ring molecular cation  $m/z$  125. This dihydroxypyridinium moiety is known to be favoured in the gas phase<sup>65</sup> and therefore it is not surprising that it is the base peak.

### 2.3.5 Ultraviolet Spectroscopy

Figure 2.5 UV Spectrum of Hmupp



The ultraviolet spectra of pyridine and its derivatives are similar to that of benzene; above 210 nm they have E (ethylinic) and B (benzoic) bands that originate from  $\pi \rightarrow \pi^*$  transitions.<sup>65</sup> There is also a weak  $n \rightarrow \pi^*$  transition (R-band) that is generally only observable in the vapor phase. The B band in pyridine lies at 257 nm in water with  $\epsilon_{\max} = 2750 \text{ L mol}^{-1} \text{ cm}^{-1}$ . When pyridine is conjugated or has electron donating substituents attached the band shifts to lower energy.<sup>66</sup> The OH and CH<sub>3</sub> groups also cause bathochromic shifts of 18 and 5 nm respectively. The B band in Hmupp is in good agreement with this and is at  $\lambda_{\max} = 280 \pm 2 \text{ nm}$  ( $\epsilon_{\max} = 1.44 \times 10^4 \text{ L mol}^{-1} \text{ cm}^{-1}$ ) for the B band. The UV spectrum for Hmupp is shown in Figure 2.5.

**CHAPTER III SYNTHESIS OF TECHNETIUM COMPLEXES  
BY THE REDUCTION ROUTE**

**3.1 Introduction**

The conjugate bases of the 3-hydroxy-4-pyridinones are bidentate ligands that can chelate a metal ion via the deprotonated 3-hydroxyl and the carbonyl oxygens. Each ligand which binds to the metal centre forms a five-membered chelate ring. (Figure 3.1) The

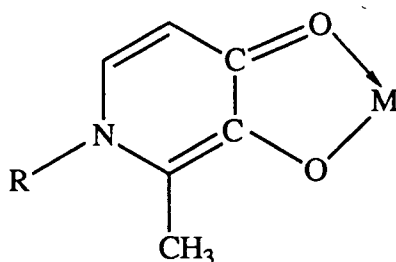


Figure 3.1 Five-membered chelate ring.

geometry of the resulting complex depends on the substrate, the ligand and the method of synthesis chosen. Using pertechnetate [TcO<sub>4</sub>]<sup>-</sup> as the substrate, the 3-hydroxy-4-pyridones and -pyridinones as the ligands, and the reduction route as the method of synthesis, one expects the formation of tris-ligand complexes of neutral or mono-cationic charge. In synthesis of tris-ligand complexes via the reduction route, it is necessary to reduce pertechnetate [TcO<sub>4</sub>]<sup>-</sup> (in which technetium is in the (+7) oxidation state) to a lower oxidation state. The oxidation state of technetium in the final product is dependant on the ligands used. If the ligands have enough back-bonding character, then the final oxidation state of technetium in the tris-ligand technetium complexes will be (+3); if they do not have enough back-bonding character then the final oxidation state of technetium in the tris-ligand technetium complexes will be (+4). In this case the ligands do not possess

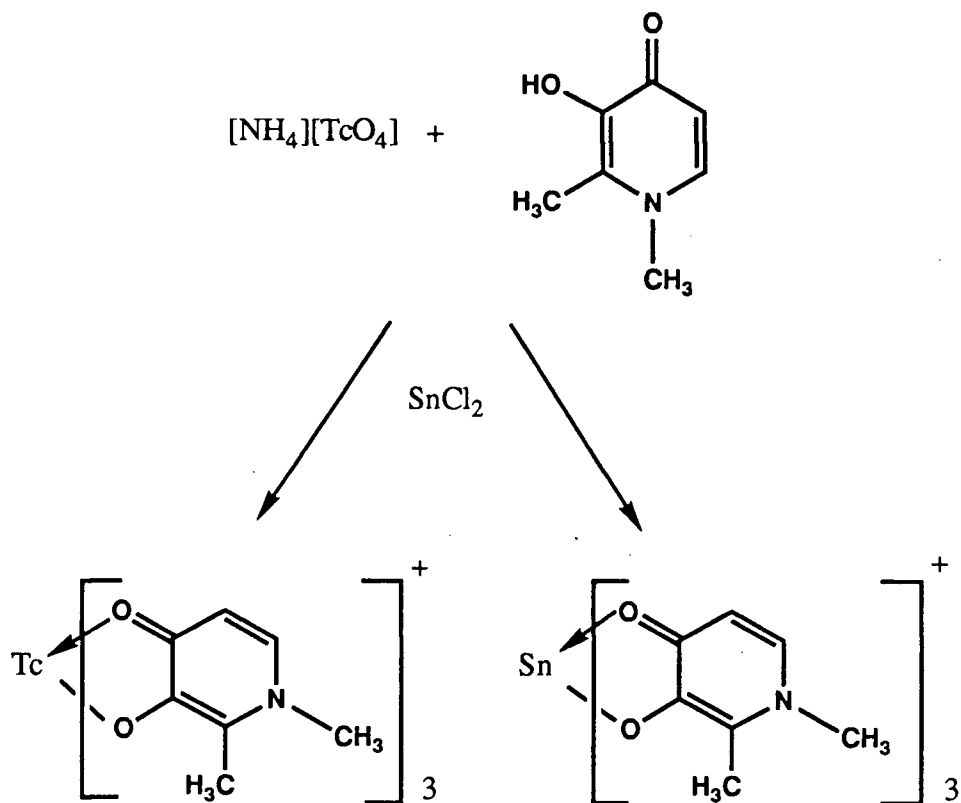
enough back-bonding character and the resulting oxidation state of technetium is (+4); thus the tris-ligand technetium complexes are mono-cationic. The reduction of pertechnetate  $[\text{TcO}_4]^-$  may be done by the addition of a ligand which is itself a reducing agent, or by the addition of a non-reducing ligand and a separate reducing agent. The 3-hydroxy-4-pyrones and the 3-hydroxy-4-pyridinones will not reduce pertechnetate  $[\text{TcO}_4]^-$  and therefore a separate reducing agent must be added.

The choice of a reducing agent can be difficult since it must react rapidly and completely and not interfere with the biodistribution of the resulting technetium complex. Many reducing agents have been examined and evaluated.<sup>67, 68, 69</sup> In general, it has been found that organic reductants tend to work slowly or only at high pH, this promoting hydrolysis and formation of  $\text{TcO}_2 \cdot n\text{H}_2\text{O}$ . Metal ions have the advantage of being fairly rapid reductants, but have been known to be incorporated into the radiopharmaceutical, to hydrolyse, or to precipitate and thereby trap some of the technetium, making them unsuitable for the desired imaging procedure. The most commonly used reducing agent in clinical applications is  $\text{SnCl}_2$ . Several reducing agents were surveyed for the synthesis of technetium complexes by the reduction route.  $\text{SnCl}_2$  was the only reducing agent tried which successfully reduced  $[\text{TcO}_4]^-$  to form tris-ligand technetium complexes. The synthetic method used for the synthesis of the 3-oxy-4-pyronato, and the 3-oxy-4-pyridinonato technetium complexes was the same. The synthetic method for the synthesis of  $[\text{M}(\text{dpp})_3]^+$  ( $\text{M} = \text{Tc}, \text{Sn}$ ) is shown in Figure 3.2.

Tin, which is usually present in much higher concentrations than technetium-99m, may compete with the reduced technetium in complex formation or may be incorporated in the final complex. If tin is incorporated, as is the case for  $[\text{Tc}(\text{DMG})_3(\text{SnCl}_3)\text{OH} \cdot 3\text{H}_2\text{O}]$ , it has been suggested that it can affect biodistribution<sup>70</sup> by enhancing the binding of some technetium complexes to liver or kidney enzymes,<sup>71</sup> and possibly alter membrane

permeability in kidneys.<sup>72</sup> However this formation of mixed complexes seems not to be a general principle, for example [<sup>99</sup>Tc(HIDA)] does not contain tin.<sup>73, 74</sup>

Figure 3.2 Synthesis of  $[M(dpp)_3]^+$  ( $M = Tc, Sn$ ) via the reduction route.



In many cases the final structure and physicochemical state of technetium radiopharmaceuticals are unknown. However, it must be remembered that the aim of administering Tc-labelled pharmaceuticals is to investigate the structure or the function of an organ. Therefore, in the past most work on <sup>99m</sup>Tc-labelled compounds has been done from the point of view of medical practice. At this time this practice is no longer acceptable and structural inferences to biodistribution are being sought out. It is therefore necessary to know the structure of the final complex which is administered.

## 3.2 Materials and Methods

The pertechnetate  $[\text{TcO}_4]^-$  obtained as the  $[\text{NH}_4]^+$  salt was used as supplied by DuPont without further purification; ammonium pertechnetate was initially supplied as a solution and later as a solid. Mimosine was available commercially and was used without further purification. The other ligands were prepared and purified as described in Section 2.2.

### 3.2.1 Reaction of 3-hydroxy-2-methyl-4-pyrone with $[\text{NH}_4][\text{TcO}_4]$ and $\text{SnCl}_2$

Maltol (0.1251 g, 1.0 mmol) and  $\text{SnCl}_2$  (0.0252 g, 0.10 mmol) were dissolved in 50 mL water. To this clear solution  $[\text{NH}_4][\text{TcO}_4]$  (0.10 mmol) was added. Upon addition of the  $[\text{NH}_4][\text{TcO}_4]$ , the clear solution immediately turned dark red. Sodium chloride (1.0 g) was then added and the solution was left to evaporate. The product was extracted with acetonitrile and recrystallized from methanol. The dark red solid was collected by filtration and dried under vacuum.

### 3.2.2 Reaction of 5-hydroxy-2-hydroxymethyl-4-pyrone with $[\text{NH}_4][\text{TcO}_4]$ and $\text{SnCl}_2$

Kojic acid (0.1420 g, 1.0 mmol) and  $\text{Sn(II)Cl}_2$  (0.0251 g, 0.10 mmol) were added to 50 mL water. To this cloudy white solution 0.10 mmol of  $[\text{NH}_4][\text{TcO}_4]$  was added. When  $[\text{NH}_4][\text{TcO}_4]$  was added the cloudy white solution immediately turned clear dark red. Sodium chloride (1.0 g) was added to the dark red solution and this was left to evaporate. The product was extracted with methanol and recrystallized from water. The dark red solid was collected and dried in vacuo.

### 3.2.3 Reaction of 3-hydroxy-2-methyl-4-(1H)-pyridinone with $[\text{NH}_4][\text{TcO}_4]$ and $\text{SnCl}_2$

Hmpp (0.1283 g, 1.0 mmol) and  $\text{Sn(II)Cl}_2$  (0.0250 g, 0.10 mmol) were dissolved in 50 mL water.  $[\text{NH}_4][\text{TcO}_4]$  (0.10 mmol) was then added to the above solution and it instantly turned red. Sodium chloride (1.0 g) was added and the red solution was left to evaporate. The product was extracted and recrystallized with methanol. The red solid was collected by filtration and dried under vacuum.

### 3.2.4 Reaction of 3-hydroxy-1,2-dimethyl-4-pyridinone with $[\text{NH}_4][\text{TcO}_4]$ and $\text{SnCl}_2$

To 50 mL of a 0.5 mg/mL  $\text{Sn(II)Cl}_2$  solution (0.10 mmol) Hdpp (0.1410 g, 1.0 mmol) was added. To this clear solution 0.10 mmol of  $[\text{NH}_4][\text{TcO}_4]$  was added. Upon addition of  $[\text{NH}_4][\text{TcO}_4]$  to the clear solution it immediately turned orange-red. Sodium chloride (1.0 g) was added and the orange-red solution was left to evaporate. The product was extracted with methanol and recrystallized from water. The orange-red solid was collected by filtration and dried in vacuo.

### 3.2.5 Reaction of 3-hydroxy-2-methyl-1-hexyl-4-pyridinone with $[\text{NH}_4][\text{TcO}_4]$ and $\text{SnCl}_2$

Hmhpp (0.0837 g, 1.0 mmol) and  $\text{Sn(II)Cl}_2$  (0.0250 g, 0.10 mmol) were dissolved in 50 mL of a 1:1 methanol water solution.  $[\text{NH}_4][\text{TcO}_4]$  (0.10 mmol) was added to the clear solution which immediately turned red. Sodium chloride (1.0 g) was added and the red solution was left to evaporate. The product was extracted with acetonitrile and recrystallized from methanol. The dark red solid was collected by filtration and dried under vacuum.

### 3.2.6 Reaction of 3-hydroxy-2-methyl-1-undecanoato-4-pyridinone with $[\text{NH}_4][\text{TcO}_4]$ and $\text{SnCl}_2$

Hmupp (0.618 g, 0.20 mmol) and  $\text{Sn(II)Cl}_2$  (0.0260 g, 0.10 mmol) were added to 50 mL of methanol.  $[\text{NH}_4][\text{TcO}_4]$  (0.05 mmol) was added to the above solution and it

immediately turned yellow and then proceeded to red. After a number of hours a red-green colour resulted. Sodium chloride (0.050 g) was added and the red-green solution was left to evaporate. Again upon standing the red-green solution turned a darker green losing some of the red colour. Some insoluble precipitate was also observed, which was concluded to be  $\text{TcO}_2 \cdot n\text{H}_2\text{O}$ . The product was extracted and recrystallized with methanol. The dark red-green solid was collected by filtration and dried in vacuo.

### 3.2.7 Reaction of mimosine with $[\text{NH}_4][\text{TcO}_4]$ and $\text{SnCl}_2$

Mimosine (0.0793 g, 0.40 mmol) and  $\text{Sn(II)Cl}_2$  (0.0250 g, 0.10 mmol) were dissolved in 50 mL of water. To this clear solution 0.10 mmol of  $[\text{NH}_4][\text{TcO}_4]$  was added, at which time the clear solution turned dark red. Sodium chloride (1.0 g) was added to the dark red solution and it was left to evaporate. The product was extracted and recrystallized from water. The light red solid was collected by filtration and dried under vacuum.

## 3.3 Discussion of the Synthetic Procedure

The preparation of the tris(3-oxy-4-pyronato)- and the tris(3-oxy-4-pyridinonato) metal (IV) chloride complexes *via* the reduction route proved to be more difficult than was initially expected. As previously mentioned in the preparation of tris-ligand technetium complexes *via* the reduction route, addition of a separate reducing agent is necessary.  $\text{SnCl}_2$  was chosen as it was the only reducing agent tried which successfully reduced pertechnetate  $[\text{TcO}_4]^-$  allowing the formation of the tris-ligand technetium chloride complexes. During the reaction, Sn (II) is oxidized to Sn (IV), thus  $\text{SnCl}_2$  is a two electron donor and must be present at a high enough molarity that it will reduce technetium from the (VII) oxidation state down to the desired lower oxidation state (IV). At the same time, since Sn (IV) is formed during the process of the reaction and has very

similar physical characteristics to technetium, it may also react with the ligand, or be incorporated into technetium complexes. We find that Sn (IV) does react with the ligand to form  $[\text{SnL}_3]^+$  complexes; however, it is not incorporated into the technetium complexes. The formation of a separate tin complex does not cause any problems with the use of the Tc complex as a radiopharmaceutical imaging agent, but it does inhibit the characterization of the technetium complex as the latter can not be obtained in a pure form. Because of the presence of this extra species in the product, no yields are reported for the reactions in Section 3.2.  $\text{SnCl}_2$  was initially used at a 2:1 (tin to technetium) stoichiometry, however, it was later lowered to 1:1 in an effort to control the formation of  $[\text{SnL}_3]^+$ . The ligand was initially added in a ten fold excess for the preparation of the tris-ligand technetium complexes, and later a 4:1 stoichiometry was tried but due to the formation of  $[\text{SnL}_3]^+$  complex this second ratio was found to be insufficient for complete formation of the  $[\text{TcL}_3]^+$  complex. This indicates that the  $[\text{SnL}_3]^+$  complex may be kinetically or thermodynamically favoured over the  $[\text{TcL}_3]^+$  complex. The syntheses of the tris-ligand metal chloride complexes were done in aqueous media except for  $[\text{M}(\text{mhpp})_3][\text{Cl}]$  and  $[\text{M}(\text{mupp})_3][\text{Cl}]$  ( $\text{M} = \text{Tc}, \text{Sn}$ ), which were done in more lipophilic media due to the higher lipophilicity of the ligands.  $[\text{M}(\text{mhpp})_3][\text{Cl}]$  was prepared in a 1:1 water:methanol solution while  $[\text{M}(\text{mupp})_3][\text{Cl}]$  was prepared in pure methanol. The  $[\text{M}(\text{mupp})_3][\text{Cl}]$  complex also showed some indications of instability when left in solution for a long period of time. A more efficient method than evaporation is needed for removal of the solvent.

Tris-ligand metal iodide, hexa-fluorophosphate and tetraphenylborate complexes were also prepared by the addition of the sodium salt of the corresponding anion to a solution of the tris-ligand metal chloride complexes.

### 3.4 Characterization of the tris(3-oxy-4-pyronato)- and the tris(3-oxy-4-pyridinonato)metal chloride complexes.

Characterization of the tris-ligand metal chloride complexes was hampered due to the Federal regulations for the transport of radioactive material and the hazards associated working with radioactive material. Special arrangements were made for transportation of the radioactive samples, for micro-analysis and also for obtaining FAB-Mass Spectra. On site, the methods available for characterization of the tris-ligand technetium metal complexes were: infrared spectroscopy, ultraviolet spectroscopy, and conductivity, with an apparatus which could be transported to the radioactive laboratory.

Infrared spectroscopy offered a quick way to identify the formation of tris-ligand metal chloride complexes, due to the characteristic changes of the ligand spectrum upon complexation with a metal. The IR spectra of the tris-ligand metal chloride complexes show diagnostic changes from those of the free ligands. The changes are consistent with metal chelation *via* the deprotonated hydroxyl and the carbonyl oxygen atoms. The IR spectra of the tris-ligand metal chloride complexes were run on a BOMEM MB-100 FTIR Infrared Spectrophotometer.

Micro-analyses were performed by the Canadian Microanalytical Service Ltd.. Micro-analysis also proved to be a problem, as no purification technique gave results within the acceptable limits. The problem was eventually worked out by the examination of FAB-MS spectra which showed the presence of tris(ligand) metal chloride species of both Tc and Sn. Due to the similar physical characteristics of Sn and Tc, and the formation of identical tris-ligand metal complexes separation was unsuccessful.

Unlike the free ligands, the tris-ligand metal chloride complexes are not volatile enough for EI-MS but rather require positive fast atom bombardment (FAB) ionization. All spectra were recorded with an AEI MS 9 and the samples were introduced on a copper

tipped probe in either glycerol or p-nitrobenzylalcohol. The molecular ions in the mass spectra are consistent with an  $ML_3^+$  formulation ( $M = Tc, Sn$ ).

### 3.4.1 Infrared Spectroscopy

IR studies on pyridine derivatives show that the substituents vibrate largely independently of the ring.<sup>75</sup> The free ligand IR spectra were consistent with this conclusion and predictably, the spectra of the tris-ligand metal complexes are quite similar. The bands are broadened somewhat but the general features of the spectra are the same. Due to the similarity of the spectra of the free ligand and the tris-ligand metal complexes, only the differences will be discussed.

There are several diagnostic differences between the spectra of the free and complexed ligand: the loss of  $\nu_{OH}$ , the bathochromic shift of  $\nu_{C=O}$ , and the appearance of several new bands below  $800\text{ cm}^{-1}$ . The new bands below  $800\text{ cm}^{-1}$  (Table 3.1) have been tentatively assigned as  $\nu_{M-O}$  but they are probably also coupled to the ring deformation modes.<sup>76</sup> Figure 3.3 is a comparison of the spectrum of Hdpp (top) and  $[M(dpp)_3][Cl]$  ( $M = Tc, Sn$ ) (bottom). The loss of  $\nu_{OH}$  is the most noticeable change in the spectrum of  $[M(dpp)_3][Cl]$  ( $M = Tc, Sn$ ).

The characteristic four band pattern of mixed  $\nu_{C=O}$  and  $\nu_{Ring}$  is shifted upon formation of the tris-ligand metal chloride complexes (Table 3.1) with the most pronounced bathochromic shift occurring for the highest energy band.

The additional  $\nu_{C=O}$  stretch in Hmupp and mimosine resulting from the carboxylic acid carbonyl does not shift upon the formation of the tris-ligand metal chloride complexes. This is thought to be due to the distance of the carboxylic acid carbonyl in Hmupp, and in mimosine, from the metal centre.

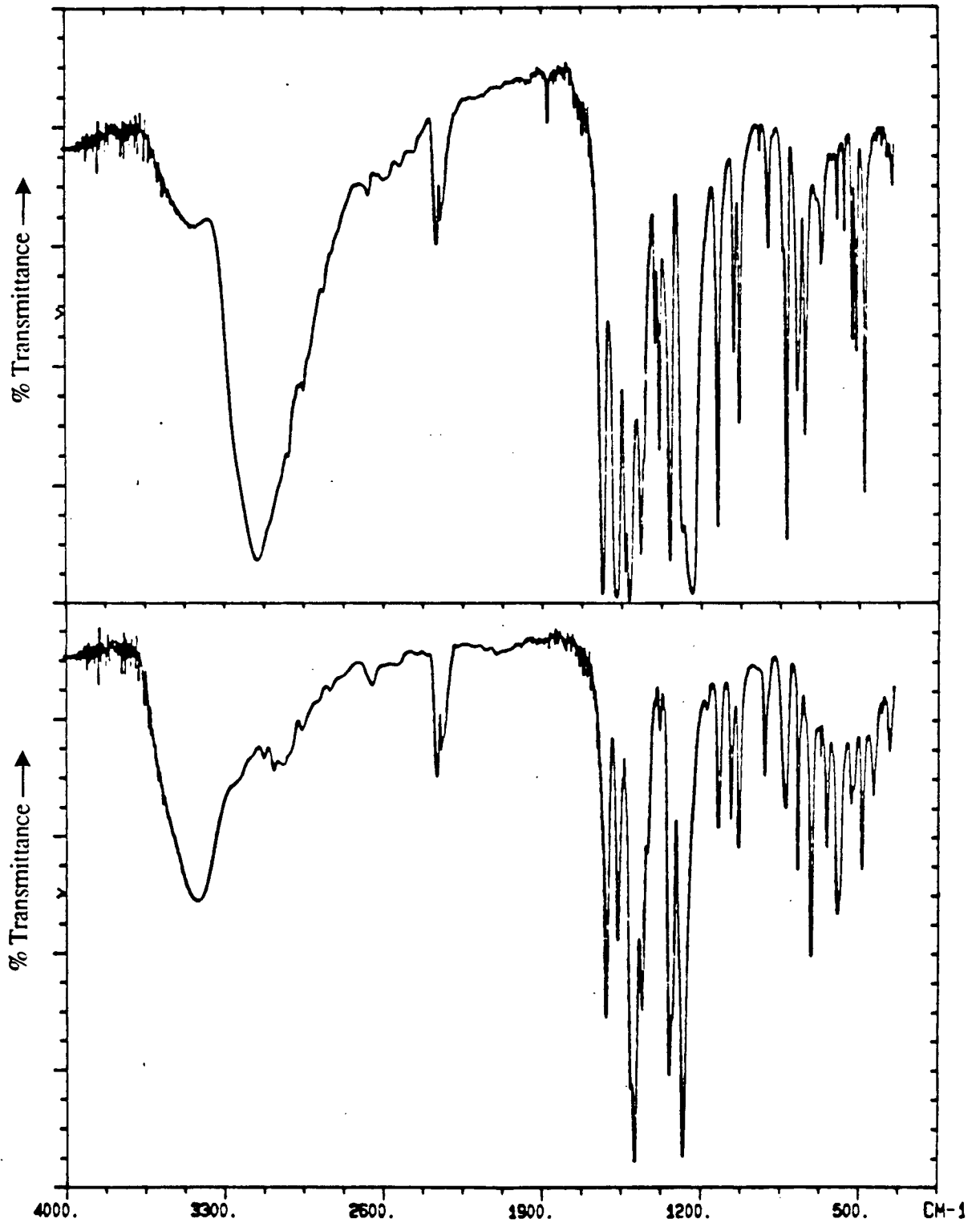
Figure 3.3 Infrared spectra of Hdpp (top) and  $[M(dpp)_3][Cl]$  ( $M = Tc, Sn$ ) (bottom).

Table 3.1 Selected infrared absorption bands ( $\text{cm}^{-1}$ ) for the tris-ligand metal chloride complexes ( $M = \text{Tc}, \text{Sn}$ ). All are strong except where noted.

Complex	Assignment $\nu_{\text{C=O}}, \nu_{\text{Ring}}$	Assignment $\nu_{\text{M-O}}$
Maltol	1654, 1611, 1558, 1459	
$[\text{M}(\text{ma})_3][\text{Cl}]$	1602, 1568 sh, 1542, 1462	728, 640, 482
Kojic acid	1662, 1612, 1580, 1465	
$[\text{M}(\text{ka})_3][\text{Cl}]$	1620, 1569, 1515, 1471	756, 695, 517
Hmpp	1646, 1620, 1542, 1500, 1420 w	
$[\text{M}(\text{mpp})_3][\text{Cl}]$	1602, 1585, 1532, 1487, 1406	736, 649, 495
Hdpp	1620, 1568, 1489, 1459	
$[\text{M}(\text{dpp})_3][\text{Cl}]$	1632, 1576, 1515, 1462	710, 640, 439
Hmhpp	1629, 1585, 1512, 1469	
$[\text{M}(\text{mhpp})_3][\text{Cl}]$	1615, 1568, 1495, 1471	720, 649, 439
Hmupp	1725, 1637, 1564, 1515, 1480	
$[\text{M}(\text{mupp})_3][\text{Cl}]$	1725, 1602, 1558, 1497, 1470	719, 649, 421
Mimosine	1637, 1576, 1532, 1498, 1462	
$[\text{M}(\text{mimo})_3][\text{Cl}]$	1637, 1568, 1521, 1489, 1455	728, 667, 505

(Abbreviations:  $M = \text{Tc}, \text{Sn}$ ; sh = shoulder; w = weak)

3.4.2 Mass Spectrometry

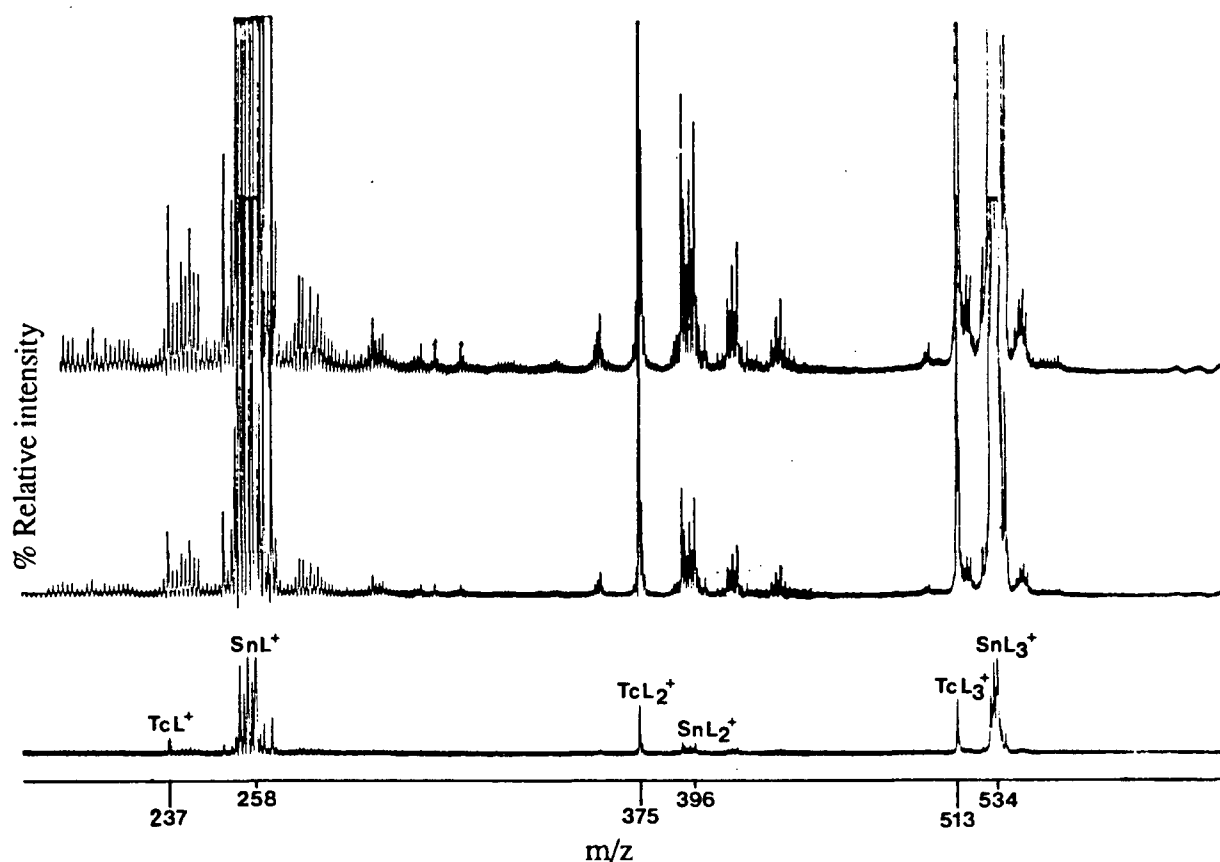
The FAB-MS spectral data are listed in Table 3.2. In most cases the molecular ion is observed as the  $TcL_3^+$  and  $SnL_3^+$  peaks. The fragments corresponding to loss of one and two ligands respectively, are also found in the majority of the spectra. The presence of peaks due to the matrix complicate the assignment of the spectra beyond this point. The molecular weights (MW) of the ligands and tris-ligand metal complexes are listed in Table A. 1 of the appendix.

Table 3.2 Data from FAB-MS spectra of the tris-ligand metal chloride complexes (m/z).

Ligand	$TcL_3^+$	$TcL_2^+$	$TcL^+$	$SnL_3^+$	$SnL_2^+$	$SnL^+$
maltol	474	349	224	495	370	245
				493	368	243
				491	366	241
kojic acid	522	381	240	543	402	261
				490	366	242
				488	364	240
Hmpp	347		223	492	368	244
				490	366	242
				488	364	240
Hdpp	513	375	237	534	396	258
				532	394	256
				530	392	254
Hmhpp	723	515	307	744		329
				742		327
				740		325
Hmupp				1044	736	428
				1042	734	426
				1040	732	424

$[M(\text{mupp})_3][\text{Cl}]$  ( $M = \text{Tc}, \text{Sn}$ ), which was of questionable stability when left in solution over a long period of time, did not show any technetium-ligand peaks; it did, however, exhibit the characteristic tin-ligand peaks. This suggests that the technetium complex is indeed unstable when left in the reaction solution for long periods. The product from the mimosine reaction did not show  $m/z$  peaks corresponding to either the technetium or the tin, tris-, bis-, or mono-ligand peaks. The only fragment which has been tentatively assigned is the  $m/z$  426 peak. The mass of this fragment corresponds to the mass of a technetium tris-ligand complex which has lost all three R groups from the ring nitrogen. The lack of any assignable peaks in the FAB mass spectrum suggests that the complex is very susceptible to fragmentation. A typical FAB-MS spectrum is shown in Figure 3.4.

Figure 3.4 FAB-MS spectrum of  $[M(\text{dpp})_3][\text{Cl}]$  ( $M = \text{Tc}, \text{Sn}$ )



### 3.4.3 Ultraviolet Spectroscopy

Concentrations were calculated as per Table A. 1 from a molecular weight averaged for M = Tc, Sn. The ultraviolet spectra for the tris-ligand metal chloride complexes (M = Tc, Sn) were run on a Beckman Model 25 spectrophotometer. The tris-ligand metal chloride complexes showed four characteristic bands. The two bands in the ultraviolet region are assigned as  $\pi \rightarrow \pi^*$  ligand transitions. The other two bands are attributed to d-d transitions, although the d-d spectra of Tc (IV) species are rarely observed, being of high energy, and usually being obscured by charge transfer absorption.<sup>77</sup> Table 3.3 gives the  $\lambda_{\max}$  (nm) and  $\epsilon$  (Lmol<sup>-1</sup> cm<sup>-1</sup>) for the observed bands in the spectra of the tris-ligand technetium and tin chloride complexes.

Table 3.3 Ultraviolet spectral data for the tris-ligand metal (M = Tc, Sn) chloride complexes.

Complex	$\lambda$ (nm)	$\epsilon$ (Lmol <sup>-1</sup> cm <sup>-1</sup> )	Complex	$\lambda$ (nm)	$\epsilon$ (Lmol <sup>-1</sup> cm <sup>-1</sup> )
[M(ma) <sub>3</sub> ][Cl]	555	300	[M(mhpp) <sub>3</sub> ][Cl]	510	400
	458	6200		340	1600
	278	13300		278	18800
	218	16200		230	12100
[M(ka) <sub>3</sub> ][Cl]	518	200	[M(mupp) <sub>3</sub> ][Cl]	425	200
	438	300		345	300
	259	14400		290	10800
	225	12900		223	10800
[M(mpp) <sub>3</sub> ][Cl]	515	3700	[M(mimo) <sub>3</sub> ][Cl]	430	500
	376	2200		350	500
	278	19200		285	6400
	223	14400		220	9100
[M(dpp) <sub>3</sub> ][Cl]	430	700			
	375	900			
	278	18200			
	225	12300			

### 3.4.4 Conductivity Measurements

The conductivity measurements were done using a Serfass Conductivity Bridge, with a commercially available dip cell. This is a Wheatstone Bridge setup where the dip cell forms one arm of a Wheatstone Bridge circuit. To measure the conductance of a solution, the dip cell is placed into the solution to be measured, and it is then connected to the test terminals of the conductivity bridge. The selector switch is set to the appropriate conductance range, and the dial is rotated until a balance is indicated by the magic eye. The conductivity is then read off the dials as a measure of resistance ( $\Omega$ ). Since absolute conductivity values are not required it is not necessary to know the cell constant. Solutions of the mixture containing the tris-ligand tin chloride and the tris-ligand technetium chloride complexes were made at the 1.0 mmol level in an appropriate solvent and were compared to known standards of the same concentration and in the same solvent. Concentrations were calculated as per Table A. 1 from a molecular weight averaged for  $M = Tc, Sn$ .

The conductivity measurements of all of the mixed Tc and Sn tris-ligand chloride complexes except  $[M(mupp)_3][Cl]$  and  $[M(mhpp)_3][Cl]$  were done in water and compared to KCl (1.0045 mM). The conductivity measurements for  $[M(mupp)_3][Cl]$  and  $[M(mhpp)_3][Cl]$  were done in methanol and compared to  $[Bu_4N][Br]$  (0.9990 mmol). The conductivity values for  $[M(mupp)_3][Cl]$  and  $[M(mimo)_3][Cl]$  were found to be very high and are not reported. This is due to the zwitterionic character of the complexes; this is expected to occur in the mid-pH regime. The resistivity values for the mixture of Tc and Sn tris-ligand complexes are reported in Table 3.4.

Table 3.4 Resistance values ( $k \Omega$ ) for the mixture of Tc and Sn tris-ligand complexes.

	Resistance ( $k \Omega$ ) (average)		Resistance ( $k \Omega$ ) (average)
H <sub>2</sub> O	550	CH <sub>3</sub> OH	420
KCl	7.85	[Bu <sub>4</sub> N][Br]	17.5
[M(ma) <sub>3</sub> ][Cl]	10.5	[M(mhpp) <sub>3</sub> ][Cl]	21.5
[M(ka) <sub>3</sub> ][Cl]	6.45		
[M(mpp) <sub>3</sub> ][Cl]	6.85		
[M(dpp) <sub>3</sub> ][Cl]	9.15		

(M = Tc, Sn)

## CHAPTER IV SYNTHESIS OF TECHNETIUM COMPLEXES BY THE SUBSTITUTION ROUTE

### 4.1 Introduction

The preparation of Tc(V) complexes *via* the substitution route has been widely investigated, and discussed in review articles.<sup>78, 79</sup> Since Davison's and Cotton's groups<sup>80</sup> determined the structure of  $[\text{TcOCl}_4]^-$  by X-ray crystal analysis, this compound has been established as a very good starting material in the synthesis of technetium complexes. The simplification of the synthesis of  $[\text{TcOCl}_4]^-$  by Davison *et al.*<sup>81</sup> also increased the use of  $[\text{TcOCl}_4]^-$  as a starting material for the synthesis of technetium (V) complexes.

The use of  $[\text{TcOCl}_4]^-$  as a starting material for the synthesis of Tc (V) complexes *via* the substitution route has resulted in the synthesis of a large number of complexes. These complexes may be arbitrarily divided into several classes depending on the type of oxo-technetium core present. The three general classes of complexes are those with  $\text{TcO}^{3+}$ , *trans*- $\text{TcO}_2^+$ , and  $\text{Tc}_2\text{O}_3^{4+}$  cores. There is also an additional class of  $\mu$ -oxo bridged technetium complexes which have been formed by reaction of  $[\text{TcOCl}_4]^-$  with various ligands.<sup>82</sup>

When the tetrabutyl-ammonium salt of  $[\text{TcOCl}_4]^-$  is used, substitutions onto  $[\text{TcOCl}_4]^-$  are usually conducted in an organic solvent, to prevent hydrolysis and disproportionation of the starting material. Small amounts of water, however, may be present with no significant detrimental effects on the reaction. Due to the simple and quick preparation of  $[\text{Bu}_4\text{N}][\text{TcOCl}_4]$  it was chosen as the starting material for the synthesis of technetium (V) complexes using the substitution route. The ligands chosen were the 3-hydroxy-4-pyrones and the 3-hydroxy-4-pyridinones.

## 4.2 Materials and Methods

The  $[\text{Bu}_4\text{N}][\text{TcOCl}_4]$  was prepared according to the literature preparation of Davison and coworkers.<sup>81</sup> The ligands were prepared and purified as described in Section 2.2. The methanol was reagent grade and was used as supplied.

### 4.2.1 Reaction of $[\text{Bu}_4\text{N}][\text{TcOCl}_4]$ with Maltol.

$[\text{Bu}_4\text{N}][\text{TcOCl}_4]$  (0.102 g, 0.20 mmol) was added to a solution of maltol (0.5180 g, 3.95 mmol) in 35 mL of methanol resulting in a yellow-brown solution. After a few minutes the yellow-brown solution began to darken. The reaction mixture was then heated at 60°C for one day giving a red solution. The red solution was left to evaporate yielding a dark red solid which was purified by recrystallization in acetonitrile to remove the excess ligand. The dark red solid was found to be a mixture of water and organic soluble products which were separated by solvent manipulation and purified by recrystallization from water and methanol respectively. The red solids were collected by filtration and were dried under vacuum.

### 4.2.2 Reaction of $[\text{Bu}_4\text{N}][\text{TcOCl}_4]$ with Kojic acid.

$[\text{Bu}_4\text{N}][\text{TcOCl}_4]$  (0.1077 g, 0.21 mmol) was added to a solution of kojic acid (0.5021 g, 3.50 mmol) in 50 mL of methanol. The light yellow-green solution was left at room temperature for two days; at which time it was reddish in colour. The red solution was left to evaporate yielding a dark red solid which was purified by recrystallization in acetonitrile to remove the excess ligand. The dark red solid was found to be a mixture of water and organic soluble products which were separated by solvent selection and purified by

recrystallization from water and methanol respectively. The red solids were collected by filtration and were dried in vacuo.

#### 4.2.3 Reaction of [Bu<sub>4</sub>N][TcOCl<sub>4</sub>] with Hmpp.

[Bu<sub>4</sub>N][TcOCl<sub>4</sub>] (0.0605 g, 0.12 mmol) was added to a mixture of Hmpp (0.4015 g, 3.20 mmol) in 50 mL of methanol. The mixture turned yellow-green upon the addition of [Bu<sub>4</sub>N][TcOCl<sub>4</sub>] and gradually turned red stirring at room temperature over two days. The red mixture was then left to evaporate. The red solution was left to evaporate yielding a dark red solid which was purified by recrystallization in acetonitrile to remove the excess ligand. The dark red solid was found to be a mixture of water and organic soluble products which were separated by solvent manipulation and purified by recrystallization from water and methanol respectively. The red solids were collected by filtration and were dried under vacuum.

### 4.3 Discussion of the Synthetic Procedure

[Bu<sub>4</sub>N][TcOCl<sub>4</sub>] is easy to prepare and was therefore chosen as the starting material for the synthesis of technetium complexes *via* the substitution route. The substitution reactions were done in methanol to prevent the hydrolysis and disproportionation of the starting material, though traces of water do not cause any problems. The ligand is present in excess in the reaction and the substitution reaction proceeds under mild conditions. Reaction of [Bu<sub>4</sub>N][TcOCl<sub>4</sub>] with maltol, kojic acid and Hmpp all yielded a mixture of water- and organic-soluble products. This was determined by thin layer chromatography on silica plates with a 9:1 methanol-water eluent. Thin layer chromatography was also used to monitor the course of the reaction. The water and organic-soluble components were separated by dissolving the water-soluble product followed by filtration to collect the

insoluble organic-soluble product. Some success was achieved in the separation of the water and organic components, however, these were later found to contain several species. At this point, column chromatography was done on the products of the  $[\text{Bu}_4\text{N}][\text{TcOCl}_4]$  and maltol reaction to separate the water-soluble mixture and the organic-soluble mixture into their individual components. Thin layer chromatography indicated that this was successful but further characterization of the two chromatographed products showed that the products were still mixtures of complexes. It was then decided that an HPLC system was required for the separation and purification of the individual complexes. This part of the project was shelved until an HPLC system could be purchased and set up.

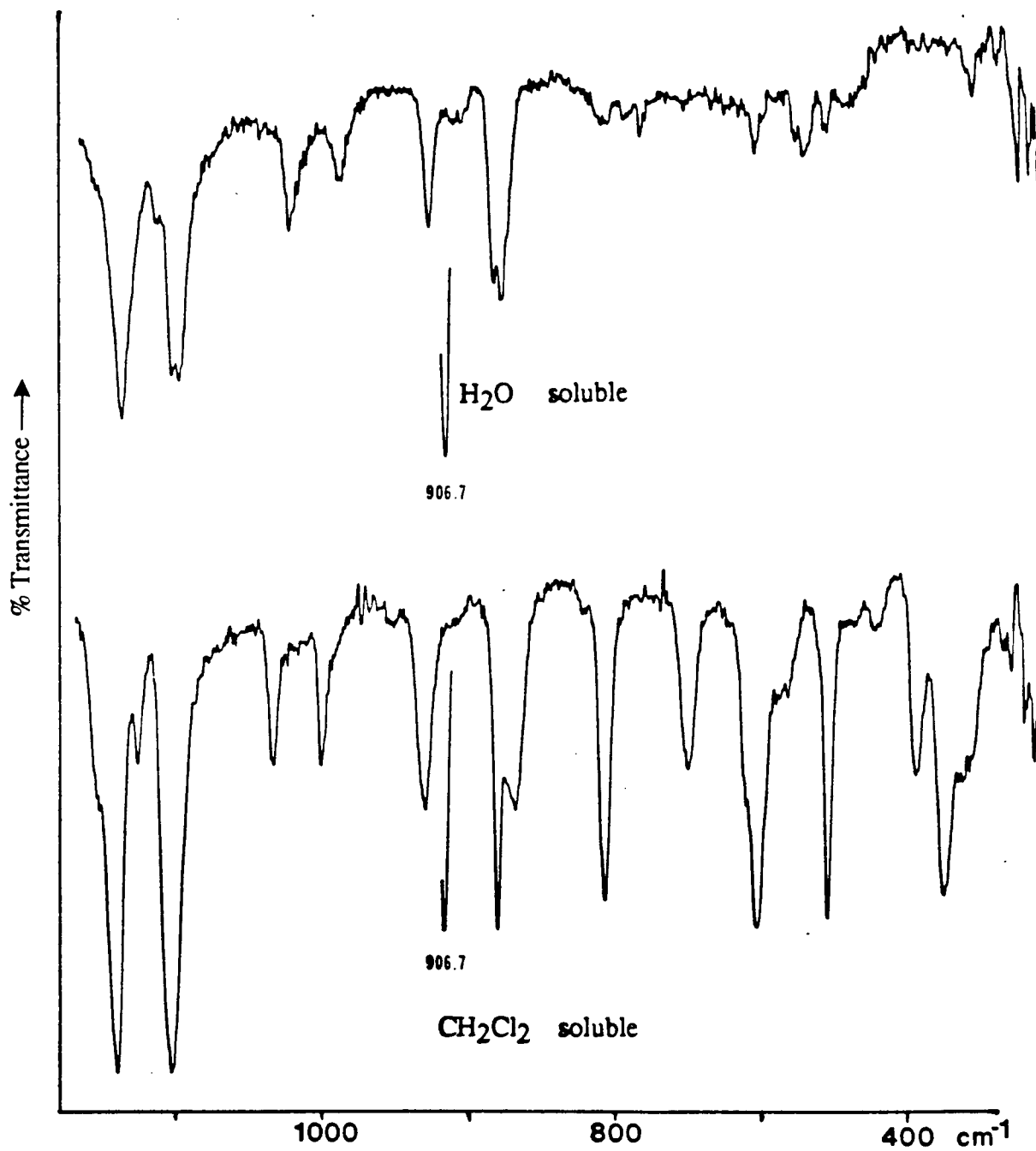
#### 4.4 Characterization

Characterization was done on the two products of the  $[\text{Bu}_4\text{N}][\text{TcOCl}_4]$  and maltol reaction after separation of the complexes was attempted. Characterization was done by infrared spectroscopy and mass spectrometry, which showed that the separation of the complexes had not been successful. Even though the separation of the complexes was not complete some information may still be obtained on the complexes that are present.

##### 4.4.1 Infrared spectroscopy

The infrared spectrum of the initial reaction mixture showed a strong infrared stretch at  $966\text{ cm}^{-1}$  which corresponds to the literature values for a  $\text{Tc}=\text{O}$  stretch. This band gradually lessened in intensity as the reaction proceeded, with the formation of two new bands at  $730\text{ cm}^{-1}$  and  $830\text{ cm}^{-1}$  which are assigned as  $\text{Tc}-\text{O}-\text{Tc}$  and  $\text{O}=\text{Tc}=\text{O}$  stretches respectively. There is also the appearance of a number of  $\text{Tc}-\text{X}$  stretches below  $400\text{ cm}^{-1}$ .

Figure 4.1 Infrared spectra of the two solids from the reaction of  $[\text{Bu}_4\text{N}][\text{TcOCl}_4]$  and maltol.



After the separation of the reaction mixture into the water and organic soluble components the two infrared spectra were run and were now found to be very different. (Figure 4.1) The water soluble part did not show any strong Tc=O, O=Tc=O, Tc-O-Tc or Tc-X stretches, while the organic soluble part showed a medium O=Tc=O stretch at  $830\text{ cm}^{-1}$ , a strong Tc-O-Tc stretch at  $730\text{ cm}^{-1}$  and several Tc-X stretches at 390, 360, 340, and  $300\text{ cm}^{-1}$ . This suggests that the majority of the water soluble product is a complex that has no oxo-technetium core present, while the majority of the organic soluble product is a  $\mu$  oxo-bridged technetium bimetallic complex.

#### 4.4.2 Mass Spectrometry

Characterization of the two products from the  $[\text{Bu}_4\text{N}][\text{TcOCl}_4]$  and maltol reaction was attempted by FAB, negative ion DCI, and positive ion DCI mass spectrometries.

Table 4.1 Negative DCI mass spectrum for the organic soluble product from the reaction of  $[\text{Bu}_4\text{N}][\text{TcOCl}_4]$  and maltol.

m/z	Assignment	m/z	Assignment
783	$\text{L}_2\text{Cl}_2\text{Tc-O-TcL}_2\text{Cl}_2$	328	$\text{LCl}_3\text{Tc}$
714	$\text{L}_2\text{Tc-O-TcL}_2$	310	$\text{LCl}_2\text{Tc-O}$
589	$\text{L}_2\text{Tc-O-TcL}$	294	$\text{LCl}_2\text{Tc}$
419	$\text{L}_2\text{Cl}_2\text{Tc}$	275	$\text{LClTc-O}$
384	$\text{L}_2\text{ClTc}$	220	$\text{Cl}_3\text{Tc-O}$
365	$\text{L}_2\text{Tc-O}$	206	$\text{Cl}_3\text{Tc}$
349	$\text{L}_2\text{Tc}$	125	L

(Abbreviations: L = Maltol)

The mass spectra for all these techniques showed that the products were mixtures of several complexes; however by examining the mass spectra while keeping in mind the complexes that might be formed, and also the information obtained from the infrared spectra, the most predominant complexes may be tentatively assigned.

The evidence from all three techniques suggests the presence of several bimetallic complexes in the organic soluble product with the  $[L_2ClTc-O-TcL_2Cl]$  complex being the predominant species. The mass spectral data for the negative DCI mass spectrum of the organic soluble product is given in Table 4.1.

The water soluble product also shows a number of peaks suggesting a mixture of complexes. The dominant peak in the FAB mass spectra is  $m/z$  419 which corresponds to a  $[TcL_2Cl_2]^+$  complex and would also explain the lack of any visible oxo-technetium stretches in the infrared spectrum. The expected fragment peaks for this complex are visible and are given in Table 4.2. The smaller peak at  $m/z$  462 suggests that a small

Table 4.2 FAB mass spectrum of the water soluble product from the reaction of  $[Bu_4N][TcOCl_4]$  and maltol.

m/z	Assignment	m/z	Assignment
637 vs	$LCl_3Tc-O-TcLCl_3$	365	$TcL_2O$
462 vs	$LTc-O-TcL$	349	$TcL_2$
419	$TcL_2Cl_2$	258	$TcLCl$
399 vs	$L_2ClTc-O$	242	$Bu_4N$
384	$TcL_2Cl$		

(Abbreviations: vs = very small; L = Maltol)

amount of  $[\text{Tc}_2\text{L}_2\text{O}]^+$  is also present. The expected fragmentation pattern for this species is also observed and is given in Table 4.2. There is also another very small peak present which indicates the presence of a tiny amount of a dimer, which has been tentatively assigned as being  $[\text{LCl}_3\text{Tc-O-TcLCl}_3]$ .

#### 4.5 Results and Discussion

Synthesis of technetium (V) complexes *via* the substitution route is presently an area of great interest in radiopharmaceutical development due to the inherent advantages of the substitution route over the reduction route. The main advantages are: the absence of a reducing agent in the final synthetic step when preparing a technetium-99m labelled radiopharmaceutical and the (usually) known oxidation state of the resulting technetium complex. The salts of  $[\text{TcOX}_4]^-$  and  $[\text{TcX}_6]^{2-}$  are presently the most commonly used starting materials; however, they are difficult to obtain in a pure form and also tend to produce complex mixtures of products. This poses a problem due to the necessity of having a single radiochemically pure technetium complex for radiopharmaceutical use. Because of this problem, this route has not been widely used to date for the synthesis of radiopharmaceuticals; however, with the development of rapid and advanced separation techniques this would be a favourable route for synthesis of radiopharmaceuticals. HPLC now provides the answer to this problem and is the most widely used technique for the separation of complex mixtures.

Our initial work with the substitution route has shown that complex mixtures are formed by the reaction of  $[\text{Bu}_4\text{N}][\text{TcOCl}_4]$  with maltol, kojic acid, and Hmpp. Further characterization on the products from the reaction of  $[\text{Bu}_4\text{N}][\text{TcOCl}_4]$  with maltol have indicated the presence of at least four complexes: two monomers  $[\text{TcL}_2\text{Cl}_2]^+$  and  $[\text{TcL}_2\text{O}]^+$ ,

and two bimetallic complexes  $[\text{LCl}_3\text{Tc-O-TcLCl}_3]$  and  $[\text{L}_2\text{ClTc-O-TcL}_2\text{Cl}]$ . The results also indicate that the two complexes  $[\text{TcL}_2\text{Cl}_2]^+$  and  $[\text{L}_2\text{ClTc-O-TcL}_2\text{Cl}]$  are predominant.

## CHAPTER V RADIOPHARMACEUTICAL APPLICATIONS OF GALLIUM AND TECHNETIUM

### 5.1 Gallium Biodistribution Studies

#### 5.1.1 Introduction

Our interest in studying the *in vitro* and *in vivo* coordination chemistry of aluminum and in the development of radiopharmaceutical imaging agents led us to investigate the *in vivo* biodistribution of a series of  $^{67}\text{Ga}$ -labelled N-substituted-3-oxy-4-pyridinone complexes. Our interest in  $^{67}\text{Ga}$  was prompted by the lack of any suitable aluminum isotopes for imaging and also by the lack of work done with this radionuclide. As already mentioned in Chapter 1 the aqueous coordination chemistry of aluminum and gallium is very similar and this similarity of *in vitro* aqueous behavior makes  $^{67}\text{Ga}$  the best model available for aluminum, although it is not a great analogue.

#### 5.1.2 Materials and Methods

The ligands Hdpp, Hmpp and Hmhpp were prepared as previously described;<sup>63</sup> *l*-mimosine (Sigma) was used without further purification. Water was purified, deionized (Barnstead D8904 and D8902 cartridges, respectively), and distilled (Corning MP-1 Megapure still).

Stock solutions of ligands were prepared in isotonic Trizma pH 7.4 buffer and dispensed in 10 mL sterile, pyrogen-free, nitrogen-purged vials. Various volumes of  $^{67}\text{Ga}$ -citrate were added (due to decay) and stirred for 10 minutes. The  $^{67}\text{Ga}$ -citrate starting material was commercially purchased from DuPont (1  $\mu\text{Ci}$  is  $2.5 \times 10^{-14}$  moles  $^{67}\text{Ga}$ ). All

injections were standardized such that a 100  $\mu\text{L}$  injection volume contained 1  $\mu\text{Ci}$  of  $^{67}\text{Ga}$ . Total ligand concentrations for each injection are listed in Table II. Radiochemical purity of greater than 98% was ascertained by thin layer chromatography prior to the injection. Tissue distribution experiments were performed in BALB/C mice (UBC). Animals were injected by tail vein and sacrificed by exsanguination 24 hours post-injection. The various organs were excised and activity (percent of injected dose per gram of organ) was determined in a well  $\gamma$  counter. The results (mean  $\pm$  standard deviation for five animals) at 24 hours post-injection are displayed in Table 5.1. The comparative clearance study ( $^{67}\text{Ga}(\text{citrate})$  vs.  $^{67}\text{Ga}(\text{dpp})_3$ ) was performed in a hypnotized and anaesthetized rabbit with a Siemens Large Field of View Gamma Camera.

### 5.1.3 Results and Discussion

The Ga complexes of the series of N-substituted-3-oxy-4-pyridinones have been characterized previously in the solid state; they are prepared in high yield from aqueous solution at neutral pH.<sup>33, 34</sup> The functionalizable ring nitrogen in the pyridinones allows some variation of the lipophilicity and water solubility. The N-H derivatives of Ga are quite water soluble ( $>1$  mM) while the N-methylated and N-ethylated analogues are less water soluble but more lipophilic, and the N-hexylated complexes are negligibly water soluble but highly lipophilic. This variation in properties led us to investigate their solution properties both *in vivo* and *in vitro*. The extraordinary solid state properties which have been reported for  $\text{ML}_3 \cdot 12\text{H}_2\text{O}$  where L = dpp, mepp,<sup>33, 34, 36</sup> (incorporating hexagonal channels of water into an exocathrate array) suggested that there might be some interesting solution properties in these  $\text{ML}_3$  systems.

The assessment of these ligands as chelating agents for  $^{67}\text{Ga}$  was done with fairly concentrated ligand solutions. The objective of a chelating agent is the removal of a metal

from the body or the direction of a metal ion to a target organ in the body; high concentrations of ligand in the blood should facilitate this goal. In long term experiments, high levels can be maintained by administering the ligand repeatedly. Shorter duration experiments were conducted to determine if the injection of saturated ligand solutions would be sufficient to produce a change in biodistribution. If this was found, it would indicate good potential for these ligands as chelating agents.

In the biodistribution experiments, values of per cent uptake per gram of organ in mice were determined 24 hours after injection of  $^{67}\text{GaL}_3$  ( L = mpp, dpp, mhpp, *l*-mimosine) for blood, liver, spleen, kidneys, heart, lung, muscle and brain. These results are summarized in Table 5.1 as per cent injected dose per gram of organ. The uptake into the blood and the liver after 24 hours is shown graphically in Figure 5.1 in order to represent the dynamic transport and terminal uptake of  $^{67}\text{Ga}$ , respectively, and this figure dramatically demonstrates the difference in biodistribution of the new complexes versus gallium citrate. The clearance of the ligand complexes from the blood was faster than that for Ga-citrate (the latter can take up to three days to clear the blood<sup>83</sup>) and the liver uptake was greater with citrate than with any of the 3-hydroxy-4-pyridinones. This difference was significant at the 99% level (based on unpaired t-tests) in 31 out of 32 cases; the other case was significantly different at the 94% level. In another study, more dilute solutions of the 3-hydroxy-4-pyridinones (concentrations before administration of 3 - 4  $\mu\text{M}$ ) with  $^{67}\text{Ga}$  showed effectively no difference from  $^{67}\text{Ga}$ -citrate injections.

To verify the differences in biodistribution (particularly in excretion behaviour) for  $^{67}\text{Ga}$  as citrate and 3-oxy-4-pyridinone complexes, a clearance experiment (comparing citrate and Hdpp) was conducted in a live rabbit. The activity in the kidneys and bladder was monitored by setting regions of interest over those organs, and the results of this experiment are shown in Figure 5.2. It is clear that the activity is rapidly excreted for  $^{67}\text{Ga}(\text{dpp})_3$ , and much more slowly excreted for Ga-citrate. Considered together, Figures

5.1 and 5.2 present a complete picture of the clearance of  $^{67}\text{Ga}(\text{dpp})_3$  and show that it is much more rapid than that of Ga-citrate. After 20 minutes, most of the former is cleared, while the latter requires more than 24 hours for complete clearance.

As discussed in the introduction, Ga-citrate is known to biodistribute similarly to Ga-transferrin.<sup>84</sup> Based on the available stability constants in the literature,<sup>85, 86</sup> it may be calculated that all of the  $^{67}\text{Ga}$  after injection as its citrate is complexed with transferrin (using constants for human serum transferrin<sup>86</sup>). Therefore, it can be safely assumed that the  $^{67}\text{Ga}$ -citrate injections reflect the  $^{67}\text{Ga}$ -transferrin distribution. As is seen in the biodistribution studies, addition of one of the 3-hydroxy-4-pyridinone ligands dramatically alters the biodistribution from that of  $^{67}\text{Ga}$ -transferrin. In the 24 hour time-frame allowed, Ga must have remained complexed to the added ligand throughout transport and uptake, ultimately to be cleared through the body via excretion. The octanol/water partition coefficient ( $\log p$ ) values for these Ga complexes<sup>87</sup> were significantly lower than ideal. Low  $\log p$  values contribute to the rapid renal elimination of the  $^{67}\text{Ga}$ -ligand complexes. New substituents are currently under active study, especially ones which will give higher  $\log p$  values. Knowledge of the difference in  $\log p$  values between the free ligands and their metal complexes is very useful since the biodistribution results further indicate their potential as chelating agents.

In summary the thermodynamic indifference of the 3-oxy-4-pyridinones to N-substitution allows the variation of the lipophilicity of the complex to alter the biodistribution without altering the stability.

Table 5.1 Biodistribution of  $^{67}\text{Ga}$  after 24 hours as a Function of Ligand in Mice (% Injected Dose per Gm Organ - 100  $\mu\text{L}$  Injection Containing  $1\mu\text{Ci}$   $^{67}\text{Ga}$  (0.25 nM) and the Ligand). Values are an Average for Five Mice.<sup>a</sup>

Tissue	citrate	Hdpp	Hmpp	<i>l</i> -mimosine	Hmhpp
Injection Concentration	47 $\mu\text{M}$	80 mM	40 mM	20 mM	5 mM
Blood	3.10 (2.47)	0.04 (0.02)	0.25 (0.07)	0.66 (0.24)	0.23 (0.11)
Liver	9.17 (4.29)	1.15 (0.21)	1.33 (0.53)	1.72 (0.55)	1.98 (0.38)
Spleen	3.94 (2.01)	0.38 (0.15)	0.51 (0.24)	0.95 (0.17)	0.73 (0.17)
Kidney	8.93 (3.24)	1.37 (0.36)	2.18 (0.49)	3.20 (0.39)	1.97 (0.24)
Heart	2.01 (0.97)	0.14 (0.02)	0.27 (0.03)	0.39 (0.11)	0.49 (0.09)
Lung	3.56 (1.91)	0.29 (0.05)	0.46 (0.09)	0.72 (0.11)	0.54 (0.09)
Muscle	1.13 (0.18)	0.15 (0.06)	0.30 (0.05)	0.24 (0.05)	0.48 (0.03)
Brain	0.24 (0.11)	0.02 (0.00)	0.05 (0.01)	0.05 (0.02)	0.06 (0.01)

<sup>a</sup> Numbers in parentheses represent standard deviations.

Figure 5.1 Per cent uptake per gram of organ for blood and liver 24 hours post-injection of various  $^{67}\text{Ga}$  - ligand solutions in mice.

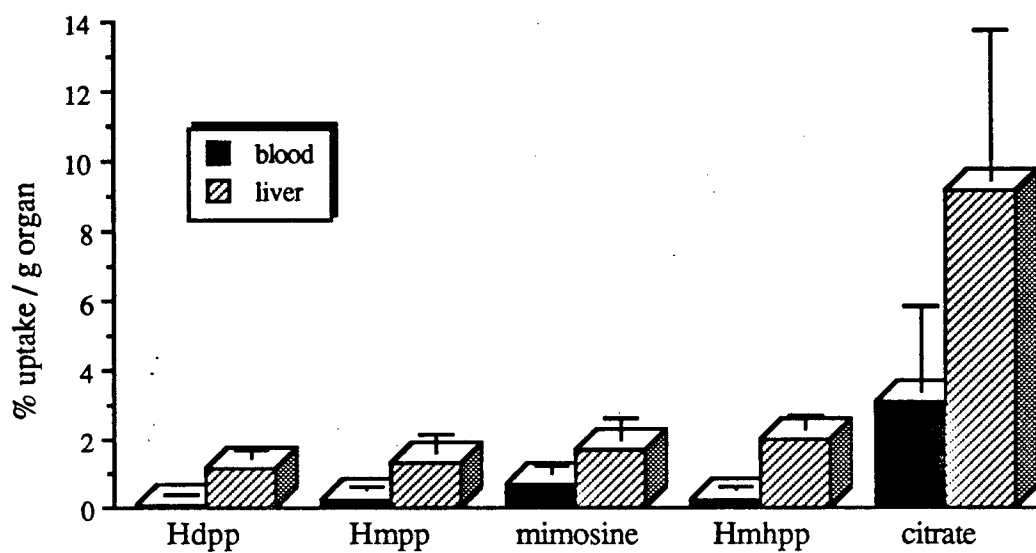
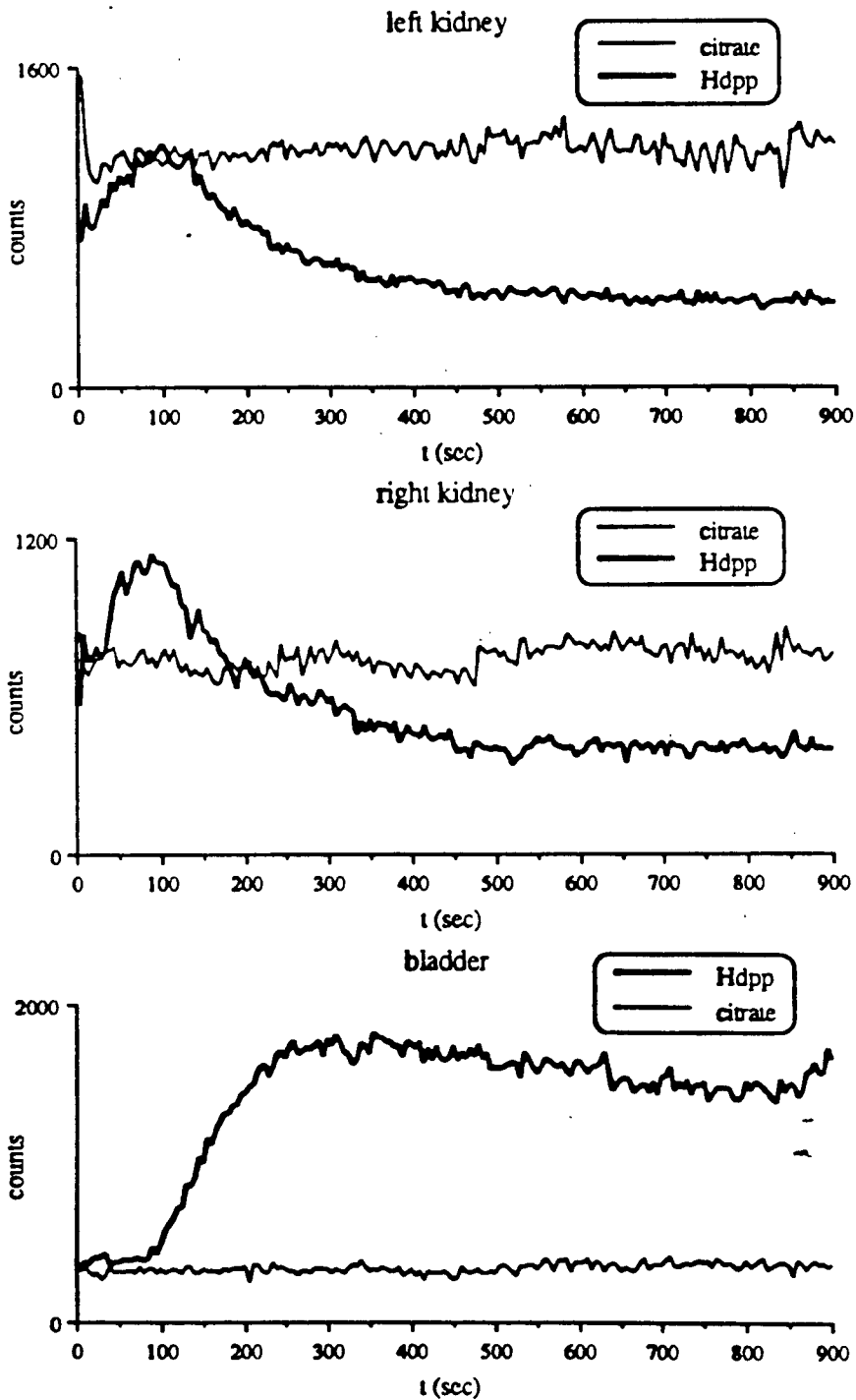


Figure 5.2 Clearance study of  $^{67}\text{Ga}(\text{dpp})_3$  (bold trace) and  $^{67}\text{Ga}(\text{citrate})$  (thin trace) in a rabbit. The time (seconds) is subsequent to injection. Regions of interest were set over each of the kidneys and the bladder.



## 5.2 Technetium Biodistribution Studies

### 5.2.1 Introduction

Our initial hopes in reacting pertechnetate with the 3-hydroxy-4-pyrones and the 3-hydroxy-4-pyridinones *via* the reduction route were for the formation of neutral technetium complexes which might localize in the brain, or for the formation of mono-cationic technetium complexes which might show heart uptake. With the formation of mono-cationic technetium complexes it was hoped that a heart imaging agent could be found. It has been known for some time that isotopes of Group I cations accumulate in normal heart muscle.<sup>88</sup> However, cationic character by itself is not sufficient to insure heart uptake, as evidenced by the fact that the majority of the cationic <sup>99m</sup>Tc complexes investigated to date do not image the heart.<sup>89</sup> Lipophilicity also seems to play a role in heart uptake. The hydrophilic limit has not been determined but if the complex is too lipophilic it seems to be extensively cleared by the liver. Thus, it was also our hope that with the easily functionalizable R group on the ring nitrogen of the 3-hydroxy-4-pyridinone ligands, the lipophilicity could be adjusted to a suitable level. Other parameters which may also influence the extent of heart uptake of <sup>99m</sup>Tc cations are the shape of the complex (complexes with more symmetrical shapes seem to be superior), the electrochemical potential for the reduction of the cation to the neutral analog (the neutral form presumably being inactive), and the degree of binding of the cation to blood proteins.

The initial cationic tris-ligand technetium complexes were prepared with <sup>99</sup>Tc, the long lived  $\beta^-$  isotope which is the preferred isotope for laboratory preparations. This work is generally done on the  $10^{-1}$  to  $10^{-3}$  M scale and must now be transferred to the world of nuclear medicine which uses <sup>99m</sup>Tc, a  $\gamma$  emitter, at the  $10^{-9}$  to  $10^{-12}$  M level.

Of all routinely available experimental techniques and procedures, only chromatography can be successfully applied to both  $^{99m}\text{Tc}$  complexes at the micromolar scale and to  $^{99}\text{Tc}$  complexes at the macromolar scale. Thus it is chromatography which provides the essential link between the inorganic chemistry of  $^{99}\text{Tc}$  and the chemistry of  $^{99m}\text{Tc}$  in the field of nuclear medicine. In a typical application of this link, the chemical properties and chromatographic profile of a new technetium complex are first well established using milligram amounts of  $^{99}\text{Tc}$ , transfer of the preparative chemistry from the  $^{99}\text{Tc}$  to the  $^{99m}\text{Tc}$  is then assessed chromatographically and finally the  $^{99m}\text{Tc}$  analogue is prepared and confirmed by concurrence of the chromatographic characteristics of the  $^{99}\text{Tc}$  and  $^{99m}\text{Tc}$  forms.

A number of chromatographic techniques have proven useful in the preparation and characterization of  $^{99}\text{Tc}$  complexes and in the quality control of  $^{99m}\text{Tc}$  radiopharmaceuticals. In our work thin layer chromatography (TLC) was the most widely used technique though a dual detection (UV-visible, radiometric) HPLC system is currently being set up and developed.

High pressure liquid chromatography (HPLC) has only recently been applied to  $^{99}\text{Tc}$  and  $^{99m}\text{Tc}$  radiopharmaceuticals, but already it has proven to be the chromatographic method of choice for a variety of experimental conditions. This is primarily because HPLC is unsurpassed in its ability to separate the components of complex mixtures. But in addition, HPLC systems can be set up with dual detection systems, for example, UV-visible and radiometric, which allow simultaneous monitoring of  $10^{-1}$  to  $10^{-3}$  M amounts of  $^{99}\text{Tc}$  by UV-visible and radiometric detection, and of  $10^{-9}$  to  $10^{-12}$  M quantities of  $^{99m}\text{Tc}$  by radiometric detection. It is this link which allows for the transfer of the chemistry from  $^{99}\text{Tc}$  to  $^{99m}\text{Tc}$ .

Thin layer chromatography (TLC) and paper chromatography currently comprise the clinically used procedures for quality control of  $^{99m}\text{Tc}$  radiopharmaceuticals. In these crude

but effective procedures the radiopharmaceutical is separated into unreduced  $[\text{TcO}_4]^-$ , hydrolysed reduced technetium  $\text{TcO}_2 \cdot n\text{H}_2\text{O}$ , and the entire class of Tc-ligand, and Tc-ligand-reductant complexes. The last category is generally treated as a single species, that is reduced labelled technetium, as no currently used procedure has the resolution necessary to separate this category into its individual complexes. The most widely used quality control procedures employ two chromatograms; the first, with one solvent system to move  $[\text{TcO}_4]^-$  leaving  $\text{TcO}_2 \cdot n\text{H}_2\text{O}$  and the reduced labelled technetium at the origin, and the second with another solvent system to move  $[\text{TcO}_4]^-$  and the reduced labelled technetium leaving  $\text{TcO}_2 \cdot n\text{H}_2\text{O}$  at the origin.

### 5.2.2 Chromatography

The chromatographic link between  $^{99}\text{Tc}$  complexes and  $^{99\text{m}}\text{Tc}$  complexes was crudely accomplished with a slight modification of a thin layer chromatography system. A TLC system was worked out for the  $[\text{}^{99}\text{TcL}_3]^+$  complexes, which involved the spotting on a silica plate of the complex which was then chromatographed in a 9:1 methanol:water solvent. Visualization of the  $^{99}\text{Tc}$  complex could then be done with the eye due to the intense colour of technetium complexes or with a UV fluorescent indicator. The  $[\text{}^{99\text{m}}\text{TcL}_3]^+$  complexes, were then chromatographed in an identical manner, however visualization of the  $^{99\text{m}}\text{Tc}$  complexes was now done by radiometric detection due to the very low concentrations of technetium-99m used in the preparation of radiopharmaceuticals. This was done by cutting the silica plate up into strips and counting them in a  $\gamma$  well counter. With this technique the  $^{99\text{m}}\text{Tc}$  complex could be located on the silica plate. The presence of the analogous  $^{99\text{m}}\text{Tc}$  complex is then confirmed by comparison of the  $R_f$  values for the  $^{99}\text{Tc}$  and  $^{99\text{m}}\text{Tc}$  forms.

The radiochemical purity of the  $[^{99m}\text{TcL}_3]^+$  complexes was also determined by thin layer chromatography. As mentioned earlier this is usually done with two systems: the first to determine the percentage of  $[^{99m}\text{TcO}_4]^-$  or "free technetium" as it is often called, and the second to determine the percentage of hydrolysed technetium  $^{99m}\text{TcO}_2 \cdot n\text{H}_2\text{O}$ . The thin layer chromatography results as recorded may be found in Table A. 2 of the appendix.

The percentage of free technetium was calculated by spotting the prepared radiopharmaceutical solution onto a silica plate, which was then chromatographed in 100% acetone. With this chromatography system, the free technetium moves with the solvent front while the hydrolysed technetium and the technetium complex stay at the origin. The silica plate is then cut into two parts and counted in a  $\gamma$  well counter. The percentage of free technetium may then be calculated. The percentage of free technetium is calculated by dividing the counts of the top portion (free Tc) by the total number of counts (hydrolysed Tc, Tc-complex, and free Tc). The percentage of free technetium is reported in Table 5.2.

The percentage of hydrolysed technetium is calculated in a similar way except now a system is developed that moves the free technetium  $[^{99m}\text{TcO}_4]^-$  and the technetium complex  $[^{99m}\text{TcL}_3]^+$  up the silica plate while leaving the hydrolysed technetium  $^{99m}\text{TcO}_2 \cdot n\text{H}_2\text{O}$  at the origin. The percentage of hydrolysed technetium in the radiopharmaceutical preparation of the  $[^{99m}\text{Tc}(\text{dpp})_3]^+$  complex was determined by using paper plates and a 1:1 water methanol solvent. The percent of hydrolysed technetium is calculated by dividing the counts of the bottom portion (hydrolysed Tc) by the total number of counts. This result is reported in Table 5.2. No system has been worked out yet to determine the percentage of hydrolysed technetium in the radiopharmaceutical preparation of the  $[^{99m}\text{Tc}(\text{mimo})_3]^+$  complex.

Table 5.2 Radiochemical Purity as Determined by Chromatography.

Complex	%Tc free [ <sup>99m</sup> TcO <sub>4</sub> ] <sup>-</sup>	%Tc Hydrolysed TcO <sub>2</sub> ·nH <sub>2</sub> O
[ <sup>99m</sup> Tc(dpp) <sub>3</sub> ] <sup>+</sup>	0.06	1.2
[ <sup>99m</sup> Tc(mimo) <sub>3</sub> ] <sup>+</sup>	0.48	

### 5.2.3 Materials and Methods

Hdpp was prepared and purified as described previously in Section 2.2; *l*-mimosine (Sigma) and SnCl<sub>2</sub>·2H<sub>2</sub>O (BDH) were used as supplied without further purification. Water was purified, deionized (Barnstead D 8904 and D8902 cartridges respectively), and distilled (Coming MP-1 Megapure Still).

Stock solutions of Hdpp and mimosine were prepared in isotonic saline at concentrations of 90 mM and 15.8 mM respectively. SnCl<sub>2</sub>·2H<sub>2</sub>O (1.0 mg, 4.43 μ mol) was added to 2.0 mL of the prepared ligand solution and shaken. [<sup>99m</sup>TcO<sub>4</sub>]<sup>-</sup> (2.0 mCi, 3.8 picomol) was then added to the ligand/tin solution and stirred for 10 minutes. The [<sup>99m</sup>TcO<sub>4</sub>]<sup>-</sup> was obtained as a salt from a commercially available pertechnetate generator in an isotonic saline solution. All injections were standardized such that 1.0 mL contained 1.0 mCi of <sup>99m</sup>Tc. Radiochemical purity of greater than 98% was ascertained by thin layer chromatography prior to injection as discussed earlier. Comparative clearance studies were then done in hypnotized and anaesthetized rabbits with a Siemens Large Field of View Gamma Camera.

#### 5.2.4 Results and Discussion

As an initial screening of the tris-ligand technetium complexes for use as radiopharmaceutical imaging agents, a clearance study was conducted in a live rabbit with the prepared  $[^{99m}\text{Tc}(\text{dpp})_3]^+$  complex. Upon injection of the  $[^{99m}\text{Tc}(\text{dpp})_3]^+$  complex into a live rabbit data accumulation was commenced. Data was collected for twenty minutes and was visualized throughout the duration of the procedure by one minute frames. Taken together Figures 5.3 and 5.4 show the distribution of the radiopharmaceutical at twenty minutes post-injection. Figure 5.3 shows some initial uptake into the heart, liver, and gall bladder, however, the majority of the labelled complex is localized in the kidneys and bladder, as shown in Figure 5.4. Figure 5.4 also shows some gut uptake; however, the gut uptake may be seen far more clearly in Figure 5.5 which shows the distribution of  $[^{99m}\text{Tc}(\text{dpp})_3]^+$  one hour post-injection and post-urination. From these results we may conclude that the majority of the complex is excreted *via* the kidneys and bladder. This is more clearly indicated by the clearance curves shown in Figure 5.6. The right and left kidney both show a rapid increase in activity, reaching a maximum at five minutes post-injection, followed by passage of the activity into the bladder. The subsequent uptake into the bladder from the kidneys is shown in Figure 5.7. No significant bladder uptake is observed until 220 seconds post-injection.

A clearance study was also done with the prepared  $[^{99m}\text{Tc}(\text{mimo})_3]^+$  complex as it was thought that mimosine, being an amino-acid, might show some biological activity. The prepared  $[^{99m}\text{Tc}(\text{mimo})_3]^+$  complex was injected into a live rabbit as before and upon injection data accumulation was started. The data was collected for twenty minutes and was visualized during the procedure by one minute frames. The results of the clearance study done with  $[^{99m}\text{Tc}(\text{mimo})_3]^+$  are displayed in a similar format to those of  $[^{99m}\text{Tc}(\text{dpp})_3]^+$  in order to compare the results. Figures 5.8 and 5.9 show the distribution of the

radiopharmaceutical at twenty minutes post-injection. Figures 5.8 and 5.9 show similar results to those of  $[^{99m}\text{Tc}(\text{dpp})_3]^+$  Figures 5.3 and 5.4. They show some activity in the heart, liver, and gall bladder, as was observed before, with the majority again being located in the kidneys and bladder. Figure 5.9 does, however, show significantly less gut uptake than Figure 5.4. Figure 5.10 shows the renal clearance of  $[^{99m}\text{Tc}(\text{mimo})_3]^+$  which again reaches a maximum at five minutes post-injection followed by a decrease of activity as it is passed on to the bladder. Figure 5.11 shows bladder activity by 120 seconds post-injection as well as significant excretion. With the  $[^{99m}\text{Tc}(\text{mimo})_3]^+$  complex (Figure 5.11) bladder activity is observed earlier than with the  $[^{99m}\text{Tc}(\text{dpp})_3]^+$  complex (Figure 5.7) and the percentage of activity excreted is also higher.

Figure 5.3 Distribution for  $[^{99m}\text{Tc}(\text{dpp})_3]^+$  twenty minutes post-injection  
(upper chest region).

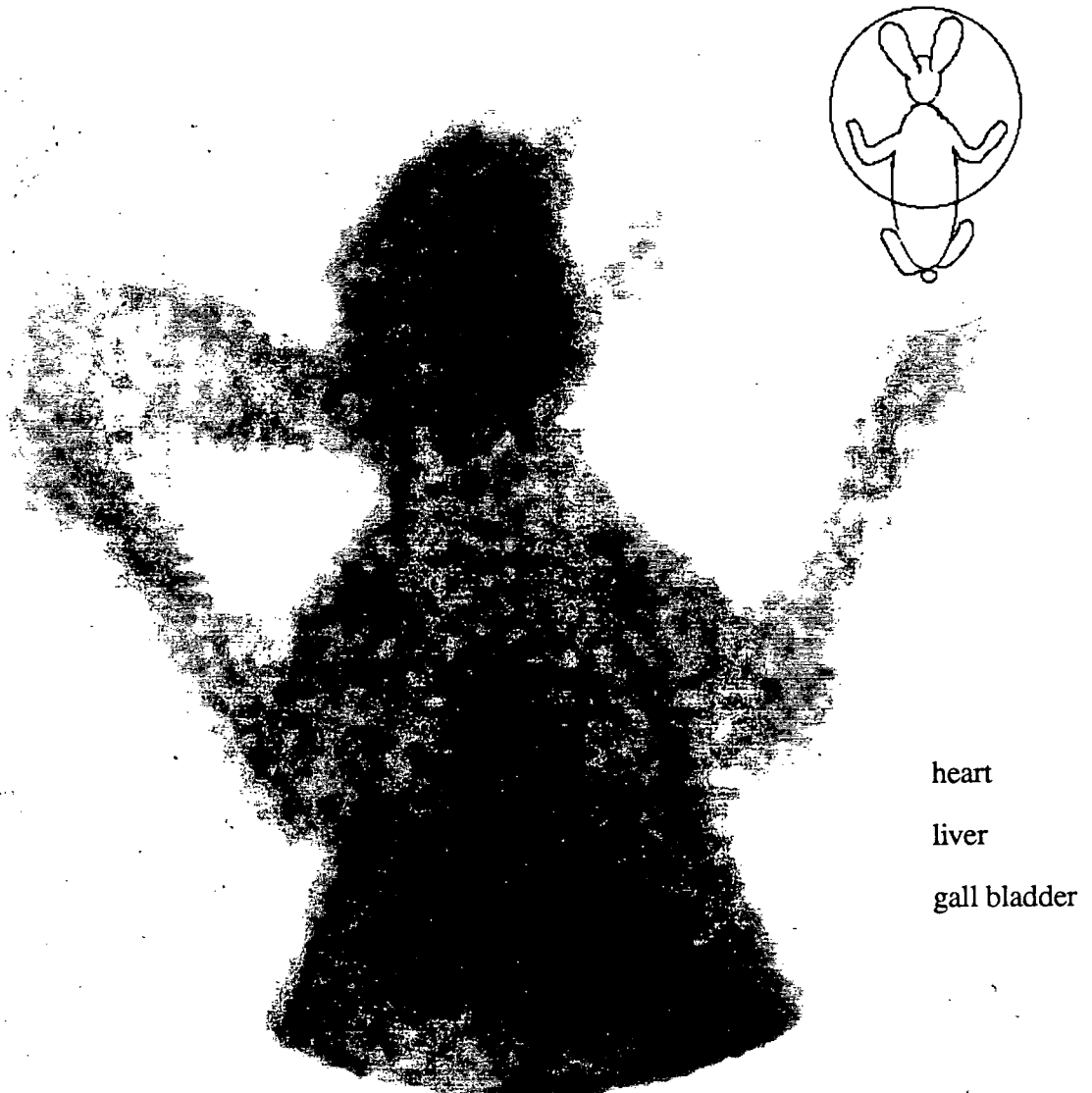


Figure 5.4 Distribution for  $[^{99m}\text{Tc}(\text{dpp})_3]^+$  twenty minutes post-injection  
(lower chest region).

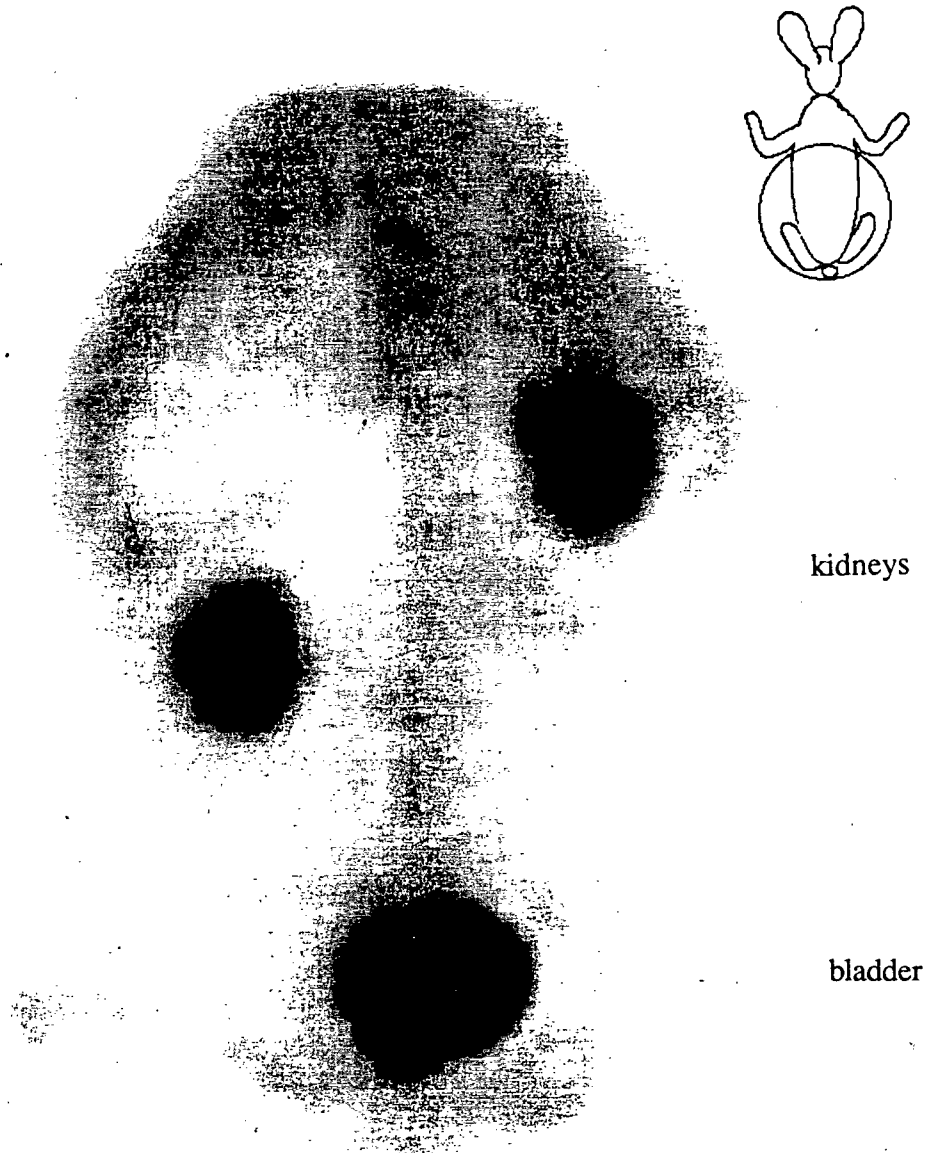


Figure 5.5 Distribution for  $[^{99m}\text{Tc}(\text{dpp})_3]^+$  one hour post-injection and post-urination (posterior view).

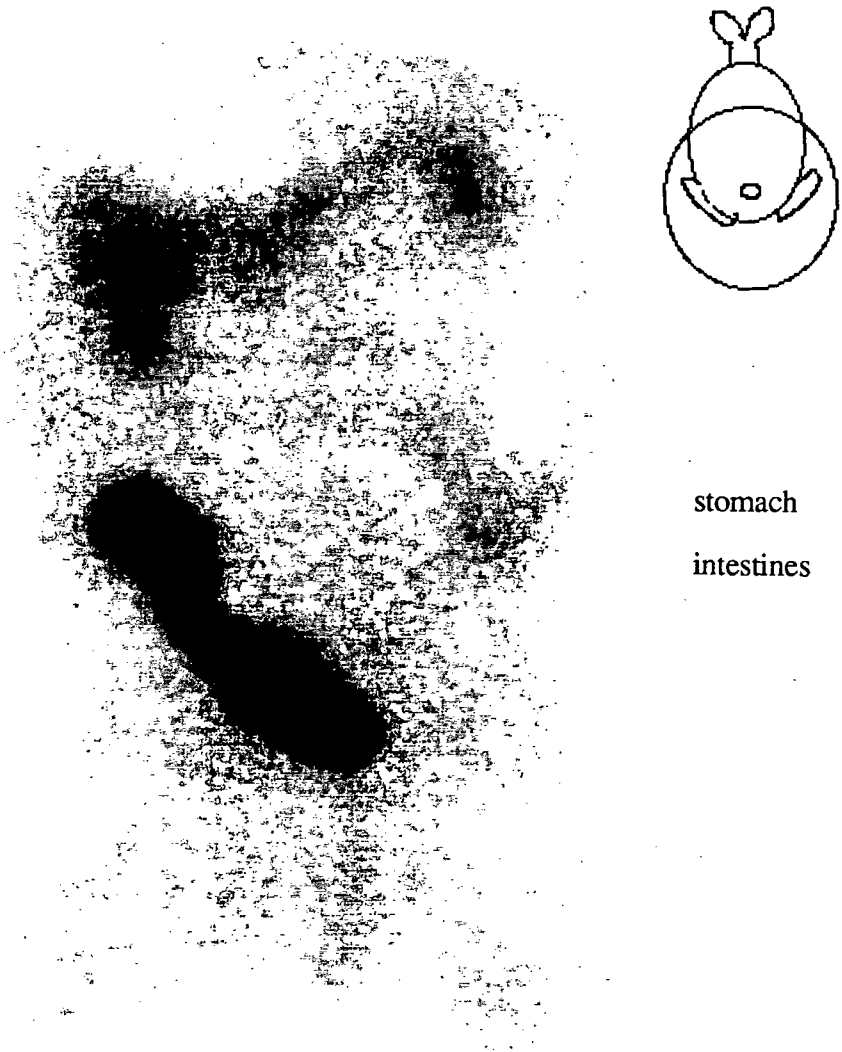


Figure 5.6 Clearance curves for  $[^{99m}\text{Tc}(\text{dpp})_3]^+$  (right kidney upper trace  
left kidney lower trace).

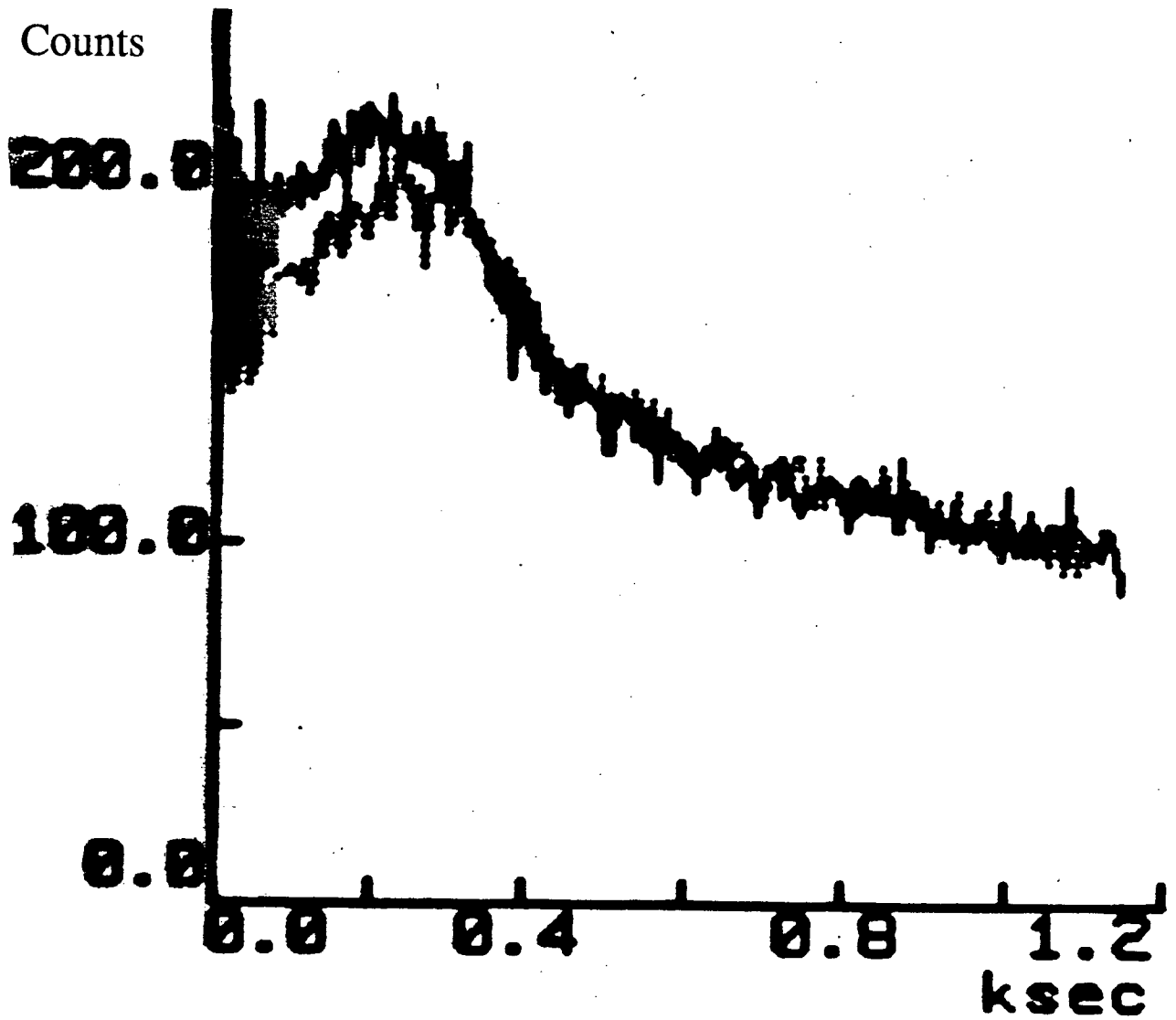


Figure 5.7 Clearance curves for  $[^{99m}\text{Tc}(\text{dpp})_3]^+$  (kidneys upper traces  
bladder lower trace).

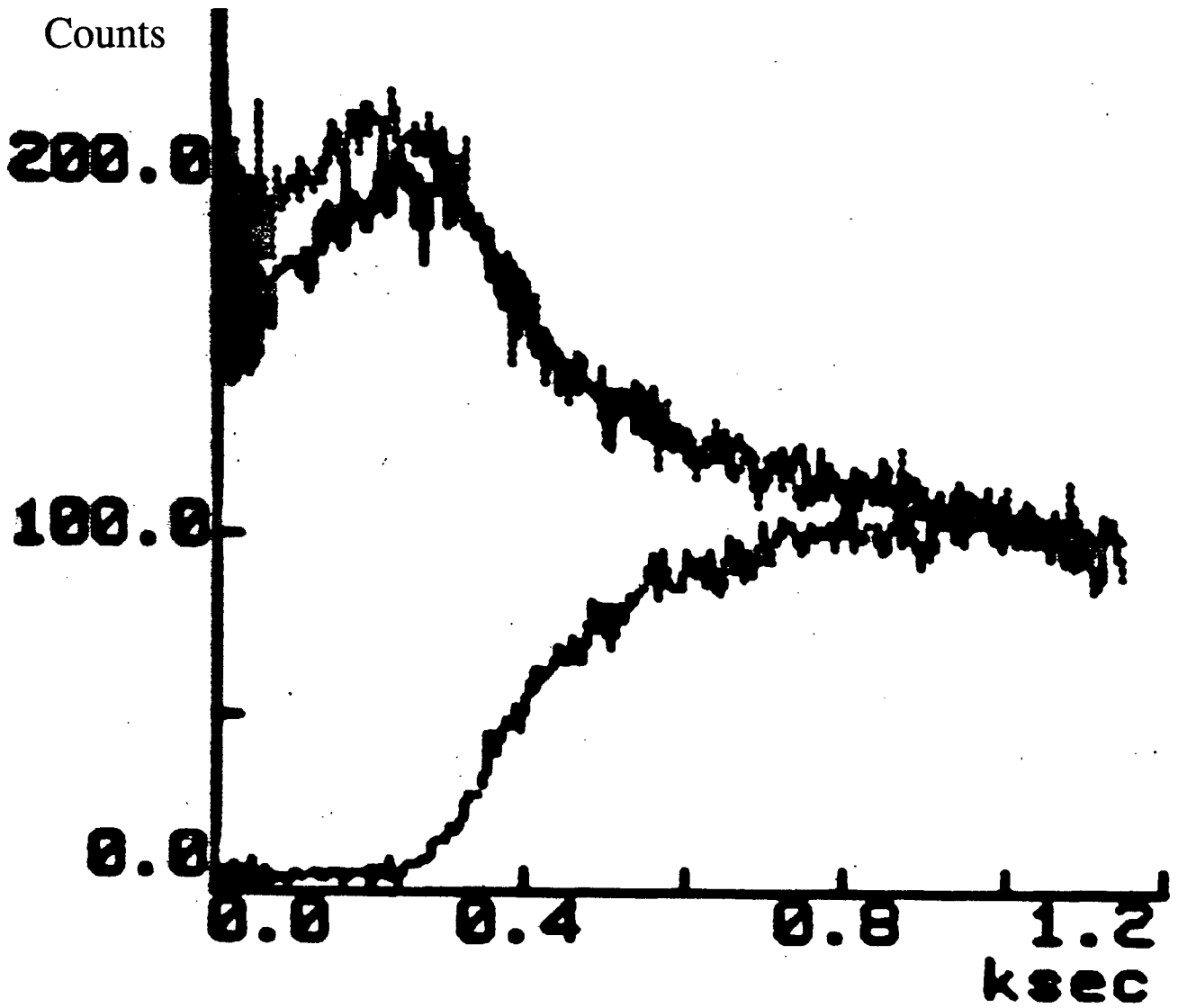
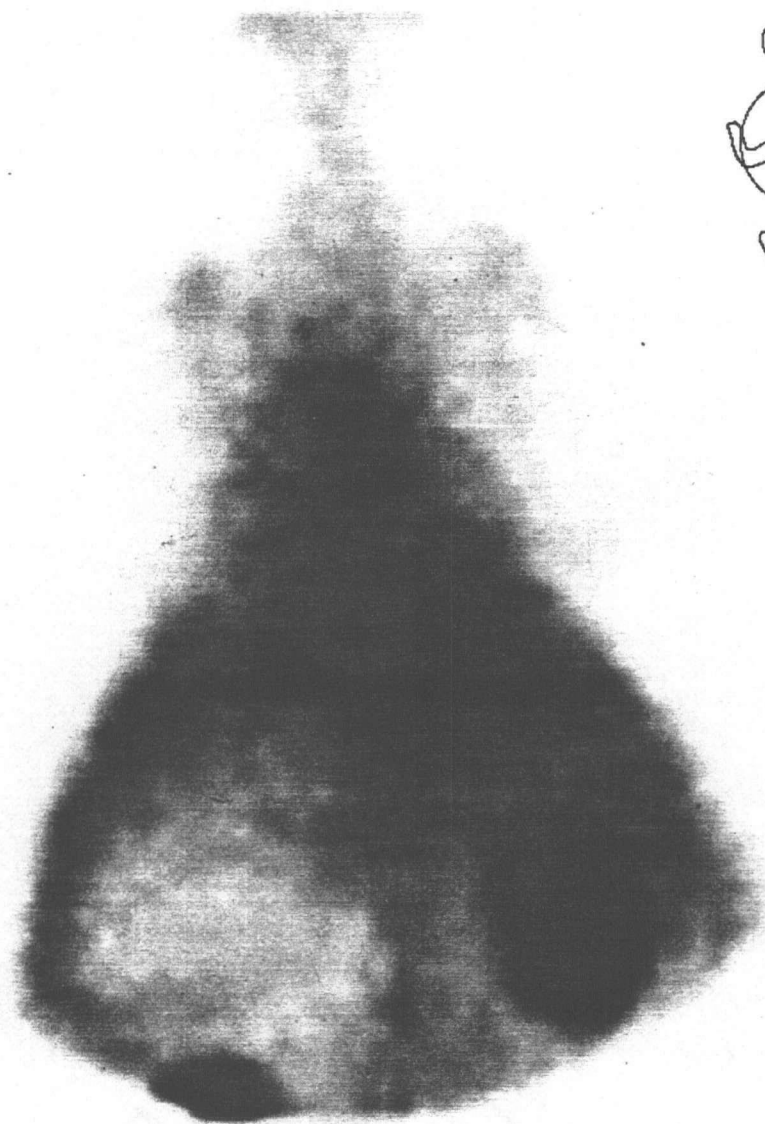


Figure 5.8 Distribution for  $[^{99m}\text{Tc}(\text{mimo})_3]^+$  twenty minutes post-injection  
(upper chest region).



heart

liver

gall bladder

Figure 5.9 Distribution for  $[^{99m}\text{Tc}(\text{mimo})_3]^+$  twenty minutes post-injection  
(lower chest region).

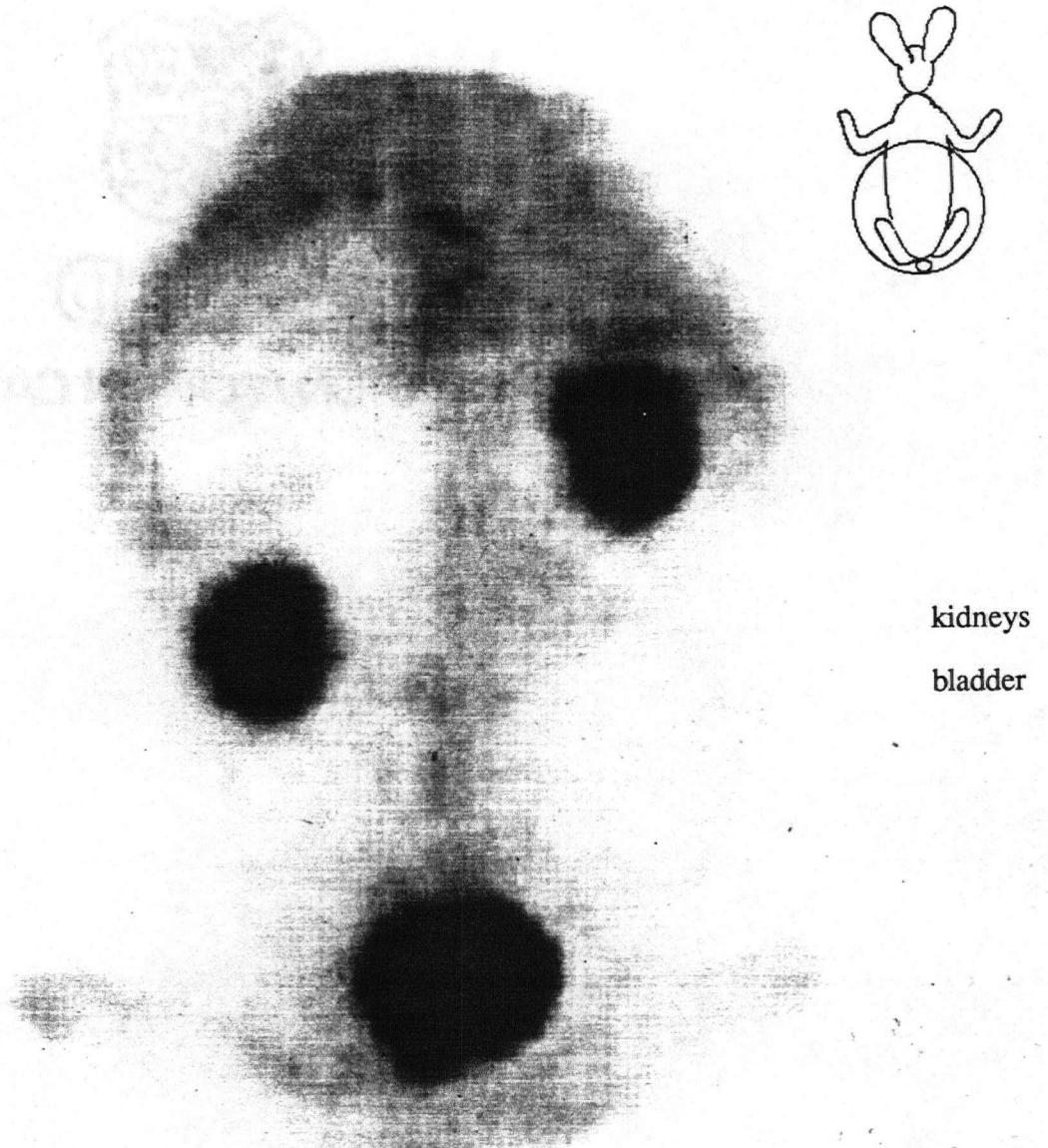


Figure 5.10 Clearance curves for  $[^{99m}\text{Tc}(\text{mimo})_3]^+$  (right kidney upper trace  
left kidney lower trace).

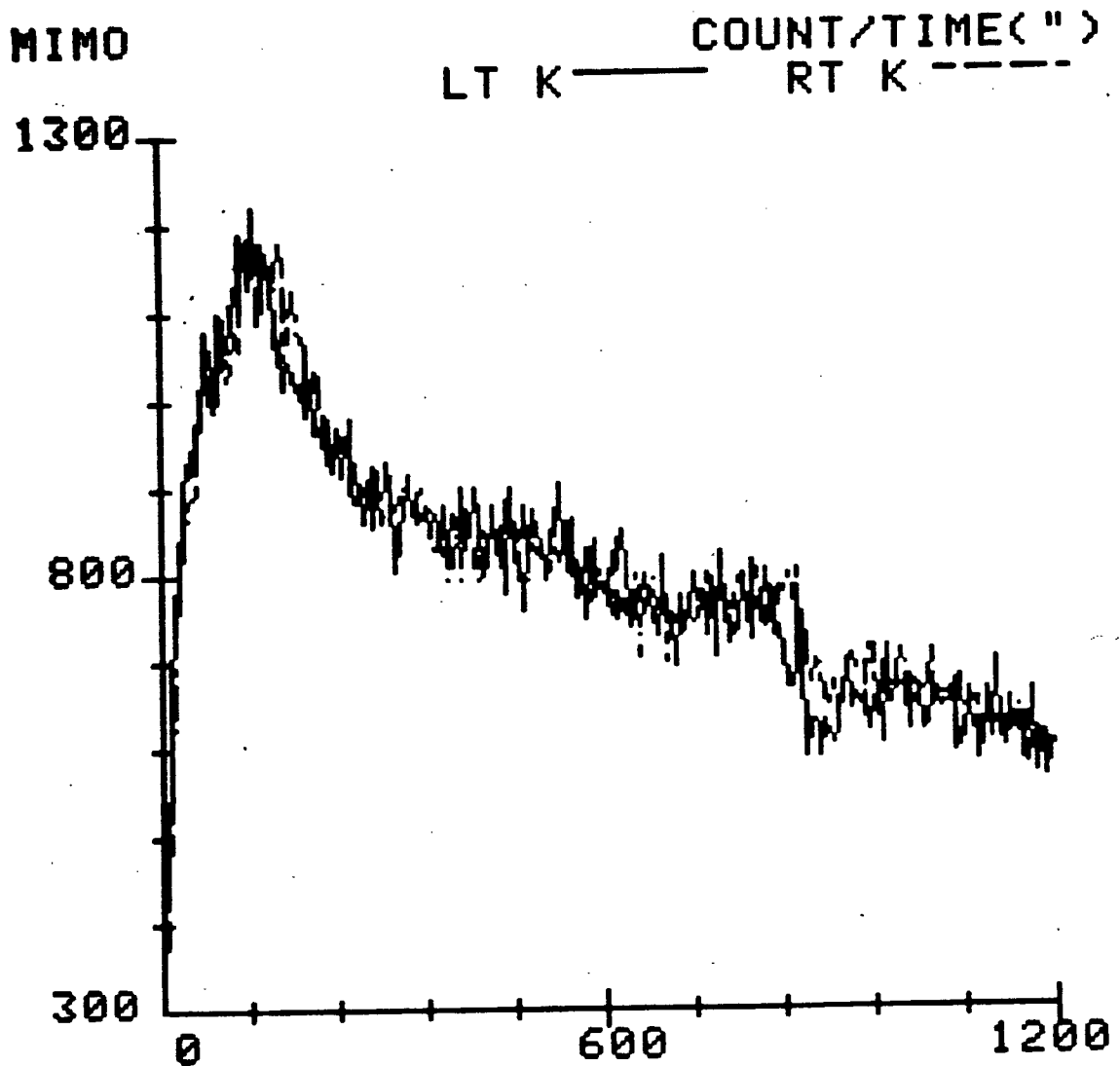
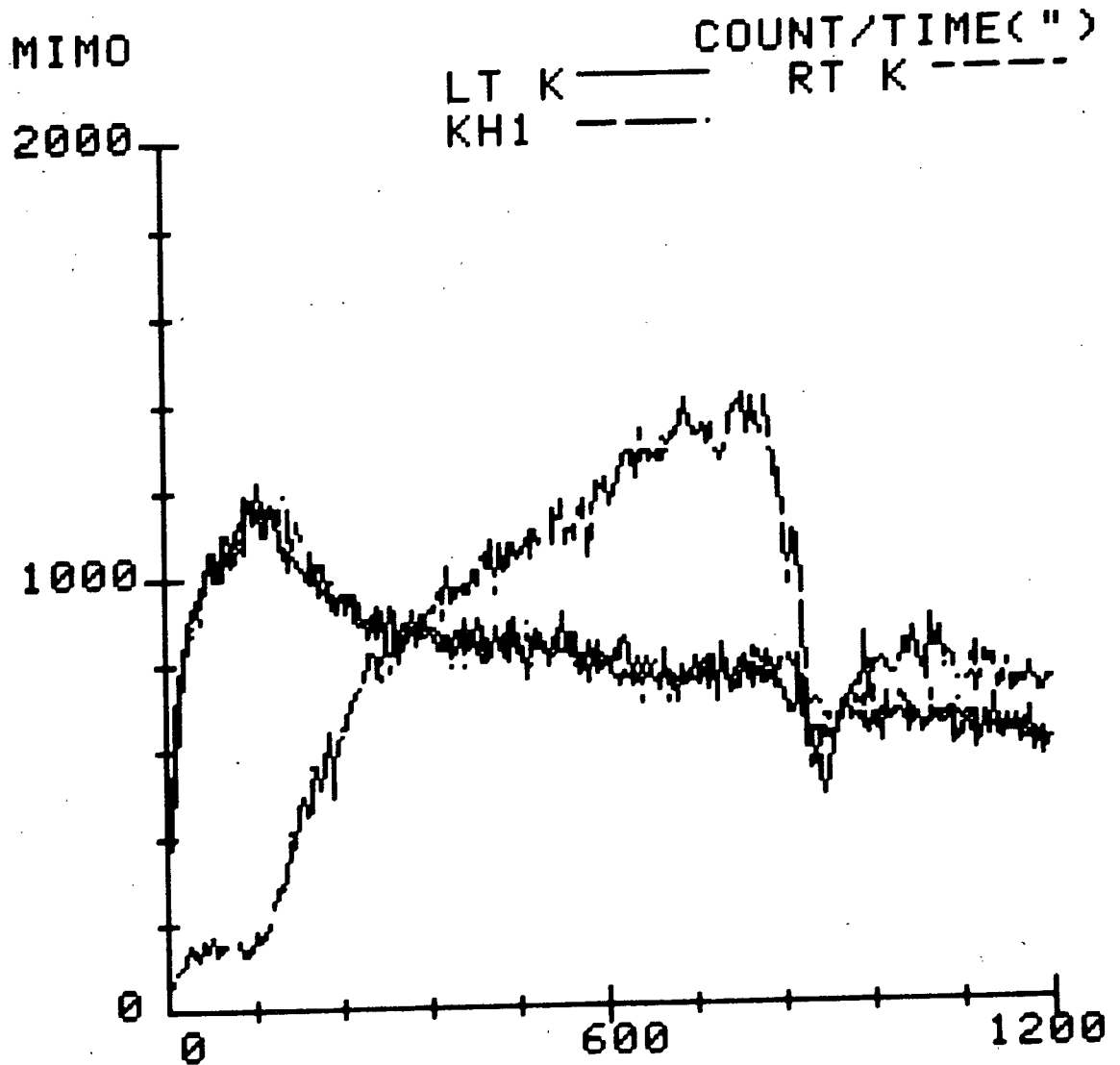


Figure 5.11 Clearance curves for  $[^{99m}\text{Tc}(\text{mimo})_3]^+$  (kidneys upper traces bladder lower trace).



## CHAPTER VI CONCLUSIONS AND SUGGESTIONS FOR FUTURE WORK

The primary objective of our research was the synthesis and characterization of technetium complexes and their subsequent investigation as radiopharmaceutical imaging agents. In addition to the technetium radiopharmaceutical work, some gallium work was also done. This work was done in collaboration with William Nelson and Don Lyster to complete an ongoing study of the *in vitro* and *in vivo* coordination chemistry of gallium 3-oxy-4-pyridinones as a model for the biodistribution of aluminum. The gallium work has been addressed in a previous chapter and it serves as both the conclusion and an indication of the direction of future work.

The main focus of our work was the synthesis and characterization of technetium-99 complexes with various 3-hydroxy-4-pyrones and pyridinones. Both the reduction and substitution routes were used for the synthesis of technetium-99 complexes; however, the majority of our work was done with the reduction route due to the applicability of this route for synthesis of radiopharmaceutical imaging agents. This applicability is a result of the availability of the starting material [ $^{99m}\text{TcO}_4$ ]<sup>-</sup>, and the short preparatory time required for complete formation of the technetium-99m complexes by this route. The short reaction time is necessary with isotopes such as  $^{99m}\text{Tc}$  because of its short half-life (6 hours). The reduction route used consists of the reduction of pertechnetate by  $\text{SnCl}_2 \cdot 2\text{H}_2\text{O}$  in the presence of a stabilizing ligand. Synthesis of technetium-99 complexes *via* this route resulted in the formation of mono-cationic tris-ligand technetium-99 complexes; however, due to the use of  $\text{SnCl}_2 \cdot 2\text{H}_2\text{O}$  as the reducing agent and the similar physical characteristics of Sn and Tc a mono-cationic tris ligand tin complex was also formed. This does not cause any problems for radiopharmaceutical use as the tin is not incorporated into the

radiopharmaceutical, on the other hand, it does cause problems in obtaining a pure technetium product. With the identification of this problem alternate reducing agents will be investigated in the future. The mixture of  $[\text{SnL}_3]^+$  and  $[\text{}^{99}\text{TcL}_3]^+$  complexes was then characterized using mass spectrometry, infrared spectrometry, ultraviolet spectroscopy and conductivity measurements. The chemistry developed for synthesis of the  $[\text{}^{99}\text{TcL}_3]^+$  complexes was used to form the analagous  $^{99\text{m}}\text{Tc}$ -labelled complexes which were then investigated for their potential as heart imaging agents. Initial clearance studies were done using  $[\text{}^{99\text{m}}\text{Tc}(\text{dpp})_3]^+$  and  $[\text{}^{99\text{m}}\text{Tc}(\text{mimo})_3]^+$  which showed some heart, liver, gall bladder, and gut uptake; though the majority of the activity was excreted rapidly by the kidneys and bladder. The rapid excretion of these complexes is thought to be due to the low lipophilicity of these ligands. In order to resolve this problem it is necessary to increase the lipophilicity, but as mentioned before if the lipophilicity is too great the complex is cleared by the liver. It was our hope that we could increase the lipophilicity and at the same time add an R group which is metabolized by the heart and thereby image the heart. Fatty acids are known to be metabolized by the heart and we decided to try attaching a fatty acid to the 3-hydroxy-4-pyridinone backbone. This was attempted by using the ring conversion reaction which has been used successfully in the past to change 4-pyrones to 4-pyridinones. The primary amine 11-aminoundecanoic acid was chosen as it is cheap, commercially available and is reported in literature to show heart uptake. Synthesis of Hmupp is reported in chapter 2 and investigation of its technetium complexes and their possible use as an imaging agent is underway.

Synthesis of technetium (V) complexes *via* the substitution route was also investigated.  $[\text{Bu}_4\text{N}][\text{TcOCl}_4]$  was chosen as the substrate and was reacted with maltol, kojic acid, and Hdpp. These reactions yielded complex mixtures of products which required advanced separation techniques which we did not have access to. Initial characterization of the products from the reaction of  $[\text{Bu}_4\text{N}][\text{TcOCl}_4]$  and maltol indicate

the presence of at least four complexes: two monomers  $[\text{TcL}_2\text{Cl}_2]^+$  and  $[\text{TcL}_2\text{O}]^+$ ; and two bimetallic complexes  $[\text{Cl}_2\text{L}_2\text{Tc-O-TcL}_2\text{Cl}_2]$  and  $[\text{Cl}_3\text{LTc-O-TcLCl}_3]$ . The results also indicate that  $[\text{TcL}_2\text{Cl}_2]^+$  and  $[\text{Cl}_2\text{L}_2\text{Tc-O-TcL}_2\text{Cl}_2]$  are the predominant species. The inability to separate these complex mixtures halted this work; however, with the purchase of a dual detection HPLC system which is presently being set up, further work will be conducted in the future.

**REFERENCES**

1. Perrier, C.; Segrè E. *Nature* (London), **1937**, *140*, 193.
2. Perrier, C.; Segrè E. *J. Chem. Physics*, **1937**, *5*, 712.
3. Perrier, C.; Segrè E. *J. Chem. Physics*, **1939**, *7*, 155.
4. Selig, H.; Malm, J. G. *J. Nucl. Chem.*, **1973**, *25*, 349.
5. Guest, A.; Lock, C. J. L. *Can. J. Chem.* **1972**, *50*, 1807.
6. Peacock, R. D.; Edwards, A. J.; Hugill, D. *Nature*, **1963**, *200*, 672.
7. Peacock, R. D. *The Chemistry of Technetium and Rhenium*, Elsevier: London, 1966.
8. Schwochau, K.; Astheimer, L.; Hauk, J.; Scheuk, H. J. *Angew. Chem.*, **1974**, *86*, 350.
9. Deutsch, E.; Heineman, W. R.; Hurst, R.; Sullivan, J. C.; Mulac, W. A.; Gordon, S. *J. Chem. Soc. Chem. Comm.*, **1978**, 1038.
10. Deutsch, E.; Libson, K.; Jurisson, S.; Lindoy, L. F. *Prog. Inorg. Chem.* **1987**, *75*.
11. Mazzi, U. *Polyhedron*, **1989**, *8*, 1683.
12. Orvig, C. Ph. D. Thesis, Massachusetts Institute of Technology **1981**.
13. Trop, H. S.; Jones, A. G.; Davison, A. *Inorg. Chem.* **1980**, *19*, 1993.
14. Kotegov, K. V.; Pavlov, O. N.; Sheredov, V. P. *Adv. Inorg. Chem. Radiochem.* **1968**, *11*, 1.
15. Dalziel, J.; Gill, N. S.; Nyholm, R. S.; Peacock, R. D. *J. Chem. Soc.* **1958**, 4012.
16. Libson, K.; Deutsch, E.; Barnett, B. L. *J. Am. Chem. Soc.* **1980**, *102*, 2476.
17. Deutsch, E. et al. *Science* **1981**, *214*, 85.
18. Münze, R. *Radiochem. Radioanal. Lett.* **1977**, *30*, 117.

19. Steigman, J.; Meinken, G.; Richards, P. *Int. J. Appl. Rad. Isotop.* **1975**, *26*, 601.
20. Bandoli, G.; Clemente, C. A.; Mazzi, U. *J. Chem. Soc. Dalton Trans.* **1978**, 373.
21. Loberg, M. D.; Porter, D. W. *Review and current status of hepatobiliary imaging agents*, in: *Radiopharmaceuticals II* (ed. Sorenson, J. A.) , Soc. of Nuclear Medicine, New York, 1979, p 519.
22. Loberg, M. D.; Fields, A. T. *Int. J. Appl. Radiat. Isot.* **1978**, *29*, 167.
23. Fergusson, J. E.; Hickford, J. H. *Aust. J. Chem.* **1970**, *23*, 453.
24. Fergusson, J. E.; Hickford, J. H. *J. Inorg. Nucl. Chem.* **1966**, *28*, 2293.
25. Cingi, M. B.; Clenente, D. A.; Magon. L.; Mazzi, U. *Inorg. Chim. Acta.* **1975**, *13*, 47.
26. Huggins, D. K.; Kaesz, H. D. *J. Am. Chem. Soc.* **1961**, *83*, 4474.
27. Hileman, J. C.; Huggins, D. K.; Kaesz, H. D. *Inorg. Chem.* **1962**, *1*, 933.
28. Hieber, W.; Lux, F.; Herget, C. *Z Naturforschung* **1965**, *206*, 1159.
29. Hileman, J. C.; Huggins, D. K.; Kaesz, H. D. *J. Am. Chem. Soc.* **1961**, *83*, 2953.
30. Michels, G. D.; Svec, H. *Inorg. Chem.* **1981**, *20*, 3445.
31. Floss, J. G.; Grosse, A. V. *J. Inorg. Nucl. Chem.* **1960**, *16*, 44.
32. Finnegan, M. M.; Lutz, T. G.; Nelson, W. O.; Smith, A.; Orvig, C. *Inorg. Chem.* **1987**, *26*, 2171.
33. Nelson, W. O.; Karpishin, T. B.; Rettig, S. J.; Orvig, C. *Inorg. Chem.* **1988**, *27*, 1045.
34. Matsuba, C.A.; Nelson, W. O.; Rettig, S. J.; Orvig, C. *Inorg. Chem.* **1988**, *27*, 3935.
35. Lutz, T. G.; Clevette, D. J.; Rettig, S. J.; Orvig, C. *Inorg. Chem.* **1989**, *28*, 715.
36. Nelson, W. O.; Rettig, S. J.; Orvig, C. *Inorg. Chem.* **1989**, *28*, 3153.

37. Baes, C. F. Jr.; Mesmer, R. E. *The Hydrolysis of Cations*; Wiley: New York, 1976.
38. Wilkinson, G.; Gillard, R. D.; McCleverty, J. A. Eds. *Comprehensive Coordination Chemistry, Vol. 3* Pergamon Press: New York, 1987.
39. Welch, M. J.; Moerlein, S. M. In *Inorganic Chemistry in Biology and Medicine*; Martell, A.E. Ed.; ACS Symposium Series 140, American Chemical Society: Washington, D. C., 1980; pp 121-140.
40. Moerlein, S. M.; Welch, M. J. *Nucl. Med. Biol.* **1981**, *8*, 277.
41. Moerlein, S. M.; Welch, M. J.; Raymond, K. N. *J. Nucl. Med.* **1982**, *23*, 501.
42. Taliaferro, C. H; Martell, A. E. *Inorg. Chim. Acta* **1984**, *85*, 9 and references contained therein.
43. Kappel, M. J.; Pecoraro, V. L.; Raymond, K. N. *Inorg. Chem.* **1985**, *24*, 2447 and references therein.
44. Green, M.A.; Welch, M.J.; Mathias, C.J.; Fox, K.A.A.; Knabb, R.M.; Huffman, J.C. *J. Nucl. Med.* **1985**, *26*, 170.
45. Green, M. A.; Welch, M. J.; Mathias, C. J.; Taylor, P.; Martell, A. E. *Nucl. Med. Biol.* **1985**, *12*, 381.
46. Mathias, C. J.; Sun, Y.; Welch, M. J.; Green, M. A.; Thomas, J. A.; Wade, K. R.; Martell, A. E. *Nucl. Med. Biol.* **1988**, *15*, 69.
47. Hunt, F. C. *Nucl. Med. Biol.* **1988**, *15*, 651, 659.
48. Foster, B. J.; Clagett-Carr, K.; Hoth, D.; Leyland-Jones, B. *Cancer Treat. Rep.* **1986**, *70*, 1311.
49. Thakur, M. L. In *Applications of Nuclear and Radiochemistry*; Lambrecht, R.M.; Morcos, N. Eds.; Pergamon: New York, 1982. p 115.

50. Thakur, M. L. In *Radiopharmaceuticals: Progress and Clinical Perspectives*. Fritzberg, A. R. Ed.; CRC: Boca Raton, FL, 1986; Vol. II, pp 1-21. 1989, Vols. 1-6.
51. Joist, J. H.; Baker, R. K.; Welch, M. J. *Semin. Thrombosis Hemostasis* **1983**, *9*, 86.
52. Thakur, M. L.; McKenney, S. L.; Park, C. H. *J. Nucl. Med.* **1985**, *26*, 518 and references therein.
53. Larson, S. M. *Semin. Nucl. Med.* **1978**, *8*, 193.
54. Welch, M. J.; Welch, T. J. In *Radiopharmaceuticals*; Subramanian, G.; Rhodes, B. A.; Cooper, J. F.; Sodd, V. J. Eds.; The Society of Nuclear Medicine: New York, 1975; pp 73-79.
55. Goodwin, D. A.; Sundberg, M. W.; Diamanti, C. I.; Meares, C. F. In *Radiopharmaceuticals*; Subramanian, G.; Rhodes, B. A.; Cooper, J. F.; Sodd, V. J. Eds.; The Society of Nuclear Medicine: New York, 1975; pp 80-101.
56. Brunetti, A.; Blasberg, R. G.; Finn, R. D.; Larson, S. M. *Nucl. Med. Biol.* **1988**, *15*, 665.
57. See issue No. 4 of *Nucl. Med. Biol.* **1986**, which is devoted to this topic.
58. Elkaschef, M. A-F.; Nosseir, M. H. *J. Am. Soc. Chem.* **1960**, *82*, 4344.
59. Brown, R. D. *J. Chem. Soc.* **1951**, 2670.
60. Meislich, H. in *The Chemistry of Heterocyclic Compounds Vol. 4: Pyridine and its Derivatives Part Three*; Klingsberg, E., Ed.; Interscience: New York, 1962; pp 509-890.
61. Harris, R. L. N. *Aust. J. Chem.* **1976**, *29*, 1329.
62. Kontoghiorghes, G. J.; Sheppard, L. *Inorg. Chim. Acta.* **1987**, *136*, L11.
63. Nelson, W. O.; Karpishin, T. B.; Rettig, S. J.; Orvig, C. *Can. Chem.* **1988**, *66*, 123.

64. Bellamy, L. J. *The Infrared Spectra of Complex Molecules, Vol. 1*, 3rd. ed.; Chapman and Hall: New York, 1975; p 453.
65. Maquestiau, A.; van Haverbeke, Y.; de Meyer, C.; Katritzky, A. R.; Cook, M. J.; Page, A. D. *Can. J. Chem.* **1975**, *53*, 490.
66. Silverstein, R. M.; Bassler, G. C.; Morrill, T. C. *Spectrometric Identification of Organic Compounds* 4th ed.; Wiley: New York, 1981; pp 305-331.
67. Fritzberg, A. R.; Lyster, D. M.; Dolphin, D. H. *J. Nucl. Med.* **1977**, *18*, 553.
68. Jones, A. G.; Orvig, C.; Trop, H. S.; Davison, A.; Davis, M. A. *J. Nucl. Med.* **1980**, *21*, 279.
69. Srivistava, S. C.; Richards, P. *Radiotracers for Medical Applications*, CRC Press, Boca.Raton, Fl, 1978.
70. Zalutsky, M. R.; Rayuda, G. V. S.; Friedman, A. M. *Int. J. Nucl. Med. Biol.* **1977**, *4*, 224.
71. Kappas, A.; Maines, M. D. *Science* **1976**, *192*, 60.
72. Stiegman, J.; Chin, E. V.; Soloman, N. A. *J. Nucl. Med.* **1979**, *20*, 766.
73. Burns, H. D.; Worley, P.; Wagner, H. N.; Marzelli; Risch, V. *Chem. Radiopharm. Text. Symp.*, Philadelphia, 1976, pp 269-289.
74. Davison, A. et al. *J. Nucl. Med.* **1983**, *24*, 353.
75. Boulton, A. J.; Mckillop, A. in *Comprehensive Heterocyclic Chemistry Vol. 2*; Katritzky, A. R., Rees, C. W., Eds.; Pergamon Press: New York, 1984; pp 1-27.
76. Nakamoto, K. *Infrared and Raman Spectra of Inorganic and Coordination Compounds*, 3rd. ed.; Wiley-Interscience: New York, 1978; pp 249-311.
77. Trop, H. S.; Davison, A.; Jones, A. G.; Davis, M. A.; Szalda, D. J.; Lippard, S. J. *Inorg. Chem.* **1980**, *19*, 1105.
78. Melnik, M.; Van Lier, J. E. *Coordination Chemistry Reviews Vol. 77*; Elsevier Science: Amsterdam, **1987**; pp 275-324.

79. Sieler, H. G. *Metal Ions Biol.* **1983**, *16*, 317.
80. Cotton, F. A.; Davison, A.; Day, V. W.; Gage, L. D.; Trop, H. S. *Inorg. Chem.* **1979**, *18*, 3024.
81. Davison, A.; Orvig, C.; Trop, H. S.; Sohon, M.; DePhamphilis, B. V. *Inorg. Chem.* **1980**, *19*, 1988.
82. Clark, M. J.; Kastner, M. E.; Podbielski, L. A.; Fackler, P. H.; Schriefels, J.; Meinken, G.; Srivastava, S. C. *J. Am. Chem. Soc.* **1988**, *110*, 1818.
83. Brunetti, A.; Blasberg, R. G.; Finn, R. D.; Larson, S. M. *Nucl. Med. Biol.* **1988**, *15*, 665.
84. Larson, S. M. *Semin. Nucl. Med.* **1978**, *8*, 193.
85. Martell, A. E.; Smith, R. M. *Critical Stability Constants*; Plenum: New York, 1974-1989, Vols. 1-6.
86. Harris, W. R.; Pecoraro, V. L. *Biochemistry* **1983**, *22*, 292.
87. Nelson, W. O. Ph.D. thesis, University of British Columbia, 1988.
88. Deutsch, E.; Glavan, K. A.; Sodd, V. J. *J. Nucl. Med.* **1981**, *22*, 897.
89. Mousa, S. A.; Williams, S. J.; Sands, H. *J. Nucl. Med.* **1987**, *28*, 1351.
90. Melnik, M.; Van Lier, J. E. *Coordination Chemistry Reviews Vol. 78*; Elsevier Science: Amsterdam, **1987**; pp 253-331.
91. Wilkinson, G.; Gillard, R. D.; McCleverty, J. A. Eds. *Comprehensive Coordination Chemistry, Vol. 6* Pergamon Press: New York, 1987, p 964.

**Appendix**

Table A. 1 Molecular weights (MW) of the 3-hydroxy-4-pyrone and pyridinone ligands and their tris-ligand metal chloride complexes.

Ligand	MW	[TcL <sub>3</sub> ][Cl]	[SnL <sub>3</sub> ][Cl]
Maltol	126.2	510.0	529.7
Kojic acid	142.1	557.8	577.5
Hmpp	125.1	506.8	526.5
Hdpp	139.1	548.8	568.5
Hmhpp	209.3	759.4	779.1
Hmupp	309.4	1059.6	1079.3
Mimosine	198.2	726.0	775.7

Table A. 2 TLC radiopharmaceutical control of  $^{99m}\text{Tc}$  complexes prior to injection.

(Counts = number of disintegrations in 30 seconds)

Complex	System 1 Determination of % free Tc	System 2 Determination of % hydrolysed Tc
$[\text{}^{99m}\text{Tc}(\text{dpp})_3]^+$	counts top = 237 counts bottom = 311,165 counts background = 38	counts top = 14,301 counts bottom = 516 counts background = 348
$[\text{}^{99m}\text{Tc}(\text{mimo})_3]^+$	counts top = 516 counts bottom = 90,537 counts background = 79	

$$\% \text{ free Tc} = \frac{\text{counts top} - \text{background}}{(\text{counts top} - \text{background}) + (\text{counts bottom} - \text{background})} \times 100$$

$$\% \text{ hydrolysed Tc} = \frac{\text{counts bottom} - \text{background}}{(\text{counts bottom} - \text{background}) + (\text{counts top} - \text{background})} \times 100$$